Far-field correlation of palaeokarstic surfaces in Mississippian successions using high-frequency foraminiferal diversity trends

Pedro Cózar[1]*, Ian D. Somerville[2], Mark W. Hounslow[3,4] and Ismael Coronado[5]

[1] *Instituto de Geociencias (CSIC-UCM), c/ Severo Ochoa 7, 28040 Madrid, Spain*

[2] *UCD School of Earth Sciences, University College Dublin, Ireland*

[3] *Lancaster Environment Centre, Lancaster University, Lancaster, UK. LA1 4YW*

[4]*Earth, Ocean and Ecological Sciences, University of Liverpool, Jane Herdman Building, Liverpool, L69 3GP*

[5] *Facultad de Ciencias Biológicas y Ambientales, Universidad de León, Campus de Vegazana s/n, 24071-León, Spain*

** Corresponding Author*

***e-mail addresses*:** p.cozar@igeo.ucm-csic.es (P. Cózar); ian.somerville@ucd.ie (I.D. Somerville); mark.w.hounslow@gmail.com (M.W. Hounslow); icorv@unileon.es (I. Coronado)

ABSTRACT

The degree to which emergent surfaces are correlated in late Asbian carbonate successions in Britain and Ireland is assessed by the integration of detailed biostratigraphy and diversity trends in foraminifers. Data are related to the Trowbarrow Quarry section in northern England, which provides a reference section for the upper Asbian because of its rich assemblages and high sampling density. Diversity trends are

shown to be non-random, possesses cyclic behaviour, and can be quantitatively correlated between sections. The assemblages allow stratigraphic segmentation into 13 intervals of foraminiferal diversity trends, which sub-divide the coarser-resolution biozones and sub-biozones. Similar foraminiferal trends are recognised in sections hundreds of kilometres away from Trowbarrow, in South Wales, and southeastern and western Ireland, facilitating a more precise correlation of strata. These highlight the coeval nature of emergent surfaces and rhythms between these regions, thus, establishing a precise stratigraphy. This new assessment also enables better discrimination of 'missing beats' and large hiatuses in the successions. The establishment of this rhythmic stratigraphy permits recognition of the late occurrence of some biostratigraphical markers, enabling amendment of biostratigraphic mismatches.

Keywords: carbonates, cyclicity, palaeokarsts, foraminifers, biodiversity, Britain, Ireland

RUNNING TITLE: Far-field palaeokarstic correlation

1. Introduction

Several authors have claimed that during the Asbian and Brigantian substages (George et al., 1976; Heckel, 2004) correlation of emergent surfaces (palaeokarsts) in carbonates was possible throughout their respective regions of study in Britain (Somerville, 1977; Davies, 1983; Berry, 1984; Ramsay, 1991). Other authors have also supported this concept (Walkden and Davies, 1983; Horbury, 1987), although admitting that the poor exposure of the outcrops, tectonic influence and existence of pre-depositional relief has led to some emergent surfaces being hidden or located at different levels within the platforms. Study of late Viséan cyclicity in Britain is an important issue in relationship to the main cooling phase of the Late Palaeozoic Ice Age (LPIA), with its onset located at the base of the Asbian for some authors (e.g., Wright and Vanstone, 2001; Barnett et al., 2002), late Asbian in Canada (Giles, 2009) or at the base -Brigantian equivalents in the USA (Smith and Read, 2000). However, the inference of cyclicity has been discarded for the late Viséan in some regions of Britain due to the inability to recognise appropriate facies stacking patterns (Manifold et al., 2020), although results using these mathematical approaches are not free of controversy (Barnett et al., 2002). There are numerous factors which can condition the observed cycles, in particular, the unfilled accommodation space, depositional topography and 'missing beats' (Eberli, 2013). It has been estimated that no more than 10-15% of rock deposited in each cycle are preserved (Eberli, 2013; Montañez, 2021). Despite these apparent problems, interpretation of vital factors such as the correlation of cycles, recognition of 'missing beats', estimation of orbital forcing, calculation of time durations and sea level amplitude changes, are only as good as the

biostratigraphic/chronostratigraphic control in these shallow water carbonates (Eberli, 2013).

Asbian cycles in central and northern England were named as 'rhythms' by some authors (Davies, 1983; Wright et al., 1997) in order to distinguish them from the classical cyclothems of the overlying Brigantian Yoredale Series, such as in the Alston Formation of northern England (Dean et al., 2011). Emergent surfaces and rhythms have been described in Asbian-age rocks, ranging in number from c. 15-20, but up to 49 in Derbyshire. However, some of these surfaces were considered as minor surfaces with impersistent lateral continuity, and thus, define internal cycles of differing hierarchical order. Detailed petrographic studies have focused on the characterization of the emergent surfaces, detailing the abundance and evolution of features related to estimated exposure times (e.g., Wright, 1994; Vanstone, 1996, 1998; Davies, 2001).

The near-field correlation of emergent surfaces in Britain is limited to regions of carbonate platforms or smaller shelves, in which the rhythms have been mostly attributed to local tectonics, regional (or plate) tectonics, eustasy, cumulative sedimentation or autogenic sedimentation processes (e.g., Somerville, 1977; Gray, 1981; Davies, 1983; Berry, 1984; Horbury, 1987, 1989; Ramsay, 1989). Paradoxically, some of the rhythmic successions of the "south Cumbria shelf" (SCS), Wales and Pennines regions (Figs. 1–2) are now recognised as being late Asbian in age, and the underlying lower Asbian interval is represented by non-rhythmic formations (Cózar and Somerville, 2020; Waters et al., 2021; Cózar et al., in press). The occurrence of lower Asbian carbonates in North Wales was questioned (or if even present) and is there of reduced thickness due to the occurrence of late Asbian markers from the Leete Formation (Cózar and Somerville, 2020).

The recognition of individual macrofossil horizons has been claimed as a correlation tool, but most of the utilised brachiopods and rugose corals are only indicative of the late Asbian, or first occur from the early Asbian or even older rocks (e.g., Riley, 1993). The macrofossil occurrences in these shallow-water facies do not allow a robust subdivision of the late Asbian, and the acmes of the species could be a result of particular palaeoecological conditions in the studied sections.

In contrast, in the shallow-water Viséan carbonate platforms of Britain and Ireland, foraminifers represent the best faunal group for providing high-resolution biostratigraphy. The upper Asbian limestones were originally included in the Cf6γ foraminiferal subzone of Conil et al. (1980), but this subzone was subsequently subdivided into Cf6γ1 and Cf6γ2 intervals by Jones and Somerville (1996), and in turn into Cf6γ1a and Cf6γ1b by Gallagher and Somerville (1997). In addition, the Cf6γ2 interval has been further subdivided by Cózar et al. (in press), into Cf6γ2a, Cf6γ2b and Cf6γ2c assemblages (Table 1). Nevertheless, these assemblages, by themselves, do not allow a rhythm-by-rhythm correlation and so establishment of a more detailed subdivision and correlation is necessary to develop a detailed rhythmic-stratigraphy. This so-far unrealised aim would be a powerful tool for correlation, for recognising orbitally-forced Milankovich cycles, and a possible astrochronological dataset for developing age models in the Viséan (Montañez, 2021).

The aims for this study are to demonstrate: (1) there is a similar pattern in the foraminiferal diversity of stratigraphic sections in Britain and Ireland within coeval upper Asbian carbonate platform facies; (2) these diversity changes permit the far-field correlation of emergent surfaces, and establishment of a precise rhythm-based-stratigraphy; (3) possible hiatuses may be detected in the succession, and (4) biostratigraphic mismatches can be precisely highlighted.

2. Studied sections

Four regions have been selected as providing representative rhythmic late Asbian shallow-water carbonate sections in Britain and Ireland: north Lancashire (Trowbarrow Quarry), South Wales (Port Eynon coast section), southeast Ireland (Ballyadams Quarry, Clogrenan B Borehole and Clogrenan Quarry) and western Ireland (Aillwee section, Burren) (Figs. 1–2). The foraminiferal assemblages from these sections are rather similar, and fossil markers (particularly foraminifers) are apparently valid for all of the regions (e.g., Conil et al., 1980; Riley, 1993). These four regions have been selected because of previous intensive sampling campaigns, whereas other less closely sampled sections do not allow inference of foraminiferal diversity trends. In total, the foraminiferal assemblages from 598 samples have been analysed (see full list of samples in Supplementary Fig. S1) comprising Trowbarrow Quarry (202), Port Eynon (64), Ballyadams Quarry (118), Clogrenan B Borehole (57), Clogrenan Quarry (23) and Aillwee (134).

2.1. South Cumbria-north Lancashire (Trowbarrow Quarry)

The reference-record for our analysis is Trowbarrow Quarry (Silverdale, north Lancashire), because it contains one of the richest and most diverse upper Asbian foraminiferal assemblages recorded anywhere in Britain and Ireland. The section of the Urswick Limestone Formation is well-known in British studies (e.g., Strank, 1981; Horbury, 1987; Athersuch and Strank, 1989) and the section contains 29 emergent surfaces recognisable in the field. Horbury (1987, 1989) recognised 12 major emergent

surfaces, thereby generating 11 rhythms. The lower 5 rhythms (numbered 1 to 5) were considered as tectonically-driven and early Asbian in age by Horbury (1987), whereas the upper 6 rhythms (labelled as A to G) were attributed to glacioeustasy during the late Asbian. However, the base of the upper Asbian is located in the uppermost part of the Park Limestone Formation (Fig. 3A), whereas the base of the Brigantian Alston Formation (formerly Gleaston Formation in this region; Rose and Dunham, 1977), is located above the Humphrey Head Limestone Member (Fig. 3A), in the first marine shale, but without an emergent surface. In the studied section, five upper Asbian foraminiferal assemblages (Table 1) are recognisable (Cózar et al., in press). The upper Asbian succession in this quarry section is approximately 170 m thick. The foraminiferal database was included in the Supplementary Appendix 1 of Cózar et al. (in press), reproduced herein in the supplementary material as Appendix A.

2.2. South Wales (Port Eynon coast section)

The upper Asbian limestones in Port Eynon (South Wales) only contains 4 thick palaeosols with clay wayboards (Cózar and Somerville, 2020), although reddish horizons (in shales and limestones) are common, as are pebbly horizons, suggesting emergent surfaces but with winnowed clays or less developed palaeokarsts (cf. Horbury and Qing, 2004; Vanstone, 1996). In total, 14 horizons can be attributed to emergent surfaces (Fig. 3B) a rather similar number of 12 palaeosols and erosion surfaces was recognised by Ramsay (1991). The overall lithostratigraphic framework of South Wales is not as well studied as the succession in North Wales (Fig. 2), where 6 to 20 rhythms were defined for the so-called lower Asbian and 8 to 13 rhythms for the upper Asbian (e.g., Somerville, 1977; Gray, 1981; Davies, 1983).

The upper Asbian in South Wales is represented by the Oxwich Head Limestone Formation, although the upper part of the formation is Brigantian in age (Fig. 2). The lower Asbian was interpreted as missing in this region, with the Oxwich Limestone Formation (late Asbian age) lying directly on the Holkerian Stormy Limestone Formation (Cózar and Somerville, 2020), although the presence of the lower Asbian strata was suggested by Waters et al. (2011). In the section, only the Cf6γ1 and Cf6γ2 subzones were formerly recognised. The rocks attributed to the upper Asbian in this region are 87 m thick. The foraminiferal database is extracted from figure 3 in Cózar and Somerville (2020), reproduced herein as Appendix B.

2.3. Southeast Ireland (Ballyadams Quarry, Clogrenan B Borehole and Clogrenan Quarry)

In southeast Ireland the Ballyadams Formation contains the entire Asbian although the lower Asbian strata are non-rhythmic (Fig. 2). It was sampled in the Ballyadams Quarry and Clogrenan B Borehole (Figs. 3C–4A), both representative sections of the rhythmic upper Asbian (Cózar and Somerville, 2005; Somerville and Cózar, 2005). To characterise the transition into the succeeding Brigantian, the lower part of the Clogrenan Quarry (Fig. 4B) is also included. Unit 1 of the upper part of the Ballyadams Formation is characterised by the rarity of palaeokarsts (except in its upper part and base; Fig. 3C), whereas the younger unit 2 contains several emergent surfaces, allowing cycles 1 to 6 to be defined (Cózar and Somerville, 2005). The Ballyadams Quarry succession contains the unit 1 and cycles 1 to 4; Clogrenan B Borehole contains cycles 3 to 6 and the base of the Brigantian, and Clogrenan Quarry (5 km south of Carlow), contains the uppermost part of cycle 6 and the entire Brigantian (Figs. 3C, 4A–4B). The

succession includes 13-14 palaeokarsts in total. The upper Asbian in the sections was not formerly subdivided into foraminiferal subzones or assemblages. The total thickness measured in the composite section is about 100 m thick. The foraminiferal database was summarised in Cózar and Somerville (2005) and Somerville and Cózar (2005), with only the most relevant biostratigraphic markers highlighted. More detailed information compiled from notes of the original investigations are included in the Appendices C-E.

2.4. Western Ireland (Aillwee section, Burren)

The succession in the Burren, western Ireland, contains the entire Asbian in the Burren Formation (Gallagher, 1992; Gallagher et al., 2006; Fig. 2), although late Asbian cyclic sedimentation is only represented in the youngest Ailwee Member, where 9 main cycles are recognised, separated by palaeokarsts (T1 to T9) (Fig. 4C). The total thickness of this member is 152 m in natural outcrops of the Aillwee section. The succession was originally subdivided into the Cf6γ1 and Cf6γ2 subzones. The database is based on the original data used by Gallagher et al. (2006), but also incorporates the details in Gallagher (1992). Most of the foraminiferal taxa were identified at genus level, and the species-level data reported were less than 10% of the assemblages, with only occurrence/absence of taxa also published. The data are reproduced in Appendix F.

3. Methodology

Foraminiferal diversity and richness indices of the sections have been generated using the Past4.05 software (https://www.nhm.uio.no/english/research/infrastructure/past/), with the database in

Appendices A to F (supplementary information), corresponding to the foraminiferal records in the above listed publications and regions. Of the many diversity indices available, the Margalef, Simpson, and Shannon-Wiener indices are more popular because of their easy calculation (Jayalakshmy and Kameswara Rao, 2006; Gamito, 2010). The Margalef richness index, D, is displayed particularly in this study, since it is known to respond to basic environmental variables (Li et al., 2019). It is defined as $D=(S-1) / \ln(n)$, where S is the number of species and n is the total number of individuals. The relationships of D to other diversity indices are shown in the supplementary information (Fig. S2). The range of values for single indices vary between sections from Britain and Ireland, a fact that depends on the state of preservation of the assemblages, particular environmental/ecological conditions, as well as species relative abundance. Thus, the Margalef D index in sections from Britain ranges from 1 (low) up to 9 (high) (abscissa axes in Fig. 3), whereas sections in Ireland range from 0 to 6−7 (Figs. 3–4).

Statistical analysis of the diversity indices was performed using R (R Development Core Team, 2005) using the sarima and geoChronR packages (McKay et al., 2021; Boshnakov, 2021). Quantitative correlations used 'sequence slotting' as implemented in CPLSlot (Hounslow and Clark, 2016), based on the methods in Clark (1985) but extended along the principles outlined by Thompson et al. (2012).

4. Do the foraminiferal diversity changes have stratigraphic significance?

To breakdown this question we examine three sub-questions.

1) Are changes random in their stratigraphic ordering? This is evaluated with a statistical assessment in Section 4.1.

2) Can the diversity changes be objectively correlated between sections? This is evaluated using sequence slotting (Gary et al., 2005; Thompson et al., 2012; Wakefield et al., in press) to correlate section data to the reference section at Trowbarrow. The slotting correlation uses only the bases of the foraminiferal subzones as correlation constraints as detailed in Section 4.2. The ability to correlate changes demonstrates evidence of consistent regional stratigraphic ordering.

3) Does the diversity data show rhythmicity and therefore reflect in some way the cyclicity shown to exist in this interval, which have been previously associated primarily with the emergent surfaces? The purpose here is not to demonstrate external forcing of such rhythms but merely to show that cyclicity exists in the foraminiferal diversity data. This is evaluated in Section 4.3.

Lastly, we show in Section 5 that the emergent surfaces provide additional points of correlation, which when integrated with the diversity changes enhance the expression of rhythmicity shown by the foraminiferal diversity data.

4.1. Stratigraphically random diversity data?

Statistical methods of recognising time series which are essentially noise are well developed and diverse (Uyanto, 2020). However, even in a rhythmic dataset, if the sample spacing is too far apart, sampling points will hit randomly points between adjacent oscillations - the so called ‘aliased data’ problem in cyclostratigraphy (Weedon, 1993). For this reason, we apply these tests to the most detailed sampling-that at Trowbarrow Quarry. However, time series methods rely on relating data to time on a regular scale, which we cannot do, so the best that is available using times-series methods is to use our sampling points as a rough proxy for time. The Durbin-Watson

statistic (shown by Uyanto (2020) to be a strongly- performing test), indicates that for all except the Fisher's-alpha index the diversity indices are significantly different from white noise (many with probability <0.01%; Table 2).

Secondly, if there is rhythmic pattern in the diversity data that is available to be sampled (and sampling is not aliased), then adjacent samples should show similarity in values. As a simple measure of consistency between adjacent samples, Hounslow and Morton (2004) used a stratal consistency function (SCF) comprising the Pearson cross-correlation between subsets X(1,...n-1) and X(2,...n) of a stratigraphic variable. This is free from assumptions of sampling regularity. A confidence limit was determined for the SCF values using bootstrap methods, with 10,000 simulations randomly drawn from a normal distribution. We apply this to the Trowbarrow diversity data (Table 2), indicating that most of the diversity indices exceed the 0.1% probability threshold (except Fisher's-alpha), indicating diversity indices are distinctly non-random. A sub-group of these have SCF >0.4, which substantially exceed the 0.1% probability threshold. Both these methods demonstrate the diversity changes are not randomly distributed in the succession.

4.2. Can the diversity changes be objectively correlated between sections?

Sequence slotting is used to quantitatively assess the correlation potential of the diversity changes between the sections. This method correlates section-data against a reference section (here Trowbarrow) and attempts to 'slot' the datasets together, such that it minimises a statistical measure of dissimilarity of the data. Sequence slotting does not utilise height (measured thickness above the base of sections), but only utilises the stratigraphic order of samples. Multiple diversity indices were used to produce a

290 multivariate correlation of the successions. In order to pre-select which diversity indices
291 to use, we selected a sub-set which had SCF >0.4 (Table 2) from the Trowbarrow data.
292 This initial subset of seven was further reduced by eliminating those diversity indices
293 with the larger between-indices cross-correlation, whilst maintaining those with the
294 larger SCF. This pre-selection results in three indices finally chosen, Shannon, Margalef
295 and Log_e (Berger-Parker). These were subsequently used in correlating the Port Eynon,
296 Ballyadams and a Clogrenan composite to Trowbarrow. A Clogrenan composite was
297 produced by joining diversity data from Clogrenan Quarry and Clogrenan B Borehole at
298 the lower of the two correlated emergent surfaces. The Aillwee section was not used,
299 since the data is based on presence- absence only, unlike the other sections. Correlations
300 were constrained using the bases of the foraminiferal subzones. A blocking constraint
301 (Thompson et al., 2012) was also applied which serves to express the differences in the
302 number of sampling points between sections, and also limit the grouping of sample
303 levels, which is an adverse feature of sequence slotting.
304 Two measures of distance in multivariate space were used, Euclidean and city-
305 block (or Manhatten) metrics. The kind of data scaling to apply to the diversity indices
306 is an important issue to evaluate, since this will impact the magnitude of the
307 dissimilarity and relative contributions (to the total distance) from each index used
308 (Gary et al., 2005; Wakefield et al., in press). No-scaling, scaling each index to a mean
309 of zero, or scaling each index to mean of zero and σ of 1 (Zscore scaling) could be used
310 in CPLSlot (that is scaling each index in each section independently- perhaps to remove
311 the effects of variable preservation). Therefore, six slotting models were produced for
312 each correlation-pair, using the two types of metric and the three types of scaling. We
313 classified the goodness of the six correlation models using several types of success

314 statistics (Table 3), and from these produced a summed ranking of the best to worst
315 models (see Supplementary Information for details).
316 Generally, the more successful correlation models produced similar correlation
317 relationships (see Supplementary Information for details). Also, either the mean-zero or
318 Zscore-scaling produced the more successful correlation models and the city-block
319 metric was also preferred in the two top correlation models (except for Trowbarrow-
320 Ballyadams where a Euclidean model was in the top two). For each of the section inter-
321 correlation pairs in Figs. 5-7 the two top-ranked city-block models using either mean-
322 zero or Zscore scaling are shown. Summary statistics from the slotting are shown in
323 Table 4. The Shannon diversity index is not shown in Figs. 5–7, since it is rather similar
324 to the Margalef index, but it is displayed in the SI, along with further details of the
325 slotting.
326 These correlation relationships (Figs. 5–7) demonstrate that quantitative correlation
327 provides good between-section coherent patterns of diversity changes. Differences
328 between correlation models normally occurs where the variations in diversity are rather
329 ambiguous (e.g. above 120 m level in Fig. 6; 170-178 m level in Fig. 7). Notably, the
330 correlations independently suggest that many of the palaeokarsts are near-coeval and so
331 linked to the diversity changes (labelled on right columns in Figs. 5–7). Sequence
332 slotting tends to perform best with roughly equal spacing of sample levels, since the
333 blocking constraint imposes some regularity in the number of samples from each
334 sequence over particular intervals. This imposition may distort the correlations, like in
335 Cf6γ2a at Port Eynon, where sampling density differs to the underlying Cf6γ1b (Fig. 5)
336 in comparison to Trowbarrow. We argue in Section 5 that many palaeokarsts provide
337 additional correlation points and are inferred to be near synchronous, and so enhance the
338 ability of diversity changes to reflect synchronous environmental change.

339

340 *4.3. Does foraminiferal diversity show evidence of rhythmic change?*

341

342 Periodograms were determined for the Margalef index at Trowbarrow, assuming
343 height scale as a proxy of time using two methods (Fig. 8). Firstly, the Lomb-Scargle
344 method which handles the unequally spaced height data (Fig. 8A). Secondly the data
345 were interpolated into equally spaced data at a median spacing of 0.95 m using linear
346 interpolation, and the multi-taper method used (Fig. 8B). This method better represents
347 likely periodicity at smaller periods compared to the Lomb-Scargle method and also
348 limits spectral leakage (McKay et al., 2021). Both the methods suggest significant
349 periodicity at around 11 m, and the multi-taper method, rather stronger periodicity
350 between 4 and 6 m. The 11 m periodicity is broadly related to the average spacing of
351 major palaeokarsts at Trowbarrow, and the smaller periods, rhythmic changes in the
352 intra-palaeokarst diversity.

353

354 **5. Foraminiferal diversity and integration with palaeokarst rhythms**

355

356 To aid description and subdivision, rhythmic changes in the Margalef index are
357 labelled as foraminiferal trends (Ft's) and subdivided into intervals Ft0 to Ft13. These
358 can be recognised in the entire upper Asbian, and mostly coincide with the major
359 palaeokarst rhythms Rh1 to Rh11 which are separated by emergent surfaces (Table 5).
360 This is also borne out by the periodograms (Fig. 8). Foraminiferal trends are recognised
361 on the basis of marked shifts, peaks or changes in the overall trend linked to emergent
362 surfaces in the Trowbarrow Quarry (which in general coincides with major emergent
363 surfaces defined by Horbury, 1987) or to the chronostratigraphical lower and upper

boundaries (early Asbian and Brigantian respectively). Factors such as the density of sampling, diagenesis or even individual richness properties condition the recognition of the Ft's in some sections, as explained in more detail below.

5.1. Trowbarrow Quarry trends (north Lancashire, N England)

Using the major emersion surfaces of Horbury (1987) (Supplementary Figs. S4–S8), biostratigraphic subdivisions, slotting results and the foraminiferal diversity, fourteen foraminiferal trends are recognised in the upper Asbian succession in the quarry (Figure 3A). The transition from the early Asbian to the late Asbian, and in turn to the Brigantian, do not coincide with any emergent surfaces, as they are based on biostratigraphical and lithological criteria (see Cózar et al., in press).

Foraminiferal trend Ft1 coincides with Rh1, the base of which coincides with the base of the Urswick Limestone Formation used by Horbury (1987) and Cózar et al. (in press). The base of the upper Asbian is c. 2.3 m below and thus, Ft0 is present in the uppermost part of the Park Limestone. Ft0 does not contain palaeokarsts or rhythms (Fig. 3A). Foraminiferal trends Ft2 to Ft10 coincide with the rhythms of the same numbers Rh2 to Rh10 (Fig. 3A). The Ft11 to Ft12 coincide in their upper and lower boundaries with those of Rh11, but not with the internal boundaries (Fig. 3A). The interval corresponding to Ft13 and the succession above, was originally considered as part of the Alston Formation by Horbury (1987), and so no rhythm was defined for this part of the succession.

The upper Asbian succession starts at the base of Ft0, which is clearly not a rhythm, because the base is within a continuous succession with a biostratigraphically-defined base (Cózar et al., in press). This interval is characterised by an increase in richness

389 compared with the earlier Asbian, up to the first developed palaeokarst with
390 development of a major clay wayboard.
391 Richness in Ft1 is high in its lower part, and shows a marked decrease in the upper
392 part, but rising again at the top, and contains the occurrence of several minor emergent
393 surfaces (Figs. 3A). Similar patterns are observed in Ft3 and Ft4, whereas Ft2 is mostly
394 a thin interval with low diversity (Fig. 3A). The marked decrease into the upper part of
395 Ft4 could be attributed to the presence of the Woodbine Shale Member (Fig. 3A),
396 although similar decreases are observed in other intervals, as well as in other sections
397 for the same interval. Thus, this shale unit has had a limited impact on the foraminiferal
398 diversity.
399 A progressive decrease occurs in Ft5 and Ft6 with a subsequent slow recovery of
400 diversity in Ft7, never reaching a high value (Figs. 3A). In contrast, the lower part of
401 Ft8 shows a marked peak in diversity and a pronounced decrease in its upper part,
402 similar to the patterns observed in Ft1, Ft3 and Ft4.
403 Trends Ft9 and Ft10 are similar, with both showing more moderate diversity, but a
404 distinctive feature is the decrease in diversity in the middle part of Ft10, followed by a
405 peak in diversity in its upper part (Fig. 3A). This latter kind of variation is shown in
406 Ft11 which is also characterised by a progressive decrease in diversity, interrupted by
407 higher diversity peaks in its upper part.
408 The Ft12 shows a small progressive increase in diversity, which passes upwards
409 into Ft13 reaching maximum diversity in the upper part of Ft13. However, Ft13 also
410 contains strong fluctuations between individual samples, as well as a decrease in
411 diversity in the uppermost samples (Fig. 3A). Ft9 to Ft12 are also characterised by
412 several minor emersion surfaces, mostly occurring in the upper part of each interval.

413 The transition into the Brigantian is marked by a strong increase in diversity and a
414 subsequent decrease. This notable change in the foraminiferal diversity trends suggests
415 that this level corresponds to a major event.
416
417 *5.2. Port Eynon trends (Gower Peninsula, S Wales)*
418
419 The Oxwich Head Limestone Formation, contains the upper Asbian and lower part
420 of the Brigantian strata (Fig. 2), although it has a diachronous upper boundary with the
421 Oystermouth Formation (Cózar and Somerville, 2020). The sampling interval is less
422 dense than in the other regions, leading to more subdued and less confident (more
423 aliased) diversity changes, particularly in the upper part of the succession (Figs. 3B, 5).
424 The first key feature is the apparent absence of Ft0, so that Ft1 rests directly on the
425 lower Asbian Stormy Limestone Formation (Fig. 3B). This fact implies the presence of
426 the first hiatus in the succession– although owing to the poor characterization of the
427 early Asbian, it is not possible to quantify how much is missing. The slotting correlation
428 model at the base of the Cf6γ1a subzone has not inserted this hiatus (Fig. 5), so the base
429 of Cf6γ1a and start of Ft1 at Port Eynon should be rather higher in Ft1 at Trowbarrow
430 (at around 24 m level; Fig. 5). Similar patterns to those recorded in Trowbarrow and
431 with numerous palaeokarsts occur in Ft1, Ft2 and Ft3. At Port Eynon the boundary
432 between Ft2 and Ft3 coincides with shaley mudstones but features of emersion have not
433 been observed.
434 The Ft4 is rather flattened and uniform, and does not exhibit decreasing diversity in
435 the upper part, like that observed at Trowbarrow- this may indicate a missing or
436 condensed upper Ft4 at Port Eynon. The upper part of the succession is poorly sampled,
437 and thus, trends are not so easily recognized, but slotting provides possible relationships

to Trowbarrow (Fig. 5), but the Ft-boundaries can be more confidently identified using the emergent surfaces. In particular, the Ft7 trend does not contain any feature which allows it to be characterized. However, the beginning of Ft5 with a marked decrease in diversity is rather characteristic, and is followed by decreasing diversity during Ft6 (Figs. 3B, 5). An increased diversity in the lower part of the interval and decrease in the upper part is characteristic of Ft8, although it is not clear if this interval is complete.

Directly succeeding the Ft8 trend are Brigantian strata. The Brigantian has a similar profile to that at Trowbarrow, with a prominent diversity increase at the base followed by a gradual decline (Fig. 3B). Thus, it is inferred that the Brigantian is more or less complete from its base at Port Eynon. However, of more significance, a major hiatus in the succession occurs, accounting for the absence of rocks representative of most of the later part of the Cf6γ2a assemblage and the entire Cf6γ2b and Cf6γ2c assemblages. This hiatus also explains why the successions in South Wales contain only a few emergent surfaces compared to those in North Wales, where the emergent surfaces are more numerous.

5.3. Ballyadams-Clogrenan trends (Carlow, southeast Ireland)

The base of the upper Asbian was located at the first palaeokarst in the Ballyadams Quarry (15 km NW of Carlow), at sample 1631 (Fig. 3C) (Cózar and Somerville, 2005). However, there were some problematic taxa below this level such as *Pseudoendothyra sublimis*. Compared with the Trowbarrow Quarry succession, the lower part of the base of a massive limestone bed (at sample 1614) can be attributed to the Ft0 trend (and assigned to the late Asbian), which shows an increased richness compared to the underlying beds (Fig. 3C).

463 Foraminiferal trends Ft1, Ft3 and Ft4 each show similar higher diversity in their
464 lower parts and lower diversity in their upper parts, with a maximum peak in richness in
465 the middle, and decreasing values in the lower and upper parts – much the same pattern
466 as in Trowbarrow (Fig. 6). The trend Ft2 is more difficult to recognise due to the fewer
467 samples in this interval. There are peaks of high and low diversity at samples 1117
468 (high) and 1119 (low), which are attributed to the Ft2 trend (Fig. 3C). In addition, this
469 interval also coincides with the appearance of foraminiferal markers for the Cf6γ1b
470 assemblage (Fig. 6). Nevertheless, this lower part of the succession is characterised by
471 the absence of emergent surfaces, and the boundaries of the Ft intervals are inferred by
472 changes in the diversity and the slotting correlations to Trowbarrow (Figs. 3C, 6).
473 In the Ft5-Ft7 interval, foraminiferal markers of the Cf6γ2a assemblage occur
474 below the minor palaeokarsts in Ft5, and so the base of Ft5 is inferred by the diversity
475 changes and slotting results (Figs. 3C, 6). The correlation to the lower part of Ft5 is
476 readily recognisable in the slotting correlation for both the Margalef and Berger-Parker
477 indices (Fig. 6). However, the upper part of Ft5-lowest Ft6 interval is less clear in the
478 slotting and visual comparison to Trowbarrow (Fig. 6). We interpreted this as a
479 significant hiatus in the upper half of the Ft5 trend, so that Ft6 sits on the lower part of
480 Ft5 across the palaeokarst at the Ft5/Ft6 boundary (Fig. 3C; see supplementary Fig.
481 S16).
482 The Ft8 is recognised by the increase in the lower part and later decrease of
483 diversity. This well-marked variation, enables correlation with the Clogrenan B
484 Borehole succession (Fig. 4A). This contrasts with the original correlation which was
485 considered at the palaeokarst at the top of Ft9 at Ballyadams, with the base of the Ft8 at
486 Clogrenan B (see Cózar and Somerville, 2005).

No obvious change in diversity, and its reduced thickness (ca. 3.5 m), are observed in Ft9 in the Clogrenan B Borehole, whereas in Ballyadams Quarry it contains richer assemblages in the lower part, which decrease to the upper part (Fig. 3C). In Ballyadams Quarry, an emergent surface was not recognized at the base and the position of the trend is recognized by foraminiferal diversity and the slotting correlation.

Similar to Trowbarrow, Ft10 is recognised by lower diversity in the lower half and higher diversity in the upper part (Fig. 7). In both Clogrenan B and Ballyadams, the first occurrence of Cf6γ2b markers are recorded in the mid-parts of Ft10 (Fig. 4A), confirming this correlation.

The lower Brigantian and Ft11 to Ft13 have no marked diversity changes, perhaps because of the low-density sampling, as well as stronger diagenetic effects (i.e. silicification). In Clogrenan B Borehole, diagenesis has had a marked affect, producing lower richness and a more flattened profile. Nevertheless, the upwards decreasing diversity in Ft11, a prominent peak in the upper part of Ft12, and lower diversity for Ft13 before the Brigantian can be observed (Fig. 4A). The bases for Ft11, Ft12 and Ft13 are interpreted to coincide with emergent surfaces. The sequence slotting with respect to Trowbarrow confirms the near synchroneity of the major palaeokarsts in the Cf6γ2a to base Brigantian interval (Fig. 7)

Owing to the poorer preservation of foraminiferal assemblages in Clogrenan B borehole, markers for Cf6γ2c do not occur, and its position is inferred by trends Ft12 and Ft13 and the slotting results. Cf6γ2c markers are identified in the Clogrenan Quarry (Fig. 4B), although less than 3 m of the upper Asbian strata is exposed and is inferred to belong to Ft13. In the Clogrenan Quarry the highest peak in diversity is in the lower Brigantian, which is more weakly expressed in the Clogrenan B Borehole (Figs. 4A–B and 7).

512 The transition into the Brigantian is marked by a prominent palaeokarst, a
513 significant feature in the Clogrenan region, and differences to Trowbarrow are indicated
514 (Fig. 7). These imply that the uppermost part of Ft13 might be missing in the Clogrenan
515 region (see supplementary Fig. S16).
516
517 *5.4. Aillwee trends (Burren, western Ireland)*
518
519 The base of the section seems to replicate the scenario in Port Eynon, with Ft0 and
520 the lower part of Ft1 missing in the basal emergent surface (Fig. 4C). In contrast, the T1
521 cycle includes the remaining parts of Ft1 and all of Ft2, which implies the authors may
522 have either overlooked an intermediate palaeokarst, or just like in Ballyadams Quarry,
523 this emergent surface may not exist in the Burren region. Ft4 appears to display the
524 amalgamation of the T3 and T4 cycles, and thus, the palaeokarst separating both cycles
525 is considered a minor feature. Markers for the Cf6γ1b assemblage are not recognised in
526 the section, and its position is inferred at the base of Ft2, close to the base of the
527 preserved upper Asbian succession (Fig. 4C). Ft4 forms a distinctive convex-shaped
528 peak of higher diversity in its mid-parts, which together with Ft3, forms the interval
529 with the largest overall diversity - similar to that seen in the Trowbarrow Quarry. The
530 other foraminiferal trends from Ft5 to Ft7 are well defined, although both Ft6 and Ft7
531 are included within the T6 cycle. Gallagher et al. (2006) divided cycle 6 into two
532 subcycles (T6A, T6B) and cycle 9 into three subcycles (T9A, T9B and T9C), which
533 were based on prominent bedding planes and pedogenic features, but there was no
534 development of clay wayboards (Fig. 4C). Markers of the Cf6γ2a are recorded in the
535 upper part of Ft7, although these markers likely should first occur at a lower horizon,

536 from Ft5 (shown by the down-pointing arrow in Fig. 4C). Further detailed sampling is
537 required to confirm this mismatch.
538 Trend Ft8 is not well expressed, since it does not display a marked higher diversity
539 as in other sections, although it does contain an overall higher diversity than the
540 preceding Ft5-Ft7 interval. This issue could be a matter of less dense sampling.
541 However, as seen in other sections, Ft8 shows marked richness fluctuations in its upper
542 part. Ft9, Ft10 and Ft11 are rather similar to those in Trowbarrow Quarry, but the lower
543 sampling density at Aillwee Member shows a rather subdued variation, but with
544 fluctuations similar to those observed in other sections. The diversity trends Ft10 and
545 Ft11 are recognised in the sub-cycles T9A and T9B, whereas the uppermost sub-cycle
546 T9C (with only two samples) does not allow inference of the Ft12 boundary. It is
547 possible that sub-cycle T9C might be an intermediate minor palaeokarst in Ft11, similar
548 to that seen at the Trowbarrow and Ballyadams quarries for this part of the succession.
549 The Aillwee Member has only 9 cycles, which implies the absence of Ft13 and also
550 most likely Ft12 in the late Asbian of the Burren region. Missing foraminiferal trends
551 Ft12 and Ft13 could have been eroded at the emergent surface below the base of the
552 Brigantian in the Burren region, forming a notable hiatus in the youngest upper Asbian
553 strata.
554 The foraminiferal response during the transition from the Aillwee Member into the
555 Balliny Member shows a decreasing richness from near its base, reaching lower values
556 than the underlying Aillwee Member (Fig. 4C). We have not observed such low values,
557 except in the Clogrenan B Borehole, where the assemblages were impoverished by
558 silicification.
559
560 *5.5. Stratigraphic and biostratigraphic results*

561

562 The foraminiferal diversity changes and slotting correlations between the regions
563 indicates three consequences:

564 Firstly, the stratigraphy and correlation between some sections can be amended: (i)
565 the lower Asbian is present in Port Eynon, below the upper Asbian where the basal part
566 is absent; (ii) the base of the late Asbian in Ballyadams Quarry is complete and
567 continuous with the early Asbian; and (iii) correlation of the Ballyadams Quarry and
568 Clogrenan B Borehole is amended to a position 19 m below that previously inferred,
569 allowing a more accurate position of the stratigraphic cycles in the sections.

570 Secondly, some foraminiferal assemblages, as indicated by their foraminiferal
571 markers, have been inferred (owing to the lack of the markers), or amended (due to their
572 later first occurrences, specifically: (i) the position of the Cf6γ2a and Cf6γ2c in
573 Clogrenan B Borehole have been inferred; (ii) the position of the Cf6γ1a has been
574 inferred in the Aillwee section; and (iii) the basal position of the Cf6γ2a has been
575 amended in the Aillwee section.

576 Thirdly, some major hiatuses have been detected in the succession: (i) the
577 uppermost lower Asbian-Ft0-basal Ft1 is absent in Port Eynon; (ii) the upper part of Ft4
578 at Port Eynon is absent or is a condensed series; (iii) the Ft9 to Ft13 are missing in Port
579 Eynon; (iv) the upper half of the Ft5 is missing in Ballyadams Quarry; (v) the upper half
580 of the Ft13 is absent in Clogrenan Quarry and Borehole; (vi) Ft0 and lower half of Ft1 is
581 missing in the Aillwee section; (vii) parts of Ft11 (?), Ft12 and Ft13 are absent in the
582 Aillwee section.

583

584 **6. Far-field correlation of emergent surfaces**

585

586 Up to 16 emergent surfaces can be correlated (surfaces 0 to XIII and 0' to VI' in
587 Figs. 9, S3), corresponding to interbasinal palaeokarsts and informally denominated as
588 major palaeokarsts. The remaining palaeokarsts do not have the same lateral continuity,
589 and thus have to be considered as more relevant for intrabasinal correlations and/or are
590 impersistent palaeokarsts.
591
592 *6.1. Palaeokarsts correlation within Britain*
593
594 The correlation between emergent surfaces from north Lancashire and South Wales
595 is rather complete in the lower part of the succession, taking into consideration the
596 limitations of the South Wales successions due to hiatuses. Most of these surfaces can
597 be considered as major palaeokarsts in both regions (Fig. 9B). Notable, is the hiatal gap
598 at the base of the upper Asbian succession in South Wales, which has amalgamated 3 or
599 4 emergent surfaces seen at Trowbarrow, possibly up to the palaeokarsts situated just
600 above the so-called surface 1 (Fig. 3A) of Horbury (1987). Thick palaeosols are only
601 developed at the boundary between Ft3 and Ft4 (Fig. 9B). The two underlying
602 prominent palaeosol horizons observed within the Ft3 interval in Port Eynon are classed
603 as secondary emergent surfaces, whereas the Ft1-Ft2, Ft4-Ft5, Ft5-Ft6 and the inferred
604 Ft6-Ft7 and Ft7-Ft8 boundaries coincide with palaeokarsts without development of
605 thick clay wayboards and palaeosols (Fig. 9B). In total, the rhythms Rh1, Rh4 to Rh7,
606 as well as their respective emergent surfaces are recognised in South Wales, whereas
607 rhythms Rh2 and Rh3 can only be inferred by the position of trends Ft2 and Ft3 (Fig.
608 9B). These rhythms are separated by some pale grey shaley and argillaceous limestones
609 at Port Eynon, where no evidence of emergence is detected, and perhaps further
610 examination of this interval in South Wales will be required to validate this.

In addition, in the upper part of Rh1, another palaeokarst may have its counterpart in Trowbarrow Quarry, and it should be considered also as a major emergent surface (horizon 0'a; Fig. 9B). In the Rh5 rhythm in the Port Eynon section there is one palaeokarst nearly coincident in stratigraphic position with an irregular surface in Trowbarrow situated at 53.5 m, which needs a closer re-examination to determine if they are both genuine subaerial exposures. Horbury (1987, fig. 5.6) recognised a further emergent surface between surfaces 5 and A in other sections in south Cumbria, which may be the lower of these palaeokarsts (see Fig. S5). As will be shown later, they also coincide stratigraphically with an emergent surface in Ireland (surface IV'a in Fig. 9B and their counterpart in Ireland IVa in Fig. 9A).

Because of the large hiatus in the upper part of the upper Asbian in the Port Eynon section, there is a sharp transition into the Brigantian, which is not seen in the more complete succession at Trowbarrow.

In conclusion, up to 8 palaeokarsts (possibly 10) and their associated foraminiferal trends recorded in South Wales can be correlated with horizons in Trowbarrow, ~ 320 km to the north (surfaces 0' to VIII' in Fig. 9B; see supplementary Figs. S4 to S8), suggesting that they should be considered as major emergent surfaces. These palaeokarsts are developed only within the biostratigraphic interval from Cf6γ1a to the lower part of Cf6γ2a. At Port Eynon a few apparently major palaeokarsts in the field, with thick clay wayboards (e.g., horizon above sample 3492; Fig. 9B), do not have equivalents in the SCS, and thus, they have to be considered as minor rhythms. In contrast, most of the correlated emergent surfaces do not present thick development of palaeosols or dramatically undulose karstic features, which confirm that factors such as the state of preservation or quality of exposure have a direct impact on the field interpretation of the surfaces.

636

637 The succession in South Wales is interrupted with significant hiatuses, and it would
638 be desirable to study in more detail the successions in North Wales, comparing
639 foraminiferal diversity with respect to the numerous shallowing-upward cycles defined
640 in that region, such as in the Eglwyseg Limestone Formation of Llangollen (see
641 Somerville, 1977, 1979; Fig. 2).

642 The occurrence of the younger rhythms in North Wales and not in South Wales can
643 be explained if South Wales was emergent land for this time interval, which could be
644 attributed to differential regional tectonics. Indeed complex synsedimentary tectonics
645 were also suggested by Ramsay (1989, 1991) for the South Wales Coalfield during the
646 Carboniferous, but mostly localised in the northerly outcrop belt. Ramsay attributed the
647 limestone cycles to pulsed subsidence followed by marine transgression and the
648 deposition of upward-shoaling and prograding sequences for the Asbian and Brigantian
649 (deposited on a southward-deepening platform). Ramsay (1989) also proposed the
650 correlation of emergent surfaces based on the facies relationships between the northerly
651 and southerly outcrops (including the Gower Peninsula), in which those in the north
652 displayed the largest hiatuses. In contrast, the southerly outcrops contained a more or
653 less continuous succession with minor hiatuses, and therefore, no evidence of major
654 uplift in the latest Asbian. The contrasting interpretation of Ramsay compared to ours, is
655 likely the result of poor biostratigraphic control, because the early Asbian is present in
656 formations traditionally considered as Holkerian (need a reference here), whose base is
657 currently unknown in the region. In addition, the Asbian-Brigantian transition had
658 traditionally been considered as continuous, which is not the case. The Port Eynon
659 Thrust, interpreted as an inverted extensional fault by Ramsay (1989), is one possible
660 cause of the latest Asbian uplift in the Gower Peninsula.

661 An alternative interpretation can be also be proposed, because in our interpretation,
662 lower Asbian rocks are not clearly documented in the cyclic successions of the northerly
663 outcrops, and neither have foraminiferal markers of the Cf6γ2b and Cf6γ2c been
664 documented or illustrated there. In South Wales the northerly outcrops show a similar
665 cyclic succession to those of the south (Ramsay 1989)- which by comparison may be
666 Rh1 to Rh8 rhythms- and hence the biostratigraphic mismatches recognised at Port
667 Eynon in the south may correspondingly also exist in the northerly outcrops. Hence, the
668 major hiatus in the latest Asbian recognised here, may have affected the entire South
669 Wales Coalfield.
670
671 *6.2. Palaeokarst correlations in Ireland*
672
673 The upper part of the Ballyadams Formation shows good correlations with some of
674 the Trowbarrow Quarry emergent surfaces, from rhythm Rh6 up into the Brigantian,
675 and thus, all of them can be considered as major palaeokarsts. There is also an
676 intermediate palaeokarst in rhythm Rh11 (Xa) which also seems be present in the
677 Trowbarrow Quarry (see surfaces IVa to XII in Figs. 7, 9A). Rhythm Rh10 is
678 recognised from the palaeokarst separating Ft10 and Ft11. One of the most striking
679 levels of correlation is that using the base of rhythm Rh9 (recognizable in Ft9), which in
680 Ballyadams Quarry is not expressed as an emergent surface, but occurs in the near-by
681 correlation to Clogrenan B Borehole (Fig. 9A). It is assumed that a closer re-
682 examination of the quarry at this position may allow recognition of a karstic feature. At
683 intermediate positions within Ft5 at both Port Eynon and Ballyadams Quarry, there is a
684 palaeokarst (surface IVa in Fig. 9A) which could also be a major emergent surface, with
685 possible interbasinal correlation. The base of the Ballyadams Quarry mimics the

686 diversity succession at the base of the Trowbarrow Quarry, with a continuous
687 foraminiferal recording of the transition between the lower and upper Asbian, with a
688 basal Ft0, overlaid by a major emergent surface (Fig. 6). In total, 10 surfaces (possibly
689 12) could be correlated between the Carlow and Trowbarrow regions.
690 The section in the Burren region shows a more or less continuous lower and middle
691 part of the succession, where the rhythms Rh3 to Rh11 can be well correlated, mostly
692 with the Trowbarrow Quarry, with only the emergent surfaces within trends Ft1 and Ft2
693 not recognised in the field (Fig. 9A). At Aillwee, the base of the upper Asbian seems to
694 be a hiatus, missing Ft0 and the lower part of Ft1 (a similar situation to the Port Eynon
695 section). In total, 9 emergent surfaces (possibly 10) are correlated with northern
696 England (> 440 km to the east; Fig. 1). The major palaeokarsts from Ft5 to the top-most
697 Asbian, can be also correlated with the Clogrenan region (Fig. 9A).
698 Significantly, from the middle part of Ft1 to the base of Ft5 in the Ballyadams
699 Formation, there are no emergent surfaces recognised (see Cózar and Somerville, 2005).
700 The absence of palaeokarsts in this lower part of the formation was also documented by
701 Gallagher et al. (2006), a little further to the south in Callan, County Kilkenny (Fig. 1).
702 This absence is rather puzzling, when taking into account the laterally equivalent
703 formations in north County Cork (Ballyclogh Formation) and in the Burren (Aillwee
704 Member of the Burren Formation), which both show a marked cyclicity from the base
705 of the late Asbian (Gallagher, 1996; Gallagher and Somerville, 2003; Gallagher et al.,
706 2006) (Fig. 2). These formations show similar facies as in the Ballyadams Formation,
707 but with palaeokarsts.
708 There are three possible explanations: (1) that the Clogrenan and Callan regions
709 (where the Ballyadams Formation is represented) corresponds to a slightly deeper-water
710 facies than in other regions of the so-called Southern Irish Platform (Gallagher, 1996;

711 Fig. 1); (2) that the Clogrenan/Callan region corresponds to shallower-water settings,
712 and that most of the clays, pebbles and other lithological features typical of emergence
713 were winnowed by wave or tides and hence not preserved; and (3) local tectonics
714 influenced the Clogrenan/Callan region, allowing higher rates of tectonic subsidence
715 preventing the emergence of the cycle tops.
716 The first hypothesis does not seem to be realistic, considering that basinal facies
717 surrounding the Southern Irish Platform are distant from this region, but in the Dublin
718 Basin, Shannon Trough and South Munster Basin (Fig. 1); whereas North Cork is
719 located on a topographic high between the Shannon Trough and South Munster Basin,
720 and the Burren (Aillwee section) is on the northern border of the Shannon Trough (Fig.
721 1). Re-examination of the Ballyadams Formation might discover possibly overlooked
722 emergent surfaces, but such surfaces have not been previously recognised, which argues
723 against the second hypothesis. Therefore, the third hypothesis, local tectonics, seem to
724 be the most feasible factor controlling the absence of emergent surfaces, although
725 foraminiferal diversity trends are well preserved. Thus, tectonics is possibly the main
726 factor controlling the subsidence rates between both regions in Ireland, where the
727 Burren section nearly duplicates the thickness in the Carlow region (Fig. 9A).
728
729 **7. Discussion**
730
731 It is difficult to determine, precisely, the origin of the foraminiferal trends (Ft's).
732 The wide recognition of these trends implies a general controlling factor, whereas local
733 factor(s) affecting individual sections, intervals or levels cannot be completely
734 discarded.

From a biological point of view, using the criteria proposed by Stanley (1990), foraminifers show a simple behaviour and high dispersal ability (Groves and Lee, 2008), and also probably a broad environmental tolerance within the shallow-water carbonate platform. These three factors in other fossil groups characterise a low rate of origination/extinction, and thus, do not facilitate the alternation between large and small populations. Thus, the richness peaks and falls are best interpreted as having been controlled by habitat fragmentation, a factor controlled exclusively by extrinsic factors.

A direct relationship between the Ft's and the facies is not recognized either, because the diversity indices are similar in sections with distinctly differing facies, as can be demonstrated even between geographically close sections, such as the Ballyadams Quarry and the Clogrenan B Borehole (see details of facies in Cózar and Somerville, 2005).

The presence of emergent surfaces, and the implied periods of emergence, do not show a correlation with the diversity indices, because the Ft's can be recognized in sections unaffected by emergent surfaces, or at least, less conditioned by them. However, the major palaeokarst spacing at Trowbarrow is clearly reflected in some periodicity in the diversity data (Fig. 8). The Ft's are also recognised in the Archerbeck Beds of the Archerbeck Borehole in Scotland (Fig. 1) (using foraminiferal data from Cózar and Somerville, 2013), whereas they are more poorly recognised, but present, in the Rookhope Borehole of the Alston Block (utilising foraminiferal data from Cózar and Somerville, 2004), and in the Silverdale Borehole of the southern Askrigg Block (utilising foraminiferal data from Waters et al., 2017) (Fig. S9). In the latter two boreholes, the sampling density is sparse, which impacts the poorer recognition of each cycle, as well as the occurrence of common barren horizons.

759 Tectonics is another potential factor, as a trigger for some of the cycles. In this
760 study, it has been demonstrated that the Ft's can also be identified in parts of the
761 sections where a larger tectonic control was presupposed, such as in the lower part of
762 the Ballyadams Quarry and the lower rhythms in the Trowbarrow Quarry (as proposed
763 by Horbury, 1989). Thus, tectonics are not directly controlling the occurrence of the
764 Ft's.
765 Horbury and Adams (1996) proposed a subdivision of the rhythms in the Urswick
766 Limestone Formation into base/middle/top, depending on lithological and
767 palaeontological features, with each part of the rhythms also characterised by lowstand,
768 transgressive and highstand system tracts. When defining these intervals in the
769 Trowbarrow Quarry and adding the regional/local first occurrences and disappearances
770 of the foraminifers, a direct relationship between these parameters and the richness
771 values is not apparent (Fig. 10). Dismissing the previously discussed factors such as
772 biological/intrinsic, environmental/facies, ecological, emergent surfaces and time
773 exposure issues, and tectonics on the foraminiferal diversity- the most likely control on
774 the Ft's seems to be glacioeustasy.
775 One reason for this is new regional occurrences happen most often during the
776 lowstand and transgressive phases of the high-frequency rhythms (for a relatively small
777 number of samples) (Fig. 10; Table 6).
778 Secondly, in relation to the phase of each cycle, there is a decreasing number of
779 regional occurrences from the base to the top of the cycles (ratio's 0.51 to 0.23; Table
780 6). The highest proportion of new local occurrences is observed in the base of the cycles
781 (ratio 1.16) and in the transgressive phase (ratio of 1.24). This situation corresponds
782 with the classical understanding of foraminiferal renovation (in the sense of Conil and
783 Lys, 1977), in which faunal renovation was produced at the transgressive phase of the

784 main event which separated the main stages or substages - similar to the Mesothems
785 described by Ramsbottom (1977), but with higher frequency cyclicity. As suggested by
786 this model, the highest concentration of new occurrences would be observed at the base
787 of the Cf6γ1a assemblage (Fig. 10), equivalent to the base of the so-called Mesothem
788 5B. However, this is not observed at the base of the Brigantian. In addition, there are
789 common new occurrences throughout the section and in different parts of the rhythms,
790 that might be the result of particular ecological conditions.
791 A third reason which supports glacioeustatic control is that fluctuations in the
792 foraminiferal diversity are more or less observed in other upper Asbian successions in
793 England and Scotland. In contrast, in lower Asbian rocks, such as the Little Asby
794 section in northern England (using foraminiferal data in Strank, 1981) or in the lower
795 part of the Ballyadams Formation in the Tankardstown Borehole, southeast Ireland
796 (using unpublished data of the authors), the diversity profiles are rather subdued.
797 Nevertheless, in these carbonates some typical peaks and troughs are observed, but not
798 ordered in trends (Fig. S9).
799 Groves and Lee (2008) and Groves and Yue (2009) proposed that accelerated rates
800 of origination in the Palaeozoic foraminifers were mostly due to the higher-amplitude
801 glacioeustasy, which repeatedly disrupted the shallow-water environments. Thus, the
802 best explanation for the Ft's and the high-frequency rhythmicity of the Urswick
803 Limestone and other analysed sections in Britain and Ireland is a glacioeustatic control
804 on the platform successions.
805 However, the precise relationship between glacioeustasy and the foraminiferal
806 diversity needs to be further investigated (merged oceans waters, variation in nutrient
807 inputs, temperature, salinity, alkalinity, etc.), and explanations do not seem as simple as
808 previous authors have proposed.

809 The foraminiferal trends in the late Asbian (in some way related to glacioeustasy),
810 and the different glacioeustatic models proposed by previous authors for Britain (e.g.,
811 Barnett et al., 2003), supports the concept of high-amplitude sea-level fluctuations
812 during severe phases of glaciation (Smith and Read, 2000; Wright and Vanstone, 2001;
813 Barnett et al., 2003; Bishop et al., 2009; Eros et al., 2012; Fielding and Frank, 2015;
814 Montañez, 2021). Records of emergent surfaces in carbonates are the best approach to
815 determining sea-level changes in low latitude regions. From the onset of cyclic
816 sedimentation, an increase in the average thickness of the cycles has been observed in
817 USA and Britain (Smith and Read, 2000; Wright and Vanstone, 2001; Fielding and
818 Frank, 2015). Smith and Read (2000) described cyclicity from the base of the
819 Chesterian Substage, and interpreted it to correspond with the Brigantian (old Belgian
820 subzone V3c). This would coincide with levels recognized in Scotland (Fielding and
821 Frank, 2015), whereas, in northern England the initial cyclicity was positioned at the
822 base of the Asbian (Wright and Vanstone, 2001; Barnett et al, 2002). However, as has
823 been demonstrated for many platform successions in Britain (e.g., Cózar and
824 Somerville, 2020; Waters et al., 2021; Cózar et al., in press), biostratigraphic revision of
825 cyclic successions suggests that cyclicity started at the base of the late Asbian, whereas
826 the lower Asbian is composed of largely non-cyclic carbonates. On the other hand, at
827 the base of the Chesterian (the Ste. Genevieve Formation in Illinois and Battleship
828 Wash Formation in Nevada), correlated with the Mikhailovian Substage (Lane and
829 Brenckle, 2005; Bishop et al., 2009), and from lower levels, these formations contain
830 typical foraminifers and conodonts which can be correlated with the late Asbian (Cózar
831 and Somerville, 2014; Cózar et al. in press). A negative shift in the $\delta^{18}O_{apatite}$ in the late
832 Viséan of northern Ireland also suggests an overall global cooling (Barham et al., 2012),
833 although the supposed base for the Asbian in northern Ireland (the Glencar Limestone

834 Formation) should be considered mostly as late Asbian (see Aretz et al., 2010, and
835 references therein). The lack of biostratigraphic precision has induced many of these
836 false mismatches with the onset of high-amplitude sea-level fluctuations in low latitude
837 regions. In reality, the onset of the main phase of cooling of the LPIA, and subsequent
838 high-amplitude sea-level changes, probably coincide in these regions, and this is likely
839 situated at the base of the late Asbian, similar to that in the Maritimes Provinces of
840 Canada (Giles, 2009).
841
842 **8. Conclusions**
843
844 Despite differences of preservation, richness and taxonomic criteria for the
845 recognition of species, there is a marked pattern of foraminiferal diversity that is
846 consistent for the upper Asbian strata between northern England, South Wales and
847 southeast and western Ireland. These patterns can be divided in intervals, referred to as
848 Foraminiferal trends (Ft's), of which fourteen have been defined for the late Asbian (Ft0
849 to Ft13), in the most complete succession in the Trowbarrow Quarry section (north
850 Lancashire). The foraminiferal trends allow the repositioning of biostratigraphic
851 mismatches due to the paucity of data and are an additional powerful tool for
852 intersection correlation (especially those with poorer exposures). These also allow the
853 recognition of potentially chronostratigraphic boundaries, based on biostratigraphy and
854 key emergent surfaces. The relationships and inferred correlations of Ft's allow
855 sedimentary gaps to be inferred at the base of the late Asbian in western Ireland and
856 South Wales. These also allow recognition of major gaps in the upper parts of the
857 successions in both regions, as well as the chronostratigraphic repositioning of

foraminiferal subzones in the western Ireland succession and the Clogrenan B borehole (in southeast Ireland).

Both minor and major emergent surfaces can be distinguished uniting the Ft intervals with the cycles and rhythms (Rh) defined by previous authors. The combined Ft's and Rh's units give additional information on the likely dominant factors controlling the cycles, providing a new perspective for the analysis of tectonics, differential subsidence rates, glacioeustacy and facies progradation of the studied sections. It may be also possible to establish a cyclostratigraphy for the region, if it can be shown they are driven by astronomical forcing. In total, sixteen major palaeokarstic surfaces have been correlated between different basins separated by hundreds of kilometres (Fig. 9), emphasizing their lateral continuity.

Supplementary data to this article can be found online at…….

Declaration of Competing Interest

The authors declare that they have not known competing financial interest or personal relationship that could have appeared to influence the work reported in this paper.

Acknowledgements

We would like to thank Galina Nestell, Paul Wright and an anonymous reviewer for their constructive comments. PC and IC were funded by the Ministerio de Ciencia e

882 Innovación (grant PID2021-124596NB-I00) and MWH was part funded by NERC
883 (grant NE/P00170X/1).
884
885

886 **References**

887 Abdi, H. 2010. Congruence: Congruence coefficient, Rv- coefficient and Mantle
888 Coefficient, in: Salkind, N. (Ed.) Encyclopaedia of Research Design, Thousand
889 Oaks, CA: Sage
890 Aretz, M., Herbig, H.-G., Somerville, I.D., Cózar, P. 2010. Rugose coral biostromes in
891 the late Viséan (Mississippian) of NW Ireland: Bioevents on an extensive carbonate
892 platform. Palaeogeogr. Palaeoclimatol. Palaeoecol. 292, 488–506.
893 Aretz, M., Nudds, J.R. 2005. The coral fauna of the Holkerian/Asbian boundary
894 stratotype section (Carboniferous) at Little Asby Scar (Cumbria, England) and its
895 implications for the boundary. Stratigraphy 2, 167–190.
896 Ashckenazi-Polivoda, S., Edelman-Furstenberg, Y., Almogi-Labin, A., Benjamini, C.
897 2010. Characterization of lowest oxygen environments within ancient upwelling
898 environments: benthic foraminifera assemblages. Palaeogeogr. Palaeoclimatol.
899 Palaeoecol. 289, 134–144.
900 Athersuch, J., Strank, A.R.E. 1989. Foraminifera and Ostracods from the Dinantian
901 Woodbine Shale and Urswick Limestone, South Cumbria, U.K. J. Micropalaeontol.
902 8, 9–21.
903 Barham, M., Murray, J., Joachimski, M.M., Williams, D.M. 2012. The onset of the
904 Permo-Carboniferous glaciation: reconciling global stratigraphic evidence with
905 biogenic apatite $\delta^{18}O$ records in the late Viséan. J. Geol. Soc. London 169, 119–122.
906 Barnett, A.J., Burgess, P.M., Wright, V.P. 2002. Icehouse world sea-level behaviour
907 and resulting stratal patterns in late Visean (Mississippian) carbonate platforms:
908 integration of numerical forward modelling and outcrop studies. Basin Res. 14, 417–
909 438.

910 Berry, J.R. 1984. The sedimentology and diagenesis of the Asbian limestones of north
911 Derbyshire. Ph.D. University of Aberdeen, 560 pp.
912 Bishop, J.W., Montañez, I.P., Gulbranson, E.L., Brenckle, P.L. 2009. The onset of mid-
913 Carboniferous glacio-eustasy: Sedimentologic and diagenetic constraints, Arrow
914 Canyon, Nevada. Palaeogeogr. Palaeoclimatol. Palaeoecol. 276, 217–243.
915 Boshnakov, G.N., 2021. Autocorrelations and white noise tests. https://cran.r-
916 project.org/web/packages/sarima/index.html
917 Clark, R.M. 1985. A FORTRAN Program for constrained sequence-slotting based on
918 minimum combined path length. Comp. Geosci, 11**,** 605–617.
919 Conil, R., Lys, M. 1977. Les transgressions dinantiennes et leur influence sur la
920 dispersion et l'évolution des foraminifères. Mém. Inst. Géol. Univ. Louvain 29, 9–55.
921 Conil, R., Longerstaey P.J., Ramsbottom, W.H.C. 1980. Matériaux pour l´étude
922 micropaléontologique du Dinantien de Grande-Bretagne. Mém. Inst. Géol. Univ.
923 Louvain 30, 1–187 (imprinted 1979).
924 Cózar, P., Somerville, I.D. 2004. New algal and foraminiferal assemblages and evidence
925 for recognition of the Asbian–Brigantian boundary in northern England. Proc. York.
926 Geol. Soc. 55, 43–65.
927 Cózar, P., Somerville, I.D. 2005. Stratigraphy of Upper Viséan rocks in the Carlow
928 area, southeast Ireland. Geol. J. 40, 35–64.
929 Cózar, P., Somerville, I.D. 2013. The Carboniferous Archerbeck Borehole, near
930 Canonbie (Dumfriesshire, southern Scotland): biostratigraphic revision of the late
931 Asbian to early Pendleian succession using foraminiferans and regional correlations.
932 Earth Environ. Sci. Trans. R. Soc. Edinb. 103, 105–122.

933 Cózar, P., Somerville, I.D. 2014. Latest Viséan-Early Namurian (Carboniferous)
934 foraminifers from Britain: implications for biostratigraphic and glacioeustatic
935 correlations. Newsl. Stratigr. 47, 355–367.
936 Cózar, P., Somerville, I.D. 2020. Foraminifers in upper Viséan-lower Serpukhovian
937 limestones (Mississippian) from South Wales: regional correlation and implications
938 for British foraminiferal zonal schemes. Proc. York. Geol. Soc. 63, pgys2020-009,
939 https://doi.org/10.1144/pygs2020-009
940 Cózar, P., Somerville, I.D., Hounslow M.W., Kamenikova, T. in press. Proposal of a
941 late Asbian (Mississippian) stratotype for England: Trowbarrow Quarry, S. Cumbria,
942 UK. Pap. Palaeontol. https://doi.org/10.1002/spp2.1451
943 Davies, J.R. 1983. Stratigraphy, sedimentology and Palaeontology of the Lower
944 Carboniferous of Anglesey. Ph.D. Thesis, University of Keele, 2 volumes, 326 pp. +
945 169 pp.
946 Davies, J.R. 1991. Karstification and pedogenesis on a late Dinantian carbonate
947 platform, Anglesey, North Wales. Proc. Yorks. Geol. Soc. 48, 297–321.
948 Dean, M.T., Browne, M.A.E., Waters, C.N., Powell, J.H. 2011. A lithostratigraphical
949 framework for the Carboniferous successions of Northern Great Britain (onshore).
950 HMSO, British Geological Survey Research Report, RR/10/07, London, 174 pp.
951 Eberli, G.P. 2013. The uncertainties involved in extracting amplitude and frequency of
952 orbitally driven sea-level fluctuations from shallow-water carbonate cycles.
953 Sedimentology 60, 64–84.
954 Eros, J.M., Montañez, L.P., Osleger, D.A., Davydov, V.I., Nemyrovska, T.I., Poletaev,
955 V.I., Zhykalyak, M.V. 2012. Sequence stratigraphy and onlap history of the Donets
956 Basin, Ukraine: Insight into Carboniferous icehouse dynamics. Palaeogeogr.
957 Palaeoclimatol. Palaeoecol. 313-314, 1–25.

958 Fielding, C.R., Frank, T.D. 2015. Onset of the glacioeustatic signal recording late
959 Palaeozoic Gondwanan ice growth: New data from palaeotropical East Fife,
960 Scotland. Palaeogeogr. Palaeoclimatol. Palaeoecol. 426, 121–138.
961 Gallagher, S.J. 1992. Lithostratigraphy, biostratigraphy and palaeoecology of Upper
962 Dinantian platform carbonates in parts of southern and western Ireland. Ph.D. thesis,
963 University College Dublin (National University of Ireland), 503 pp.
964 Gallagher, S.J. 1996. The stratigraphy, and cyclicity of late Dinantian platform
965 carbonates in parts of southern and western Ireland, in: Strogen, P. Somerville, I.D.,
966 Jones, G.LL. (Eds.), Recent Advances in Lower Carboniferous Geology (Eds),
967 Geological Society, London, Special Publications, 107, Oxford, pp. 239–251.
968 Gallagher, S.J., Somerville, I.D. 1997. Late Dinantian (Lower Carboniferous) platform
969 carbonate stratigraphy of the Buttevant area North Co. Cork, Ireland. Geol. J. 32,
970 313–335.
971 Gallagher, S.J., Somerville, I.D. 2003. Lower Carboniferous (Late Viséan) platform
972 development and cyclicity in southern Ireland: foraminiferal biofacies and lithofacies
973 evidence. Riv. Ital. Paleontol. Stratigr. 109, 152–165.
974 Gallagher, S.J., MacDermot, C.V., Somerville, I.D., Pracht, M., Sleeman, A.G. 2006.
975 Biostratigraphy, microfacies and depositional environments of Upper Viséan
976 limestones from the Burren region, County Clare, Ireland. Geol. J. 41, 61–91.
977 Gamito, S. 2010. Caution is needed when applying Margalef diversity index. Ecol.
978 Indic. 10, 550–551.
979 Gary, A.C., Johnson, G.W., Ekart, D.D., Platon, E. and Wakefield, M.I. 2005. A method
980 for two-well correlation using multivariate biostratigraphical data. in; Powell, A.J.
981 and Riding, J.B. (Eds) Recent Developments in Applied Biostratigraphy. The

982 Micropalaeontological Society, Special Publications, pp205-217.
983 https://doi.org/10.1144/TMS001.12
984 George, T.N., Johnson, G.A.L., Mitchell, M., Prentice, J.E., Ramsbottom, W.H.C.,
985 Sevastopulo, G.D., Wilson, R.B. 1976. A correlation of Dinantian rocks in the
986 British Isles. HMSO, Geological Society London, Special Report **7**, 87 pp.
987 Giles, P.S., 2009. Orbital forcing and Mississippian sea level change: time series
988 analysis of marine flooding events in the Viséan Windsor Group of eastern Canada
989 and implications for Gondwana glaciation. Bull. Can. Petrol. Geol. 57, 449–572.
990 Gray, D.I. 1981. Lower Carboniferous carbonate palaeoenvironments in North Wales.
991 Ph.D. Thesis, University of Newcastle, 524 pp.
992 Groves, J.R., Lee, A. 2008. Accelerated rates of foraminiferal origination and extinction
993 during the Late Paleozoic ice age. J. Foram. Res. 38, 74–84.
994 Groves, J.R., Yue, W. 2009. Foraminiferal diversification during the late Paleozoic ice
995 age. Paleobiology 35, 367–392.
996 Heckel, P. H. 2004. Chairman's column. Newsl. Carbonif. Stratigr. 22, 1–4.
997 Horbury, A.D. 1987. The sedimentology of the Urswick Limestone in south Cumbria
998 and north Lancashire. Ph.D. thesis, University of Manchester, 668 pp.
999 Horbury, A.D. 1989. The relative roles of tectonism and eustacy in the deposition of the
1000 Urswick Limestone in south Cumbria and north Lancashire, in: Arthurton, R.S.,
1001 Gutteridge, P. and Noland, S.C. (Eds.), The role of tectonics in Devonian and
1002 Carboniferous sedimentation in the British Isles, Yorkshire Geological Society
1003 Occasional Publication, 6, York, pp. 153–169.
1004 Horbury, A.D., Adams A.E. 1996. Microfacies associations in Asbian carbonates: an
1005 example from the Urswick Limestone Formation of the southern Lake District,
1006 northern England, in: Strogen, P. Somerville, I.D., Jones, G.LL. (Eds.), Recent

1007 Advances in Lower Carboniferous Geology, Geological Society, London, Special
1008 Publications, 107, Oxford, pp. 221–238.
1009 Horbury, A.D., Qing, H. 2004. ‘Pseudobreccias’ revealed as calcrete mottling and
1010 bioturbation in the late Dinantian of southern Lake District, UK. Sedimentology 51,
1011 19–38.
1012 Hounslow, M.W. and Clark, R.M., 2016. CPLSlot a program for objective correlation
1013 between successions using sequence slotting.
1014 https://doi.org/10.13140/RG.2.2.17513.29288.
1015 Hounslow, M.W. and Morton, A.C., 2004. Evaluation of sediment provenance using
1016 magnetic mineral inclusions in clastic silicates: comparison with heavy mineral
1017 analysis. Sed. Geol. 171, 3–36.
1018 Jayalakshmy, K.V., Rao, K.K. 2006. Aspects of the biodiversity of brackish water
1019 foraminifera. Environ. Forensics 7, 353–367.
1020 Jones, G.LL., Somerville, I.D. 1996. Irish Dinantian biostratigraphy: practical
1021 application, in: Strogen, P. Somerville, I.D. and Jones, G.LL. (Eds.), Recent
1022 Advances in Lower Carboniferous Geology, Geological Society, London, Special
1023 Publications, 107, Oxford, pp. 253–262.
1024 Josse, J., Pagès, J. and Husson, F., 2008. Testing the significance of the RV
1025 coefficient. CSDA 53, 82–91.
1026 Lane, H.R., Brenckle, P.L. 2005. Type Mississippian subdivisions and biostratigraphic
1027 succession, in: Heckel, P.H. (Ed.), Stratigraphy and Biostratigraphy of the
1028 Mississippian Subsystem (Carboniferous System) in its Type Region, the Mississippi
1029 Valley of Illinois, Missouri, and Iowa. Illinois State Geological Survey Guidebook,
1030 34, pp. 76–105.

1031 Li, M., Lei, Y., Li, T., Jian, Z. 2019. Impact of temperature on intertidal foraminifera:
1032 Results from laboratory culture experiment. J. Exp. Mar. Biol. Ecol. 520,
1033 https://doi.org/10.1016/j.jembe.2019.151224
1034 Manifold, L., Hollis, C., Burgess, P. 2020. The anatomy of a Mississippian (Viséan)
1035 carbonate platform interior, UK: Depositional cycles, glacioeustasy and facies
1036 mosaics. Sed. Geol. 401, https://doi.org/10.1016/j.sedgeo.2020.105633
1037 McKay, N.P., Emile-Geay, J. and Khider, D., 2021. geoChronR–an R package to
1038 model, analyze, and visualize age-uncertain data. Geochronology 3, 149–169
1039 Montañez, I.P. 2021. Current synthesis of the penultimate icehouse and its imprint on
1040 the Upper Devonian through Permian stratigraphic record, in: Lucas, S. G.,
1041 Schneider, J. W., Wang, X., Nikolaeva, S. (Eds.), The Carboniferous Timescale.
1042 Geological Society, London, Special Publications 512,
1043 https://doi.org/10.1144/SP512-2021-124
1044 R Development Core Team, 2005. R: A language and environment for statistical
1045 computing. R Foundation for Statistical Computing, Vienna, Austria. ISBN 3-
1046 900051-07-0, http://www.R-project.org.
1047 Ramsay, A.T.S. 1989. Tectonics and sedimentation of Late Dinantian limestones in
1048 South Wales, in: Arthurton, R.R., Gutteridge, P. and Nolan S.C. (Eds.), The role of
1049 tectonics in Devonian and Carboniferous sedimentation in the British Isles,),
1050 Yorkshire Geological Society occasional publication 6, Leeds, pp. 225–241.
1051 Ramsay, A.T.S. 1991. Sedimentation and tectonics in the Dinantian limestones of South
1052 Wales, in: Macdonald, D.I.M. (Ed.), Sedimentation, Tectonics and Eustasy – Sea-
1053 level changes at active margins. International Association of Sedimentologists,
1054 Special Publication 12, Oxford, pp. 485–511.

1055 Ramsbottom, W.H C. 1977. Major cycles of transgression and regression in the
1056 Namurian. Proc. York. Geol. Soc. 41, 261–291.
1057 Riley, N.J. 1993. Dinantian (Lower Carboniferous) biostratigraphy and
1058 chronostratigraphy in the British Isles. J. Geol. Soc. London 150, 427–446.
1059 Rose, W.C.C., Dunham, K.C. 1977. Geology and Hematite deposits of South Cumbria.
1060 Economic Memoir of the Geological Survey of Great Britain, Sheets 58 and part of
1061 48. HMSO, London, 170 pp.
1062 Smilde, A.K., Kiers, H.A.L., Bijlsma, S., Rubingh, C.M. and van Erk, M.J. 2009.
1063 Matrix correlations for high-dimensional data: the modified RV-coefficient.
1064 Bioinformatics 25, 401–405
1065 Smith, L.B., Read, J.F. 2000. Rapid onset of late Paleozoic glaciation on Gondwana:
1066 evidence from Upper Mississippian strata of the Mid-continent, United States.
1067 Geology 28, 279–282.
1068 Somerville, I.D. 1977. The sedimentology and stratigraphy of the Dinantian limestones
1069 in the Llangollen area and east of Clwydian range, North Wales. Ph.D., Queen's
1070 University of Belfast, 234 pp.
1071 Somerville, I.D. 1979. Minor sedimentary cyclicity in late Asbian (upper D1)
1072 Limestones in the Llangollen district of North Wales. Proc. Yorks. Geol. Soc. 42,
1073 317–342.
1074 Somerville, I.D., Cózar, P. 2005. Late Asbian to Brigantian (Mississippian) foraminifera
1075 from south–east Ireland: Comparison with Northern England assemblages. J.
1076 Micropalaeont. 24, 131–142.
1077 Stanley, S.M. 1990. The general correlation between rate of speciation and rate of
1078 extinction: fortuitous causal linkages, in: Ross, R.M., Allmon, W.D. (Eds.), Causes

of evolution: a paleontological perspective. University of Chicago Press, Chicago, pp. 103–127.

Strank, A.R.E. 1981. Foraminiferal biostratigraphy of the Holkerian, Asbian and Brigantian stages of the British Lower Carboniferous. Ph.D. Thesis, University of Manchester, 391 pp

Thompson, R., Clark, R.M. and Boulton, G.S. 2012. Core correlation. in; Birks, H.J.B., Lotter, A.F., Juggins, S. and Smol, J.P (Eds) Tracking environmental change using lake sediments. Springer, Dordrecht. pp. 415–430.

Uyanto, S.S., 2020. Power comparisons of five most commonly used autocorrelation tests. Pakistan J., Stat, Oper.Res. 16 119-130.

Vanstone, S. 1994. Late Dinantian palaeokarst of England and Wales: implications for exposure surface development. Sedimentology 45, 19–37.

Vanstone, S. 1996. The influence of climatic change on exposure surface development: a case study from the Late Dinantian of England and Wales, in: Strogen, P. Somerville, I.D. and Jones, G.LL. (Eds.), Recent Advances in Lower Carboniferous Geology. Geological Society, London, Special Publications, 107, Oxford, pp. 281–302.

Wakefield, M.I., Hounslow, M.W., Edgeworth, M., Marshall, J.E.A. Mortimore, R.N. Newell, A.J., Ruffell, A., Woods. M.A. in press. Chapter 17: Examples of correlating, integrating and applying stratigraphy and stratigraphical methods, in: Coe, A.L. (Ed.), Deciphering Earth's history: the practice of stratigraphy. The Geological Society press.

Walkden, G. Davies, J. 1983. Polyphase erosion of subaerial omission surfaces in the Late Dinantian of Anglesey, North Wales. Sedimentology 30, 861–878.

Waters, C.N., Cózar, P., Somerville, I. D., Haslam, R.B., Millward, D. Woods, M. 2017. Lithostratigraphy and biostratigraphy of Lower Carboniferous (Mississippian) carbonates of the southern Askrigg Block, North Yorkshire, UK. Geol. Mag. 154, 305–333.

Waters, C.N., Waters, R.A., Barclay, W.J., Davies, J.R., Jones, N.S., Cleal, C.J. 2011. Chapter 5. South Wales, in: Waters, C.N., Somerville, I.D., Jones, N.S. et al. (Eds.), A revised correlation of Carboniferous rocks in the British Isles. The Geological Society, London, Special Report 26, pp. 29–36.

Waters, C.N., Burgess, I.C., Cózar, P., Holliday, D.W. Somerville, I.D. 2021. Reappraisal of Arundian–Asbian successions of the Great Scar Limestone Group across northern England. Proc. York. Geol. Soc. 63, https://doi.org/10.1144/pygs2021-002.

Weedon, G.P., 2003. Time-series analysis and cyclostratigraphy: examining stratigraphic records of environmental cycles. Cambridge University Press.

Wright, V.P. 1994. Paleosols in shallow marine carbonate sequences. Earth-Sci. Rev. 35, 367–395.

Wright, V.P. Vanstone, S.D. 2001. Onset of Late Palaeozoic glacio-eustasy and the evolving climates of low latitude areas: a synthesis of current understanding. J. Geol. Soc. London 158, 579–582.

Wright, V.P., Vanstone, S.D. Marshall, J.D. 1997. Contrasting flooding histories of Mississippian carbonate platforms revealed by marine alteration effects in palaeosols. Sedimentology 44, 825–842.

Captions

Table 1. Main foraminiferal markers of the late Asbian assemblages (based on Cózar et al., in press).

Table 2. Results of tests for randomness on the diversity indices for the Trowbarrow data (202 sample levels). For the stratal consistency function (SCF) of Hounslow and Morton (2004), the parametric bootstrap-derived probability threshold for randomness (obtained with 10,000 re-sampling from a normal distribution) are 5%, 1% and 0.1% are 0.114, 0. 0.162, 0.209. Indices were also examined for similarity to a normal distribution. *= test performed with index Log_e transformed to make it a closer to a normal distribution. The (p%) probability is shown for the Durbin-Watson test for autocorrelation shown by Uyanto (2020) to be the most powerful (small p indicates data is not noise).

Table 3. Measures of slotting success. CPL is the combined path length. Wakefield et al. (in press) has more details about these measures.

Table 4. Statistics for success of sequence slotting for the highest ranked city block-based correlation models (see Table 3). Ratio in [] is the block constraint used for slotting [Trowbarrow: section concerned]. All the correlations pass a 5% threshold for association using the RV-based P_{ass} value.

Table 5. Summary of foraminiferal trends Ft0 to Ft13 within the five late Asbian subzones (Cf6γ1a - Cf6γ2c) and related emergent surfaces.

Table 6. Ratio by the number of samples (n) of Local (in the Trowbarrow section) and regional (in northern England) occurrences and disappearances

Fig. 1. Location of the main sections and boreholes mentioned in the text. (1-column)

Fig. 2. Schematic lithostratigraphy of the main regions discussed in the text. The formal lithostratigraphy and substage ages are included in the columns labelled A, as they were originally described (from left to right) by Gallagher and Somerville (2003), Gallagher et al. (2006), Cózar and Somerville (2005), Horbury (1987), Davies (1983), Somerville (1977), Gray (1981) and Cózar and Somerville (2020). Age of reinterpreted lithostratigraphy is located in columns labelled B. Foraminiferal diversity has been analysed in the regions with grey shading on the formations. Abbreviation B.b. basement beds; Fm Formation; Lst. Limestone; N. North; S. South; SCS=South Cumbria shelf. (2-columns)

Fig. 3. Margalef diversity index (ranging from 1 (low) up to 9 (high) in abscissa axis) in A. Trowbarrow Quarry (1 to 5 and A to G are major emergent surfaces of Horbury, 1987), B. Port Eynon, C. Ballyadams Quarry sections. The asterisks in the biostratigraphy column marks the position where guides of the foraminiferal assemblages/subzones are recorded sensu Cózar et al. (in press), Cózar and Somerville (2020) and Cózar and Somerville (2005). Rh 1-11 are rhythms defined between the major emergent surfaces 1 to 5 and A to G in the Trowbarrow Quarry. The major emergent surfaces are interpreted as those with thick palaeosols and common pedogenic features, whereas dashed lines represent minor palaeokarsts with poorer development of

1175 palaeosols. Ft 0-Ft13 are Foraminiferal trends with boundaries (dotted lines). Samples
1176 in all sections are placed equidistant, and differ in meter spacing. W.S. Woodbine Shale.
1177 (2-columns)
1178
1179 Fig. 4. Margalef diversity index in A. Clogrenan B Borehole, B. base of Clogrenan
1180 Quarry, C. Aillwee sections. The asterisks in the biostratigraphy column mark the
1181 position where guides of the foraminiferal assemblages/subzones are recorded sensu
1182 Cózar and Somerville (2005) and Gallagher et al. (2006). Foraminiferal Assemblage
1183 Cf6γ2c in the Clogrenan B Borehole and Cf6γ1b in Aillwee section are in grey because
1184 foraminiferal guides are not recognised in this section. Cycles in the Clogrenan B
1185 Borehole with asterisks are the corrected position after correlation by foraminiferal
1186 diversity and slotting. Other remarks as in Fig. 3. (2-columns)
1187
1188 Fig. 5. The city block slotting-based correlation models for Port Eynon showing the
1189 Magalef and Log_e(Berger-Parker) indices. Data in each case shows the zero-scaled data
1190 for all sections in a sample position scale. Black lines represent the correlation
1191 constraints applied to the data at the foraminiferal subzone boundaries. Palaeokarst
1192 positions (in blue) are shown on the right side of each panel, with labelling as in Fig. 9.
1193 For many of the points for the two types of correlation models (orange and black
1194 squares and dots) the inferred slotted position at Trowbarrow overlap in showing the
1195 similarity in the slotting solutions irrespective of the scaling used. More data is shown
1196 in the SI, including the Shannon index not shown here. (1.5-column)
1197
1198 Fig. 6. The city block slotting-based correlation models for Ballyadams showing the
1199 Margalef and Log_e(Berger-Parker) indices. Dashed-blue lines for palaeokarsts indicate

1200 the two possible positions of the karsts, based on the two slotting models shown. See
1201 Fig. 5 for details. (1.5-column)
1202
1203 Fig. 7. The city block slotting-based correlation models for the composite Clogrenan
1204 section showing the Margalef and Log_e(Berger-Parker) indices. See Figs. 5 for details.
1205 (1.5-column)
1206
1207 Fig. 8 Assessment of the periodicity in the Margalef index at Trowbarrow, using data in
1208 height scale of metres. A. Lomb-Scargle method for unequally spaced data. B. the
1209 periodogram determined using the Multitaper method. The lines in both represent the
1210 confidence intervals for a power-law function, as is normally the case in palaeoclimatic
1211 data (McKay et al. 2021), with periods (in metres) marked in B which exceed the 95%
1212 confidence threshold. (1.5-column)
1213
1214 Fig. 9. Correlation of the foraminiferal trends (Ft), sedimentological rhythms (Rh) and
1215 major and minor emergent surfaces in the studied basins (all vertical scales in metres).
1216 Emergent surfaces in roman numbers are considered as major palaeokarsts (see Fig. 1
1217 for location of sections). Sample numbers are only included in the last sample below
1218 any of the important levels (biostratigraphic and palaeokarstic levels), beginning or end
1219 of the sections, whereas the full sample numbers are included in Figs. 3–4. Lines have
1220 been relocated at stratigraphic scales according to the position of the sample in the
1221 section. A. correlation between Trowbarrow, Carlow and Burren (western Ireland), B.
1222 correlation between Trowbarrow and Port Eynon (south Wales). Location of section
1223 lines in inset in B. (2-columns)
1224

1225 Fig. 10. Foraminiferal disappearances and occurrences in the Trowbarrow Quarry
1226 section compared with the high-frequency rhythms recognised in the section, the
1227 interpreted phases of the system tracts, the number of local and regional disappearances,
1228 and number of local and regional occurrences. LST lowstand system tract, TST
1229 transgressive system tract, HST highstand system tract. W.S. Woodbine Shale. (2-
1230 columns)


N
Archerbeck Bh.
Rookhope Bh.
Little Asby
Trowbarrow
Silverdale Bh.
Anglesey
Aillwee
Dublin Basin
Ballyadams
Llangollen
Oswestry
Southern
Irish
Platform
Shannon
Trough
Tankardstown Bh.
Clogrenan
Callan
N Cork
Port Eynon
South
Munster
Basin
0 km 100 200

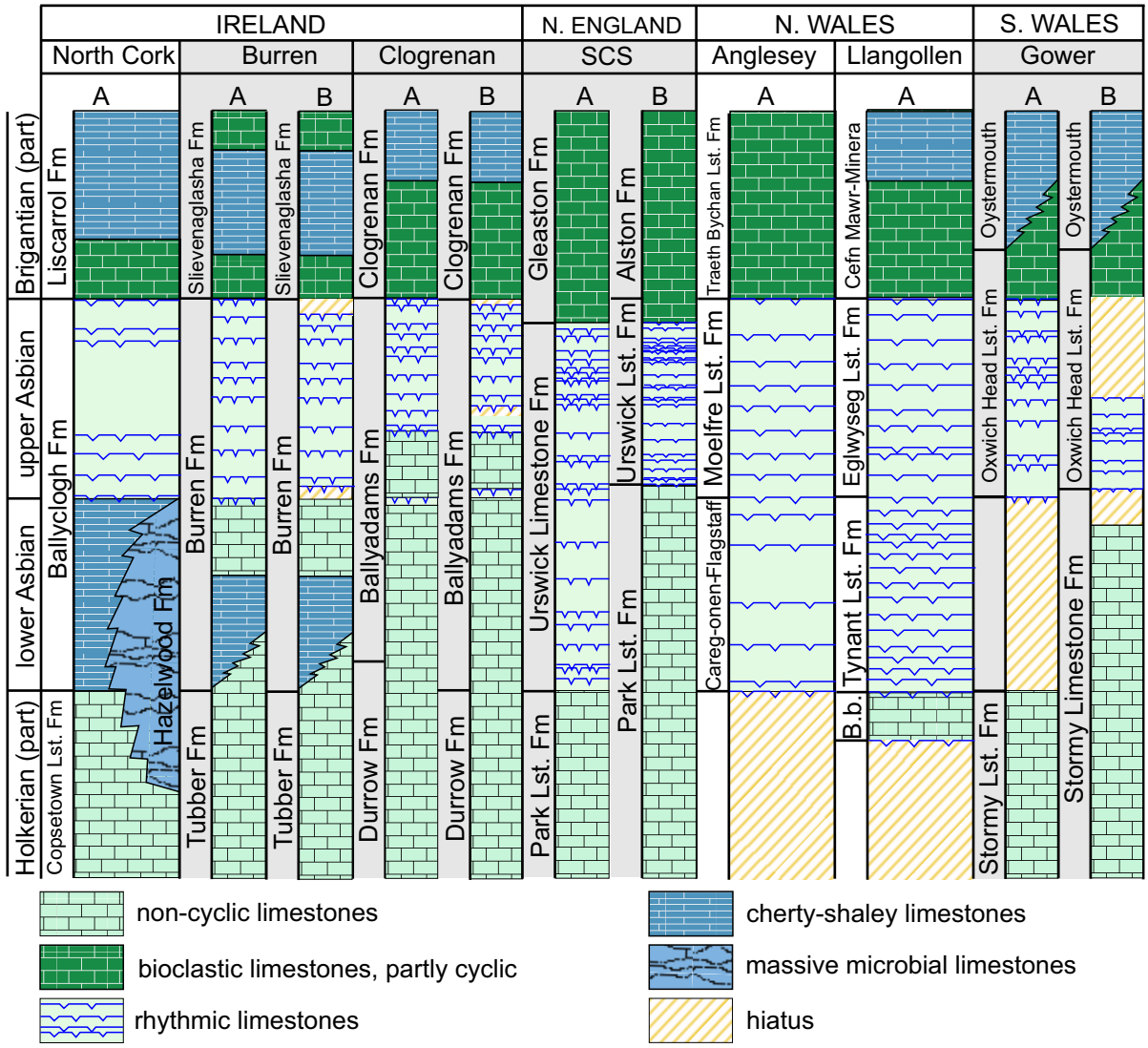
IRELAND
N. ENGLAND
N. WALES
S. WALES
North Cork
Burren
Clogrenan
SCS
Anglesey
Llangollen
Gower
A
B
Brigantian (part)
upper Asbian
lower Asbian
Holkerian (part)
Liscarrol Fm
Ballyclogh Fm
Hazelwood Fm
Copsetown Lst. Fm
Slievenaglasha Fm
Burren Fm
Tubber Fm
Clogrenan Fm
Ballyadams Fm
Durrow Fm
Gleaston Fm
Urswick Limestone Fm
Park Lst. Fm
Alston Fm
Urswick Lst. Fm
Traeth Bychan Lst. Fm
Moelfre Lst. Fm
Careg-onen-Flagstaff
Cefn Mawr-Minera
Eglwyseg Lst. Fm
Tynant Lst. Fm
B.b.
Oystermouth
Oxwich Head Lst. Fm
Stormy Lst. Fm
Stormy Limestone Fm
non-cyclic limestones
bioclastic limestones, partly cyclic
rhythmic limestones
cherty-shaley limestones
massive microbial limestones
hiatus

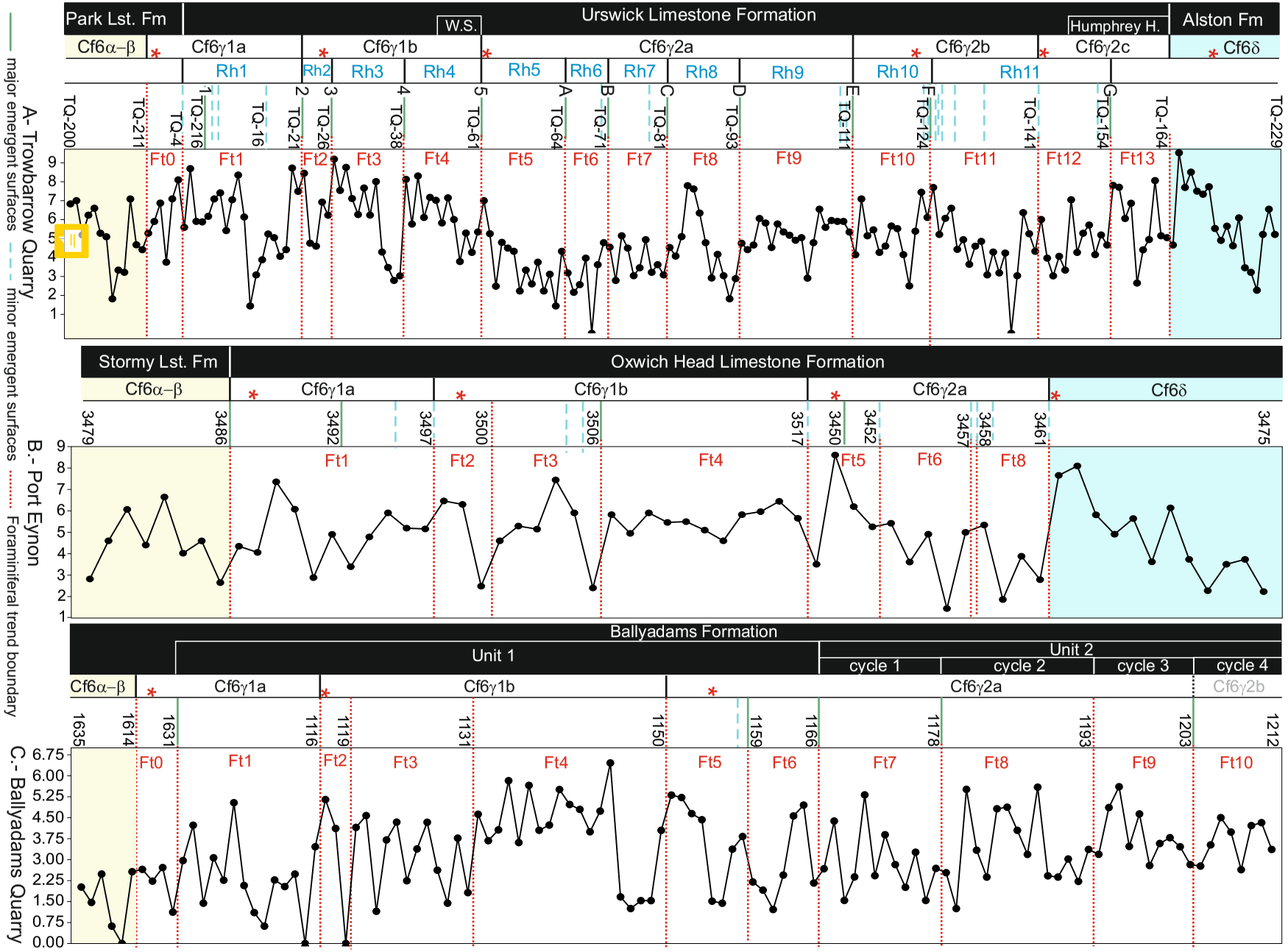
major emergent surfaces
minor emergent surfaces
Foraminiferal trend boundary
A- Trowbarrow Quarry
Park Lst. Fm
Urswick Limestone Formation
W.S.
Humphrey H.
Alston Fm
Cf6α–β
Cf6γ1a
Cf6γ1b
Cf6γ2a
Cf6γ2b
Cf6γ2c
Cf6δ
Rh1
Rh2
Rh3
Rh4
Rh5
Rh6
Rh7
Rh8
Rh9
Rh10
Rh11
TQ-200
TQ-211
TQ-4
TQ-216
TQ-16
TQ-21
TQ-26
TQ-38
TQ-61
TQ-64
TQ-71
TQ-81
TQ-93
TQ-111
TQ-124
TQ-141
TQ-154
TQ-164
TQ-229
Ft0
Ft1
Ft2
Ft3
Ft4
Ft5
Ft6
Ft7
Ft8
Ft9
Ft10
Ft11
Ft12
Ft13
B.- Port Eynon
Stormy Lst. Fm
Oxwich Head Limestone Formation
3479
3486
3492
3497
3500
3506
3517
3450
3452
3457
3458
3461
3475
Ft1
Ft2
Ft3
Ft4
Ft5
Ft6
Ft8
C.- Ballyadams Quarry
Ballyadams Formation
Unit 1
Unit 2
cycle 1
cycle 2
cycle 3
cycle 4
1635
1614
1631
1116
1119
1131
1150
1159
1166
1178
1193
1203
1212
Ft0
Ft1
Ft2
Ft3
Ft4
Ft5
Ft6
Ft7
Ft8
Ft9
Ft10

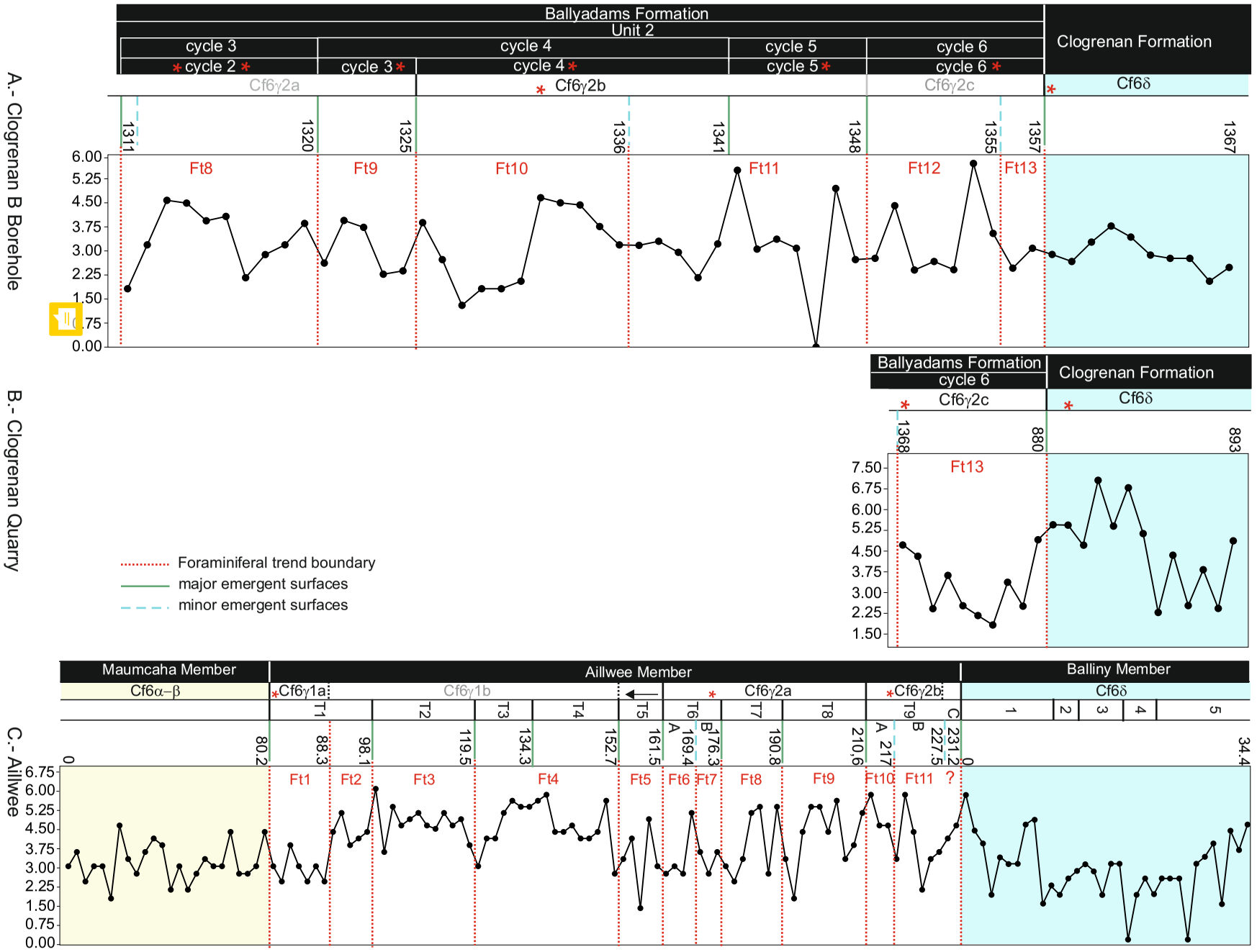
A.- Clogrenan B Borehole
Ballyadams Formation
Unit 2
Clogrenan Formation
cycle 3
cycle 4
cycle 5
cycle 6
cycle 2
cycle 3
cycle 4
cycle 5
cycle 6
Cf6γ2a
Cf6γ2b
Cf6γ2c
Cf6δ
1311
1320
1325
1336
1341
1348
1355
1357
1367
Ft8
Ft9
Ft10
Ft11
Ft12
Ft13
6.00
5.25
4.50
3.75
3.00
2.25
1.50
0.75
0.00
B.- Clogrenan Quarry
Ballyadams Formation
cycle 6
Clogrenan Formation
Cf6γ2c
Cf6δ
1368
880
893
Ft13
7.50
6.75
6.00
5.25
4.50
3.75
3.00
2.25
1.50
Foraminiferal trend boundary
major emergent surfaces
minor emergent surfaces
C.- Aillwee
Maumcaha Member
Aillwee Member
Balliny Member
Cf6α–β
Cf6γ1a
Cf6γ1b
Cf6γ2a
Cf6γ2b
Cf6δ
T1
T2
T3
T4
T5
T6
T7
T8
T9
A
B
C
1
2
3
4
5
0
80.2
88.3
98.1
119.5
134.3
152.7
161.5
169.4
176.3
190.8
210.6
217
227.5
231.2
34.4
Ft1
Ft2
Ft3
Ft4
Ft5
Ft6
Ft7
Ft8
Ft9
Ft10
Ft11
?
6.75
6.00
5.25
4.50
3.75
3.00
2.25
1.50
0.75
0.00

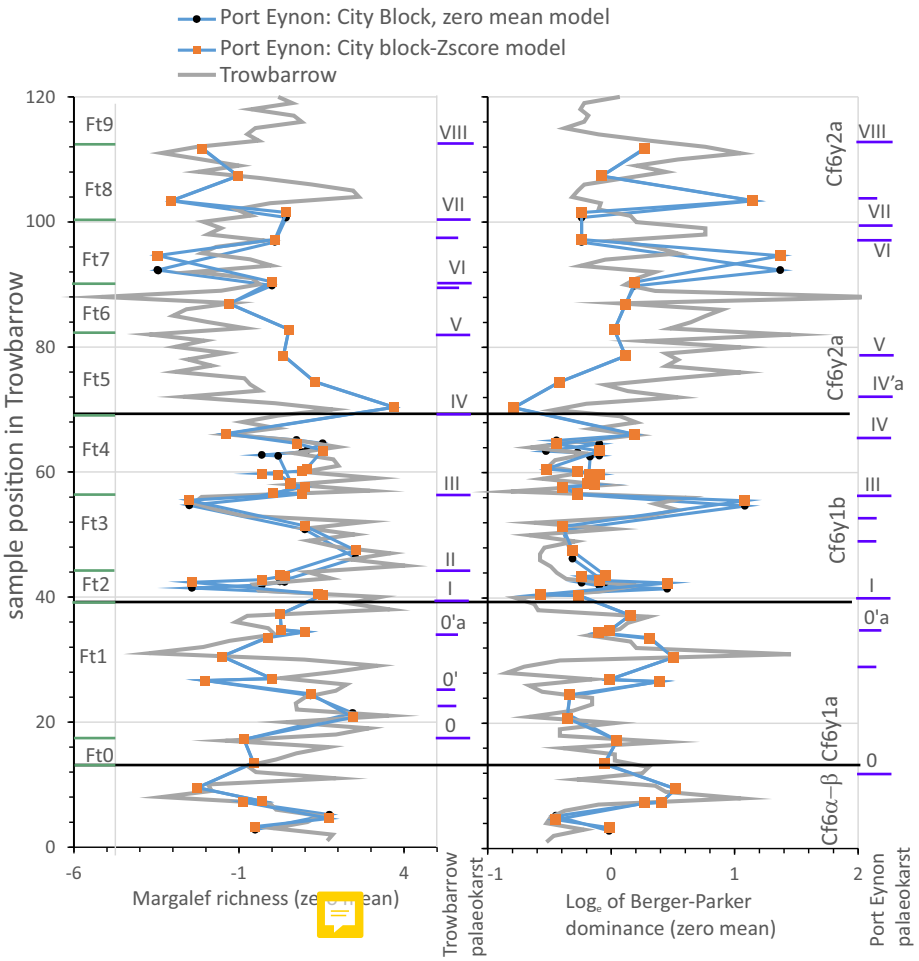
Port Eynon: City Block, zero mean model
Port Eynon: City block-Zscore model
Trowbarrow
sample position in Trowbarrow
120
100
80
60
40
20
0
Ft9
Ft8
Ft7
Ft6
Ft5
Ft4
Ft3
Ft2
Ft1
Ft0
VIII
VII
VI
V
IV
III
II
I
0'a
0'
0
-6
-1
4
Margalef richness (zero mean)
Trowbarrow palaeokarst
Cf6y2a
Cf6y2a
Cf6y1b
Cf6y1a
Cf6α–β
VIII
VII
VI
V
IV'a
IV
III
I
0'a
0
-1
0
1
2
Log$_e$ of Berger-Parker dominance (zero mean)
Port Eynon palaeokarst

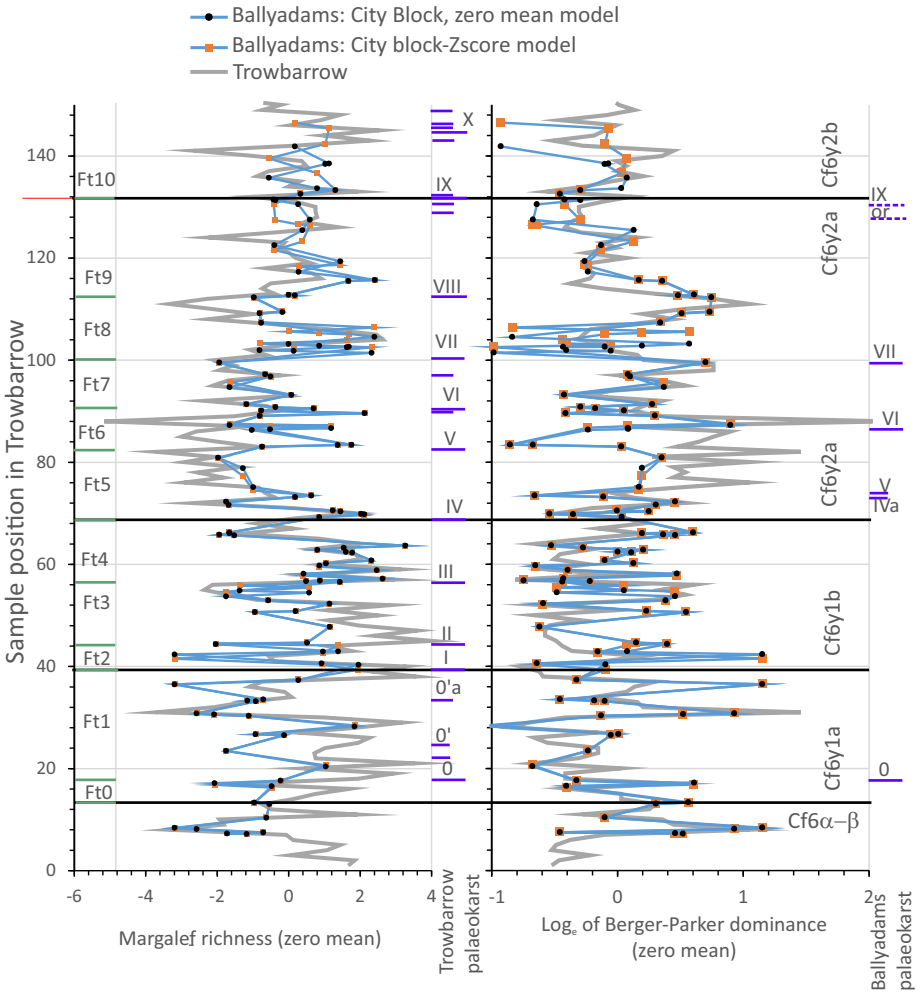
Ballyadams: City Block, zero mean model
Ballyadams: City block-Zscore model
Trowbarrow
Sample position in Trowbarrow
Ft10
Ft9
Ft8
Ft7
Ft6
Ft5
Ft4
Ft3
Ft2
Ft1
Ft0
X
IX
VIII
VII
VI
V
IV
III
II
I
0'a
0'
0
Cf6y2b
Cf6y2a
Cf6y1b
Cf6y1a
Cf6α–β
IX
αr
VII
VI
V
IVa
0
Margalef richness (zero mean)
Log$_e$ of Berger-Parker dominance (zero mean)
Trowbarrow palaeokarst
Ballyadams palaeokarst

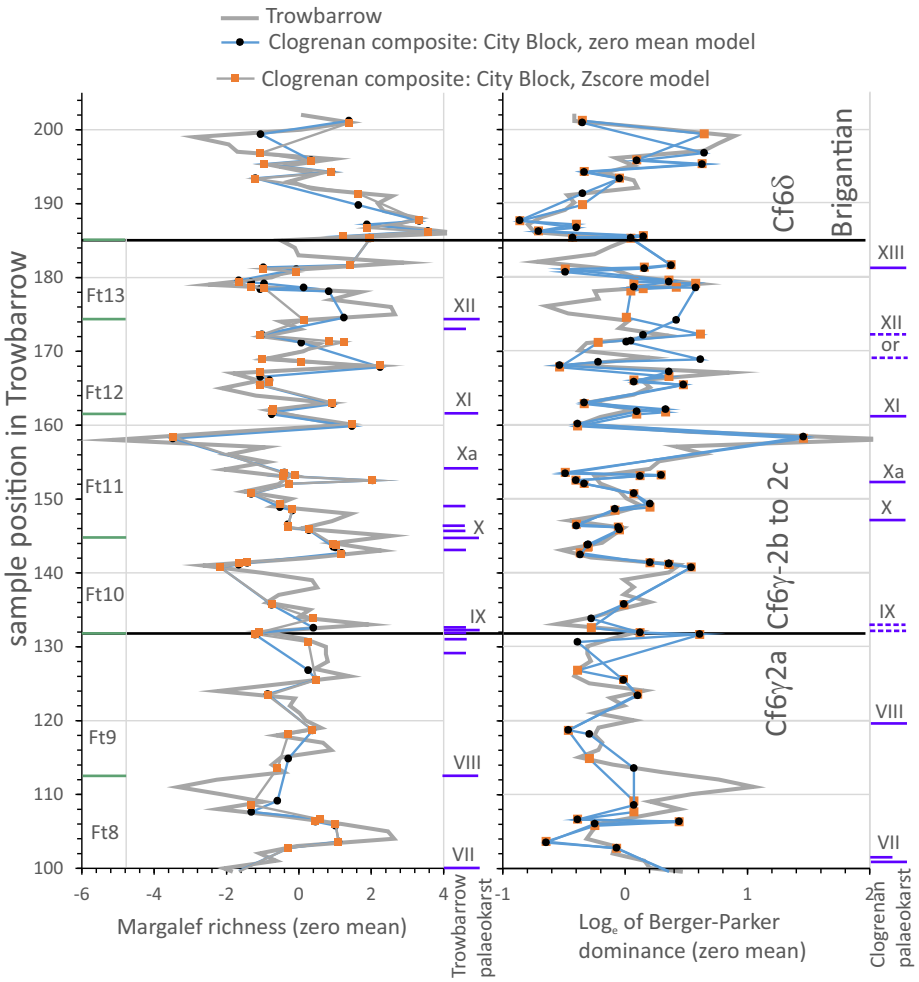
Trowbarrow
Clogrenan composite: City Block, zero mean model
Clogrenan composite: City Block, Zscore model
sample position in Trowbarrow
200
190
180
170
160
150
140
130
120
110
100
Ft13
Ft12
Ft11
Ft10
Ft9
Ft8
XII
XI
Xa
X
IX
VIII
VII
-6
-4
-2
0
2
4
Margalef richness (zero mean)
Trowbarrow palaeokarst
Cf6δ
Brigantian
Cf6γ-2b to 2c
Cf6γ2a
XIII
XII
or
XI
Xa
X
IX
VIII
VII
-1
0
1
2
Log$_e$ of Berger-Parker dominance (zero mean)
Clogrenan palaeokarst

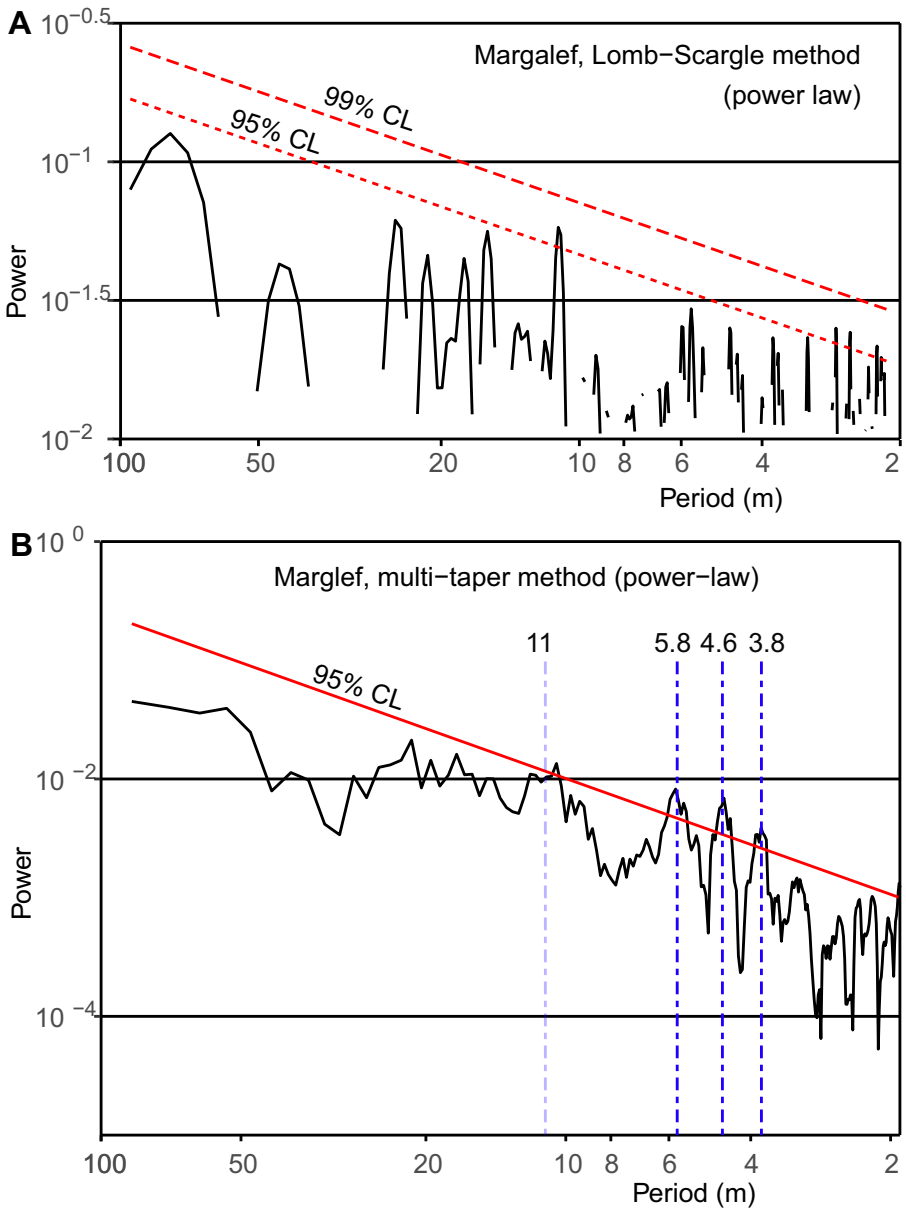
A
Margalef, Lomb−Scargle method
(power law)
99% CL
95% CL
Power
Period (m)
B
Marglef, multi−taper method (power−law)
95% CL
11
5.8
4.6
3.8
Power
Period (m)

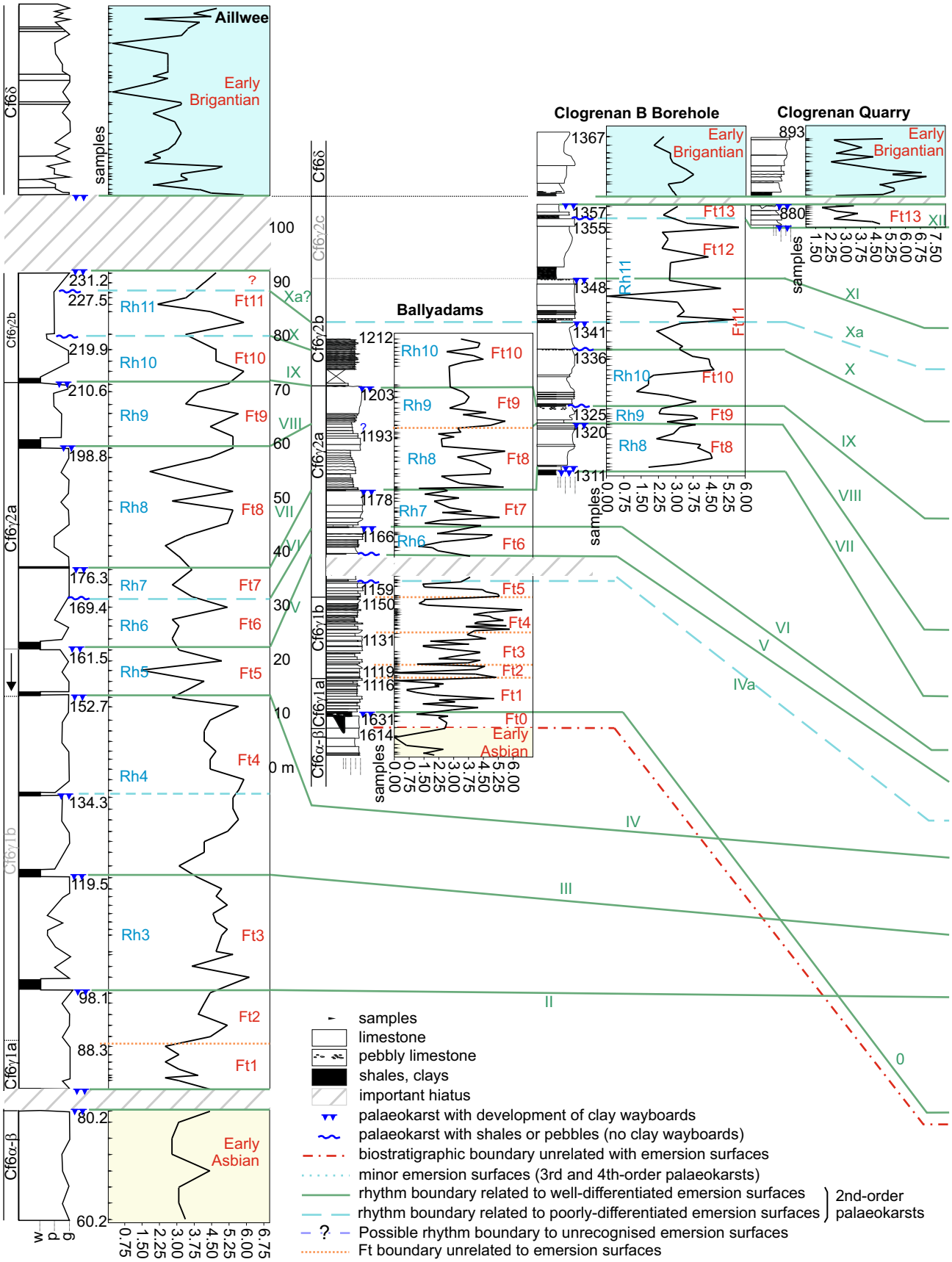
Aillwee
Early Brigantian
Clogrenan B Borehole
Clogrenan Quarry
Ballyadams
Early Asbian
samples
limestone
pebbly limestone
shales, clays
important hiatus
palaeokarst with development of clay wayboards
palaeokarst with shales or pebbles (no clay wayboards)
biostratigraphic boundary unrelated with emersion surfaces
minor emersion surfaces (3rd and 4th-order palaeokarsts)
rhythm boundary related to well-differentiated emersion surfaces
rhythm boundary related to poorly-differentiated emersion surfaces
2nd-order palaeokarsts
Possible rhythm boundary to unrecognised emersion surfaces
Ft boundary unrelated to emersion surfaces

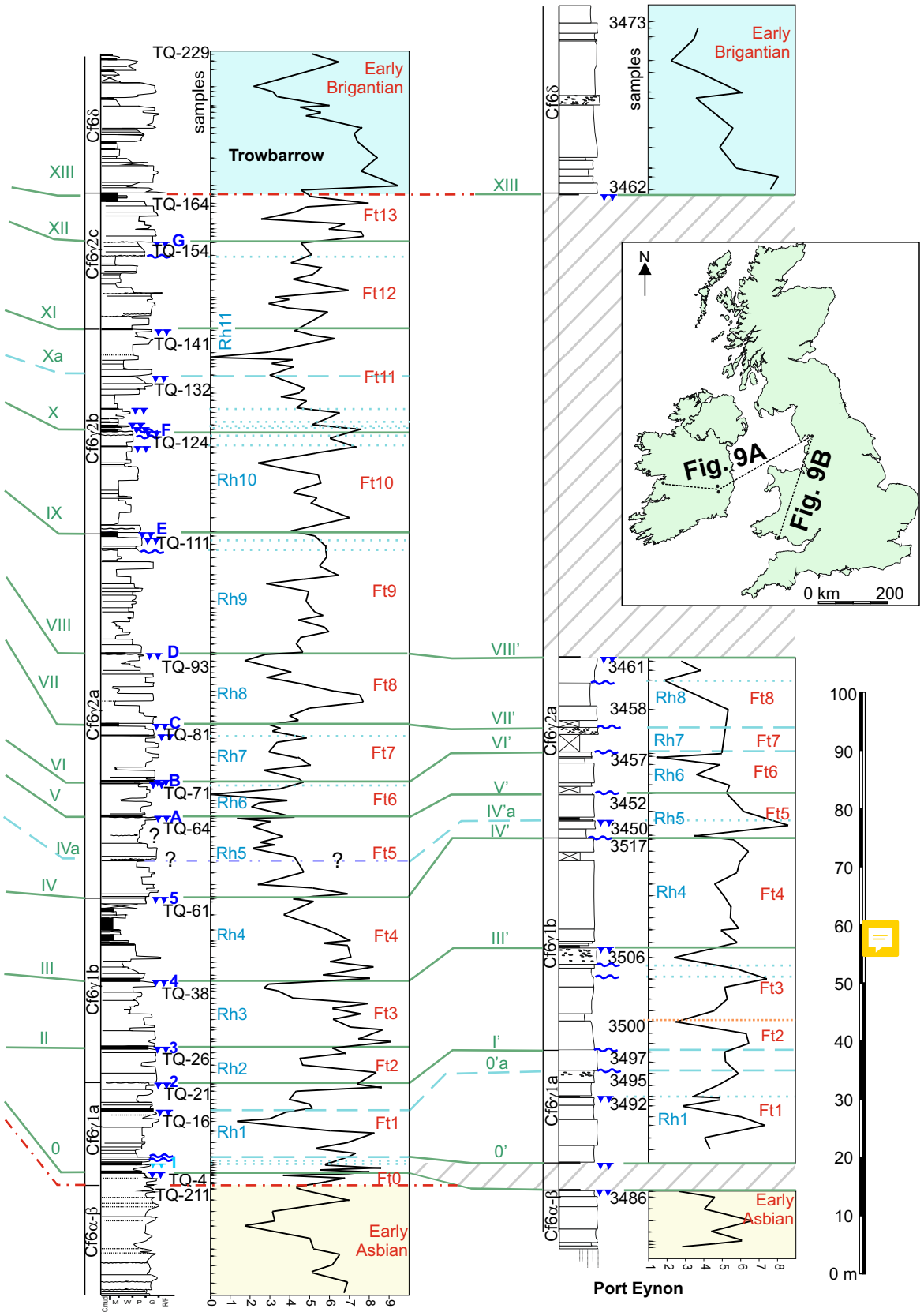
TQ-229
samples
Early Brigantian
Trowbarrow
TQ-164
TQ-154
TQ-141
TQ-132
TQ-124
TQ-111
TQ-93
TQ-81
TQ-71
TQ-64
TQ-61
TQ-38
TQ-26
TQ-21
TQ-16
TQ-4
TQ-211
Cf6δ
Cf6γ2c
Cf6γ2b
Cf6γ2a
Cf6γ1b
Cf6γ1a
Cf6α-β
XIII
XII
XI
Xa
X
IX
VIII
VII
VI
V
IVa
IV
III
II
0
Rh11
Rh10
Rh9
Rh8
Rh7
Rh6
Rh5
Rh4
Rh3
Rh2
Rh1
Ft13
Ft12
Ft11
Ft10
Ft9
Ft8
Ft7
Ft6
Ft5
Ft4
Ft3
Ft2
Ft1
Ft0
Early Asbian
3473
samples
3462
Early Brigantian
N
Fig. 9A
Fig. 9B
0 km
200
VIII'
VII'
VI'
V'
IV'a
IV'
III'
I'
0'a
0'
3461
3458
3457
3452
3450
3517
3506
3500
3497
3495
3492
3486
Rh8
Rh7
Rh6
Rh5
Rh4
Rh1
Ft8
Ft7
Ft6
Ft5
Ft4
Ft3
Ft2
Ft1
Early Asbian
Port Eynon
100
90
80
70
60
50
40
30
20
10
0 m

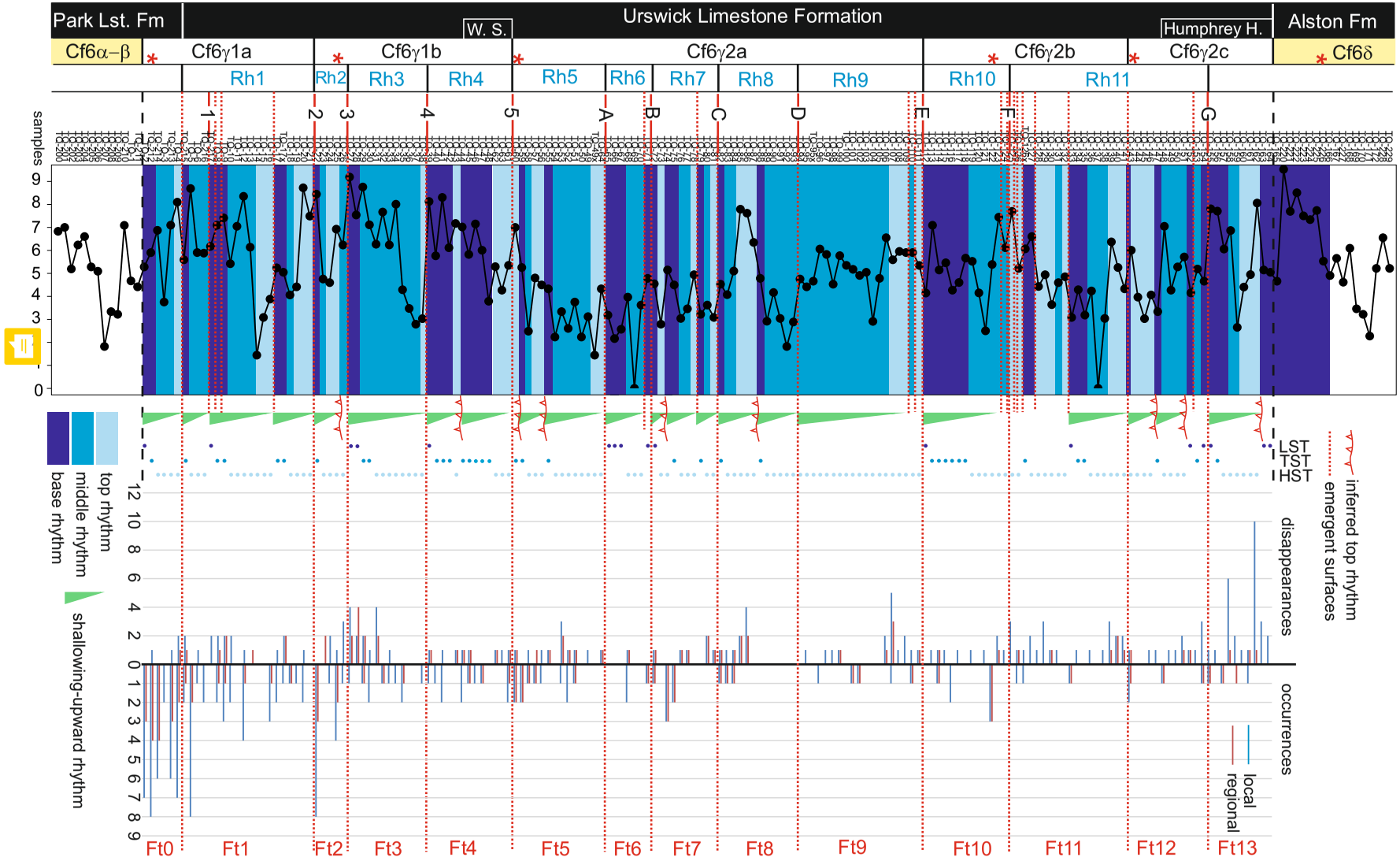
Park Lst. Fm
Urswick Limestone Formation
W. S.
Humphrey H.
Alston Fm
Cf6α–β
Cf6γ1a
Cf6γ1b
Cf6γ2a
Cf6γ2b
Cf6γ2c
Cf6δ
Rh1
Rh2
Rh3
Rh4
Rh5
Rh6
Rh7
Rh8
Rh9
Rh10
Rh11
samples
base rhythm
middle rhythm
top rhythm
shallowing-upward rhythm
LST
TST
HST
inferred top rhythm
emergent surfaces
disappearances
occurrences
local
regional
Ft0
Ft1
Ft2
Ft3
Ft4
Ft5
Ft6
Ft7
Ft8
Ft9
Ft10
Ft11
Ft12
Ft13

	Assemblages	main foraminiferal markers
LATE ASBIAN	Cf6γ2c	common *Archaediscus karreri* group common *Neoarchaediscus* common *Eostaffella ikensis*
	Cf6γ2b	*Bradyina rotula* *Euxinita efremovi*
	Cf6γ2a	*Neoarchaediscus* s.s. large *Cribrospira* species
	Cf6γ1b	*Bibradya* small *Cribrospira* species
	Cf6γ1a	*Eostaffella ikensis* *Cribrostomum* *Koskinobigenerina* *Endothyranopsis crassa*

Table 1. Main foraminiferal markers of the late Asbian assemblages (based on Cózar et al., in press).

Diversity index	*Dominance (1-Simpson index)	Shannon	Evenness	Brillouin	Menhinick	Margalef	Equitability	*Fisher's-alpha	*Berger-Parker	*Chao-1
SCF	0.433	0.438	0.424	0.499	0.424	0.486	0.259	0.012	0.442	0.274
Durbin-Watson	<0.01%	<0.01%	<0.01%	<0.01%	<0.01%	<0.01%	0.01%	42	<0.01%	<0.01%

Table 2. Results of tests for randomness on the diversity indices for the Trowbarrow data (202 sample levels). For the stratal consistency function (SCF) of Hounslow and Morton (2003), the parametric bootstrap-derived probability threshold for randomness (10,000 samples from a normal distribution) are 5%, 1% and 0.1% are 0.114, 0. 0.162, 0.209. Indices were examined for similarity to a normal distribution. *= test performed with index Log_e transformed to make it a closer to a normal distribution. The (p%) probability is shown for the Durbin-Watson test for autocorrelation shown by Uyanto (2020) to be the most powerful (small p indicates data is not noise).

Indicator	What the measure indicates
D- value	Measure of success with smaller values indicate better success (Clark, 1985). This generally expresses a measure of short-range success in the slotted data.
N-CSTAT	The normalised sensitivity statistic. A measure of the robustness of the fit, largely independent of changes in the CPL between different slotting solutions. Values below 1 indicate the average sensitivity statistic is less than the average distance between adjacent points. Smaller N-CSTAT values are generally associated with better, more robust slotting solutions.
RV2, RV_{std}data_textoutput.	The RV-coefficients (Abdi, 2010) are measures of similarity (or association) of the two multivariate datasets. They express the overall, or long-range similarity. They have useful ranges of 0 to +1 for positive association. The modified RV-coefficient (RV2) of Smilde et al. (2009) is used, since it behaves more-like familiar regression coefficients. RV_{std} is the standardized RV coefficient, and is larger for better association. A probability of association of the datasets (P_{ass}) when slotted together is also determined (Josse et al., 2008).

Table 3. Measures of slotting success. CPL is the combined path length. Wakefield et al. (in press) has more details.

Success measure	Mean-Zero model	Zscore model
Trowbarrow- Port Eynon [4:2]		
D	0.837	0.830
RV2	0.292	0.275
P_{ass} (%)	4	4
Trowbarrow- Ballyadams [3:3]		
D	0.670	0.652
RV2	0.323	0.350
P_{ass} (%)	4	3
Trowbarrow- Clogrennan [5:3]		
D	0.664	0.648
RV2	0.682	0.525
P_{ass} (%)	3	3

Table 4. Statistics for success of sequence slotting for the highest ranked city block based correlation models (see Table 3). Ratio in [] is the block constraint used for slotting [Trowbarrow: section concerned]. All the correlations pass a 5% threshold for association using the RV-based P_{ass} value.

Rhythm-Trend	subzone	Diversity trend	Subsidiary emergent surfaces [position]
Brigantian	Cf6δ	Peak in the lower part, decreasing upwards	
Ft13	Cf6γ2c	Minimum in mid parts	
Rh11-Ft12	Cf6γ2c	Increasing mildly throughout	Tr[0.82]
Rh11-Ft11	Cf6γ2b	Declining, with low in upper part	Tr[0.04, 0.07, 0.09, 0.22, 0.55], Cl[0.47]
Rh10-Ft10	Cf6γ2b	Peak in upper part, similar but low in lower part	Tr[0.85, 0.95]
Rh9-Ft9	Cf6γ2a	Similar throughout	Tr[0.86,0.96]
Rh8-Ft8	Cf6γ2a	Peak in upper part of lower half, declining to top	
Rh7-Ft7	Cf6γ2a	Similar throughout	Tr[0.80], Ba[0.25]
Rh6-Ft6	Cf6γ2a	Low in lower parts	Tr[0.87]
Rh5-Ft5	Cf6γ2a	Declining from base to top	PE[0.11,0.28,0.56,0.71], Ba[0.32,0.46]
Rh4-Ft4	Cf6γ1b	Declining from lower part	Al[0.45]
Rh3-Ft3	Cf6γ1b	Declining in upper part to top	PE[0.62, 0.76]
Rh2-Ft2	Cf6γ1b	Declining from lower to top	
Rh1-Ft1	Cf6γ1a	Peak in lower, minimum in mid parts	Tr[0.09, 0.14, 0.19, 0.70], PE[0.58, 0.81]
Ft0	Cf6γ1a	Increasing upwards	

[position]= position of emergent surface as proportion of the thickness from base of the rhythm. Tr=Trowbarrow, PE= Port Eynon, Al=Aillwee, Ba= Ballyadams, Cl=Clogrenan.

Table 5. Summary of foraminiferal trends Ft0 to Ft13 within the five late Asbian subzones (Cf6γ1a - Cf6γ2c) and related emergent surfaces.

	Base cycle	Middle cycle	Top cycle	Lowstand	Transgressive	Highstand
n	51	77	44	16	37	119
Local first occurrences	59/1.16	60/0.78	30/0.68	12/0.75	46/1.24	87/0.73
Regional first occurrences	26/0.51	30/0.38	10/0.23	9/0.56	18/0.49	39/0.32
Local disappearances	48/0.94	56/0.72	58/1.32	21/1.31	29/0.78	112/0.94
Regional disappearances	21/0.41	22/0.28	24/0.55	11/0.69	12/0.32	44/0.37

Table 6. Local and regional occurrences and disappearances of foraminifers in absolute number and their ratio by the number of samples (n) in Trobarrow Quarry.

Supplementary information for “Far-field correlation of palaeokarstic surfaces in Mississippian successions using high-frequency foraminiferal diversity trends”

BY PEDRO CÓZAR, IAN D. SOMERVILLE, MARK W. HOUNSLOW AND ISMAEL CORONADO

The supplementary information contains the following:

Figs S1, S2. Additional plots of the Margalef diversity indices in the sections, and comparison of all the diversity indices initially considered at Trowbarrow.

Fig. S3. Summary plot of the cross-correlations between all sections.

Figs S4 to Fig. S8. Photographs of all the major palaeokarsts and surfaces proposed.

Fig. S9. Margalef diversity indices for other Asbian sections in Britain.

Tables S1 to S5. Additional information about variable section for the slotting analysis and selection of the slotting models for the Trowbarrow-Port Eynon, Trowbarrow-Clogrenan and Trowbarrow-Ballyadams.

Figs. S10-S15. Intersection correlations for the various slotting models, and plots of the Shannon-H diversity index

Fig. S16. Summary plots of the Margalef and Berger-Parker indices within the frame of the final correlation model (i.e. Fig. S3) to Trowbarrow.

Fig. S17. The composite diversity index plots for the late Asbian using data for all sections.

Table S6 to S9. Lists of the sets of diversity indices using in the sections, and slotting and their inferred position with respect to the Trowbarrow sampling psoitions.

Dominance, D	1						
Shannon H	-0.99875878	1					
Bruillouin	-0.98554659	0.9890905	1				
Margalef	-0.94884474	0.9477882	0.9526661	1			
Fisher-Alpha	-0.70475595	0.7098739	0.667396	0.639784	1		
Chao-1	-0.8456208	0.8473593	0.3470224	0.3634769	0.1648191	1	
berger-parker	0.95258787	-0.942023	-0.929929	-0.898603	-0.559554	-0.76573	1

	Dominance, D	Shannon H	Bruillouin	Margalef	Fisher-Alpha	Chao-1	Berger-Parker
SCF	0.43	0.44	0.50	0.49	0.01	0.27	0.44
Mean	**-2.60**	**2.68**	**2.01**	**5.16**	**3.16**	**3.28**	**-2.15**
SD	**0.57**	**0.59**	**0.54**	**1.78**	**0.96**	**0.64**	**0.49**

Table S1. Statistics for the primary diversity indices considered. The upper matrix are the Pearson correlation coefficients. The lower matrix are the stratal consistency function (SCF) and the mean and standard deviation (SD) of the respective indices. Green=good values, purple are adverse values.

	Ln(Berger-Parker)	**Margalef**
Ln (Berger-Parker)	1	
Margalef	-0.896629	1
Shannon_H	-0.927809	0.9574534

Table S2. The Spearman correlation coefficient's between the diversity indices (for Trowbarrow data) used in the sequence slotting for all sections.

PORT EYNON

Model	Delta	N-CSTAT	Na/Nb	RV2	RVstd	Delta	N-CStat	RV2	RVstd	Score total
Slot [Eucl,none]{6 cons}	0.838	7.293	202/50	0.2409	0.4947	3	1	3	3	10
Slot [Eucl,Zero]{6 cons}	0.834	7.262	202/50	0.2392	0.4912	1	0	5	5	11
Slot [Eucl,ZSco]{6 cons}	0.839	8.682	202/49	0.2967	0.6109	4	4	0	1	9
Slot [City,none]{6 cons}	0.841	7.944	202/50	0.2407	0.4943	5	2	4	4	15
Slot [City,Zero]{6 cons}	0.837	7.974	202/49	0.292	0.6098	2	3	1	2	8
Slot [City,ZSco]{6 cons}	0.830	9.315	202/49	0.2752	1.0378	0	5	2	0	7

Table S3. Slotting model assessment table for the Trowbarrow to Port Eynon sequence slotting models. Orange indicates the best two values of the corresponding result. In the Model text [x,y] indicates the metric used (Euclidean, or city-block) and the type of scaling (none=no scaling, zero= scaling to mean of zero, ZSc= scaling to mean zero and SD=1. Score total= sum of the scores, with top-ranking having a score of 0 and bottom ranking score of 5. Top two score totals in green. Na/Nb= number in Trowbarrow/Port Eynon dataset slotted together.

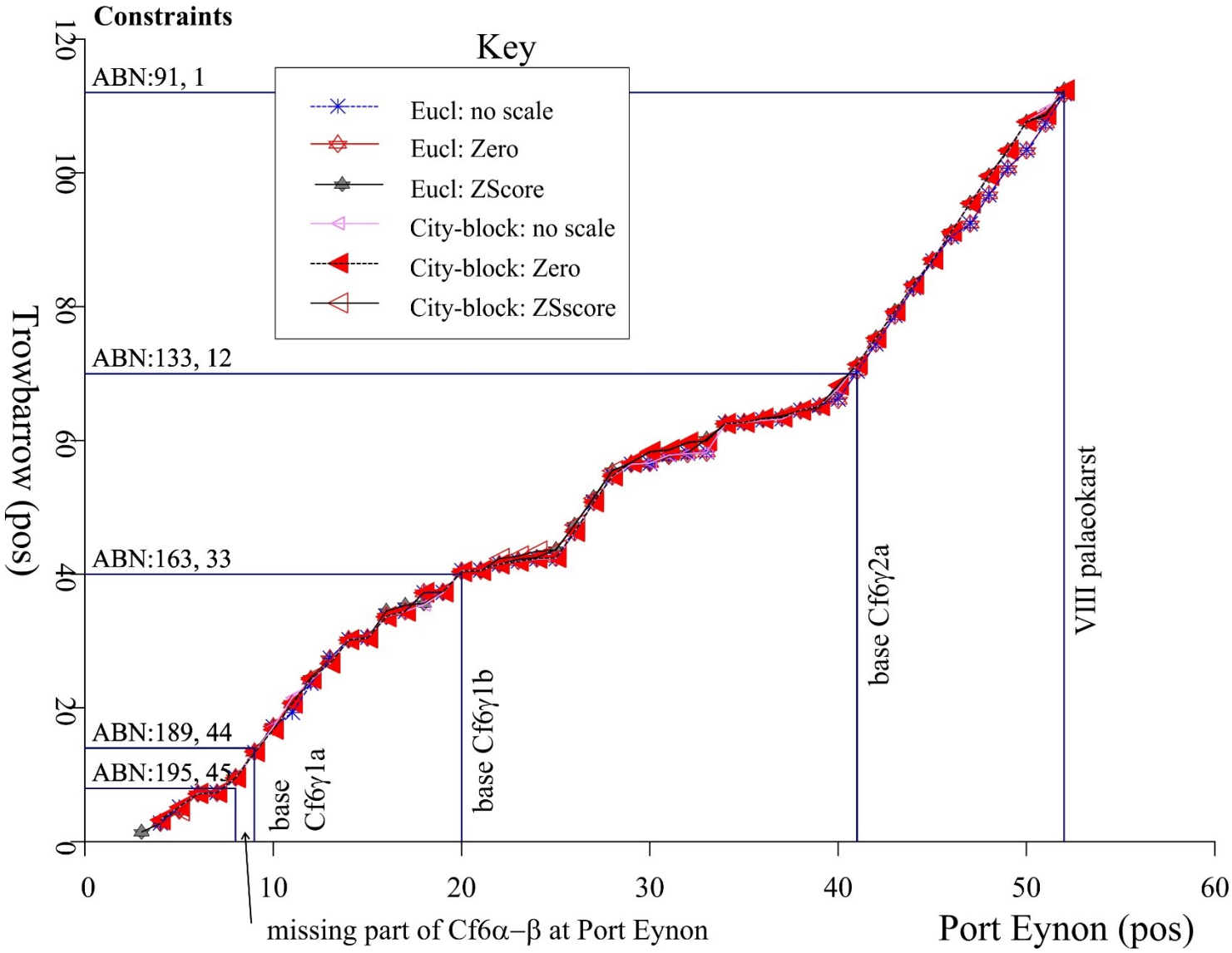

Fig. S10. The correlation models for the six slotting solutions at Port Eynon. On each axis are the sample numbers ordered with relative position from the base. The correlation-tie point constraints (ABN from CPLSlot) are labelled with the row number in the data files (on the horizontal tie), and the level used in the stratigraphy of the sections (on the vertical tie).

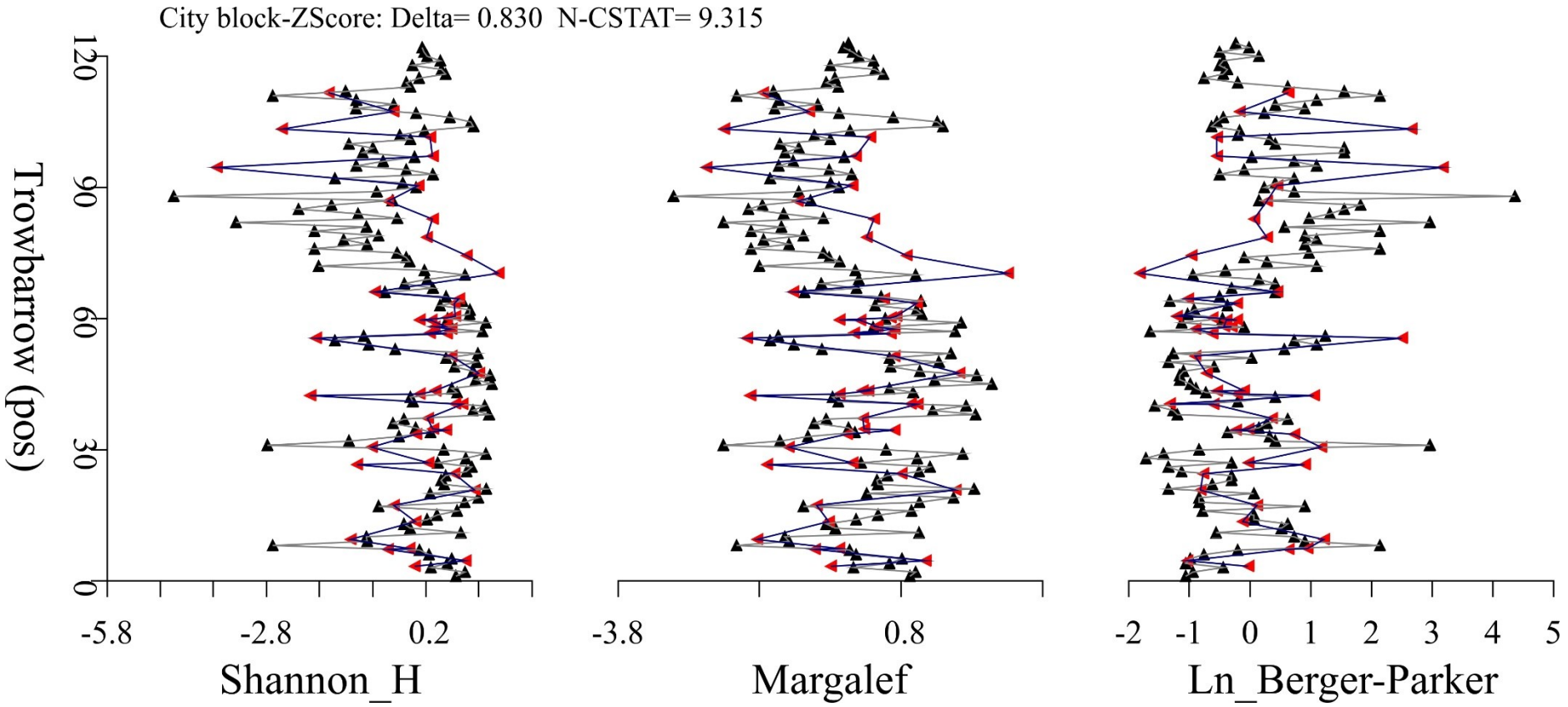

Fig. S11. The overlaid slotted diversity data for Trowbarrow (in black) and Port Eynon (in red). Diversity indexes have been plotted with data scaled to a mean of zero and a standard deviation of 1 (i.e. Zscore). The y-axis is the sample position at Trowbarrow, which in the case of the Port Eynon data are the position (possibly non integer) of the estimated positions using the slotting metrics and scaling shown.

CLOGRENAN COMPOSITE

Model	Delta	N-CSTAT	Na/Nb	Rc	RV2	Rvstd	Delta	N-Cstat	RV2	RVstd	Score Total
Slot [Eucl,none]{3 cons}	0.84	0.801	202/69	0.559	0.3183	0.6416	4	1	5	4	14
Slot [Eucl,Zero]{3 cons}	0.672	1.274	202/69	0.753	0.5831	2.1182	3	5	1	0	9
Slot [Eucl,ZSco]{3 cons}	0.671	1.115	202/69	0.682	0.4756	1.4729	2	3	3	2	10
Slot [City,none]{3 cons}	0.842	0.783	202/69	0.577	0.339	1.2317	5	0	4	3	12
Slot [City,Zero]{3 cons}	0.664	1.237	202/69	0.814	0.6818	2.1163	1	4	0	1	6
Slot [City,ZSco]{3 cons}	0.648	1.108	202/69	0.715	0.5246	0.3616	0	2	2	5	9

Table S4. Slotting model assessment table for the Trowbarrow to Clogrenan composite sequence slotting models. See Table S3 for details.

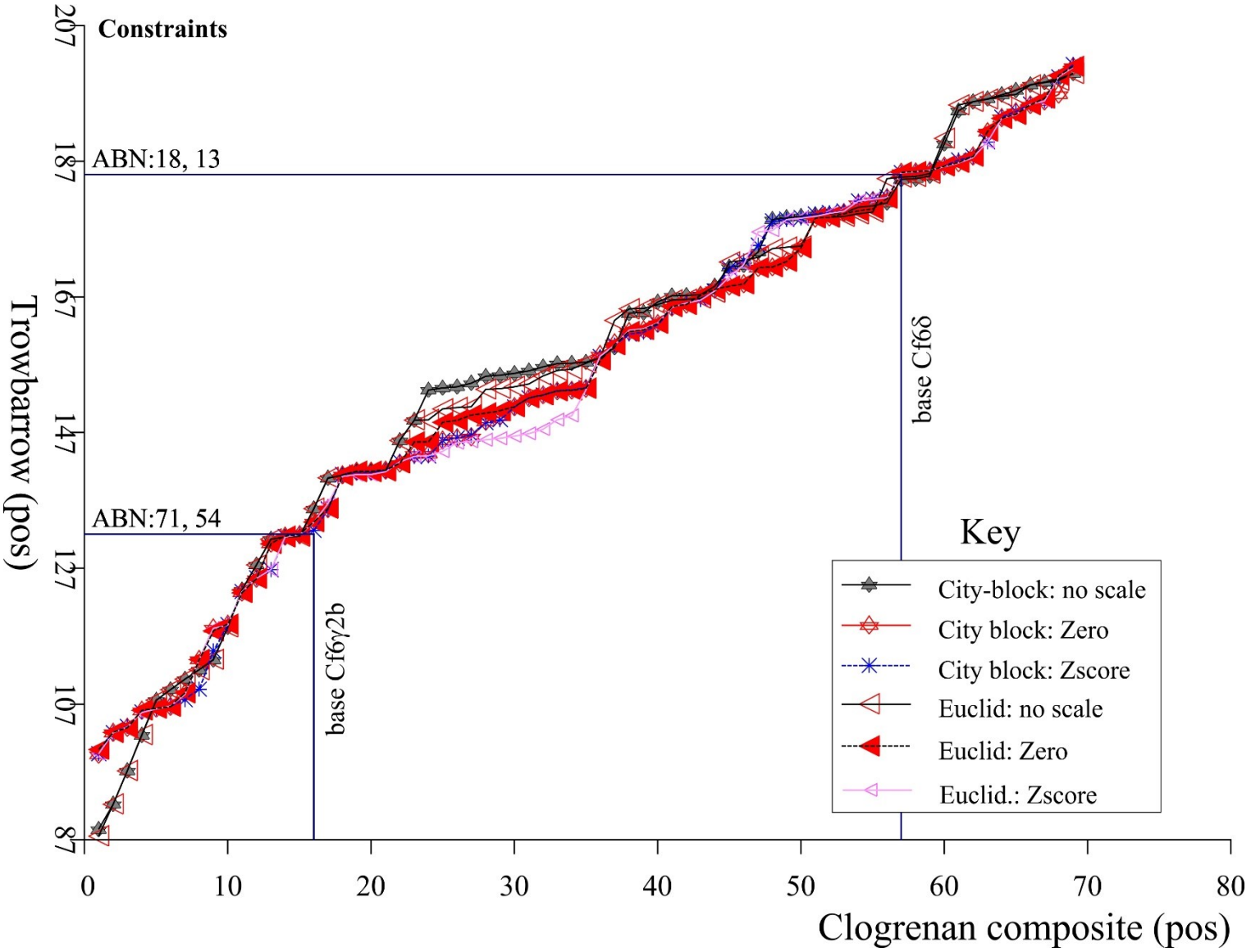

Fig. S12. The correlation models for the six slotting solutions at the composite Clogrenan section. See Fig S10 for details.

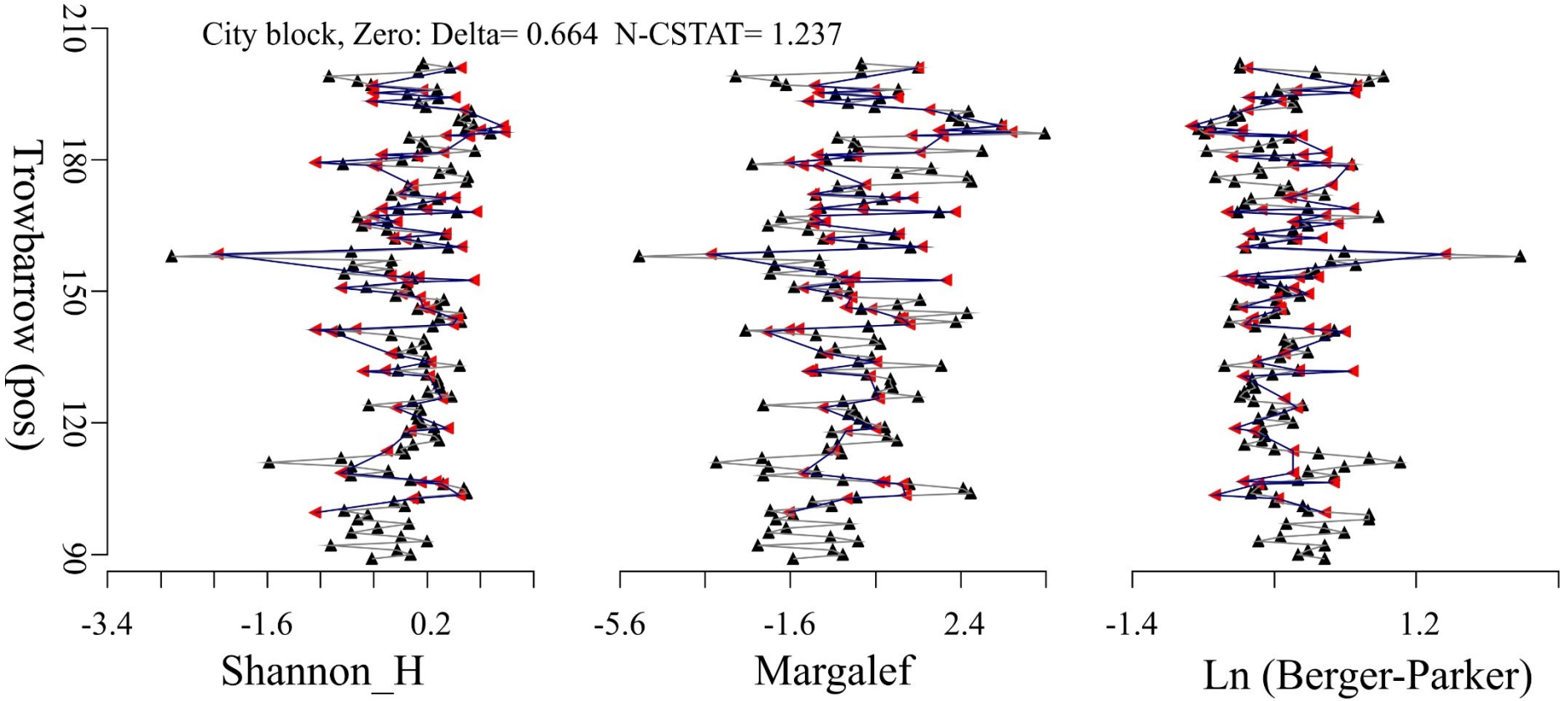

Fig. S13. The overlaid slotted diversity data for Trowbarrow (in black) and Clogrenan (in red). Diversity indexes have been plotted with data scaled to a mean of zero. The y-axis is the sample position at Trowbarrow, and in the case of the Clogrenan data are the position (possibly non integer) of the estimated position using the slotting method indicated.

BALLYADAMS

Model	Delta	N-CSTAT	Na/Nb	RV2	RVstd	Delta	N-CStat	RV2	RVstd	Score total
Slot [Eucl,none]{5 cons}	1.042	2.626	202/118	0.3156	0.8139	4	5	5	4	18
Slot [Eucl,Zero]{5 cons}	0.686	0.32	202/118	0.3232	0.8336	3	2	3	1	9
Slot [Eucl,ZSco]{5 cons}	0.682	-0.321	202/118	0.3269	0.8216	2	0	1	2	5
Slot [City,none]{5 cons}	1.055	2.551	202/118	0.3175	0.8188	5	4	4	3	16
Slot [City,Zero]{5 cons}	0.67	0.246	202/118	0.3233	0.8338	1	3	2	0	6
Slot [City,ZSco]{5 cons}	0.652	-0.67	202/118	0.3502	0.4806	0	1	0	5	6

Table S5. Slotting model assessment table for the Trowbarrow to Ballyadams sequence slotting models. See Table S3 for details.

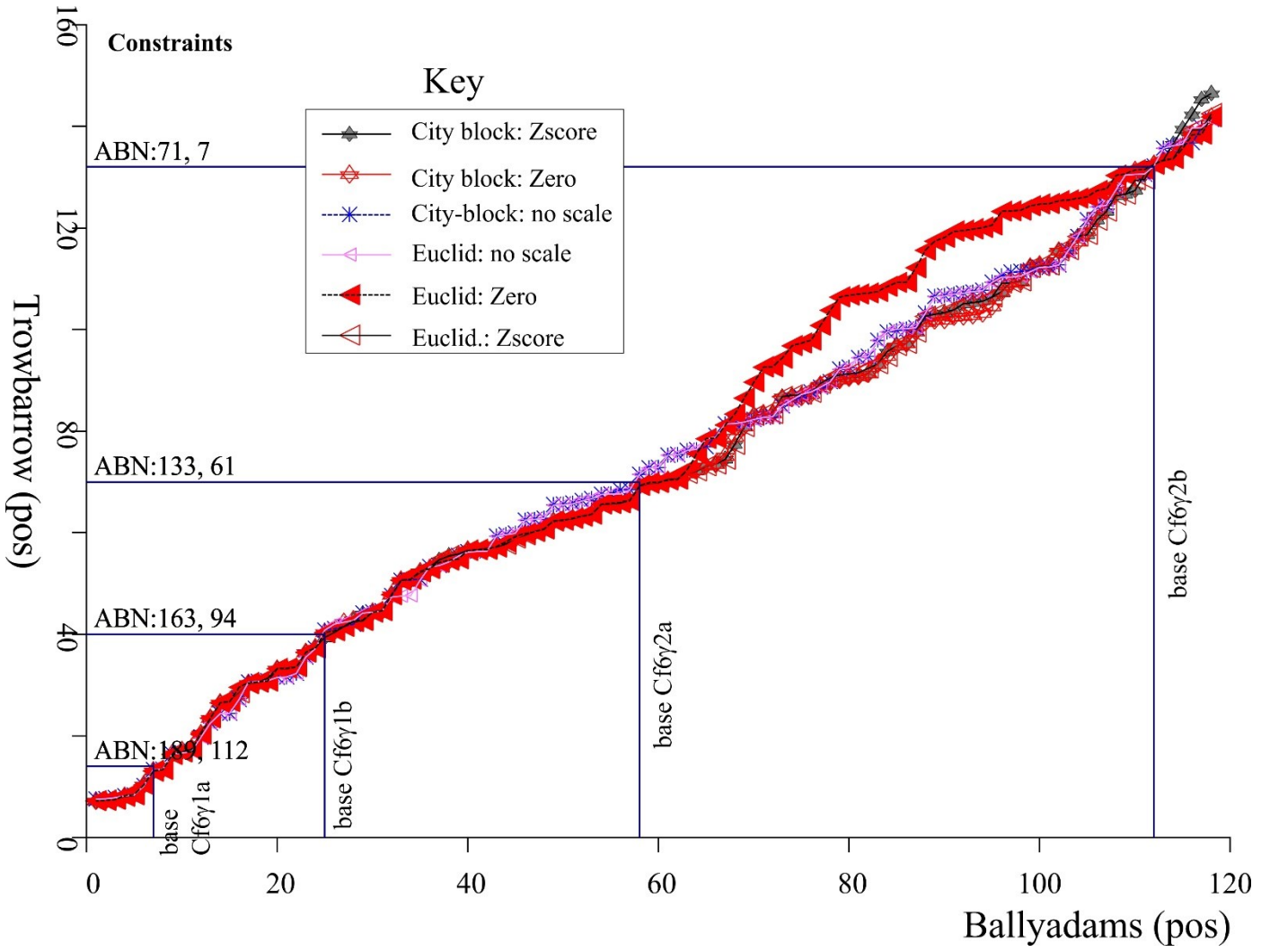

Fig. S14. The correlation models for the six slotting solutions at the Ballyadams section. See Fig S10 for details.

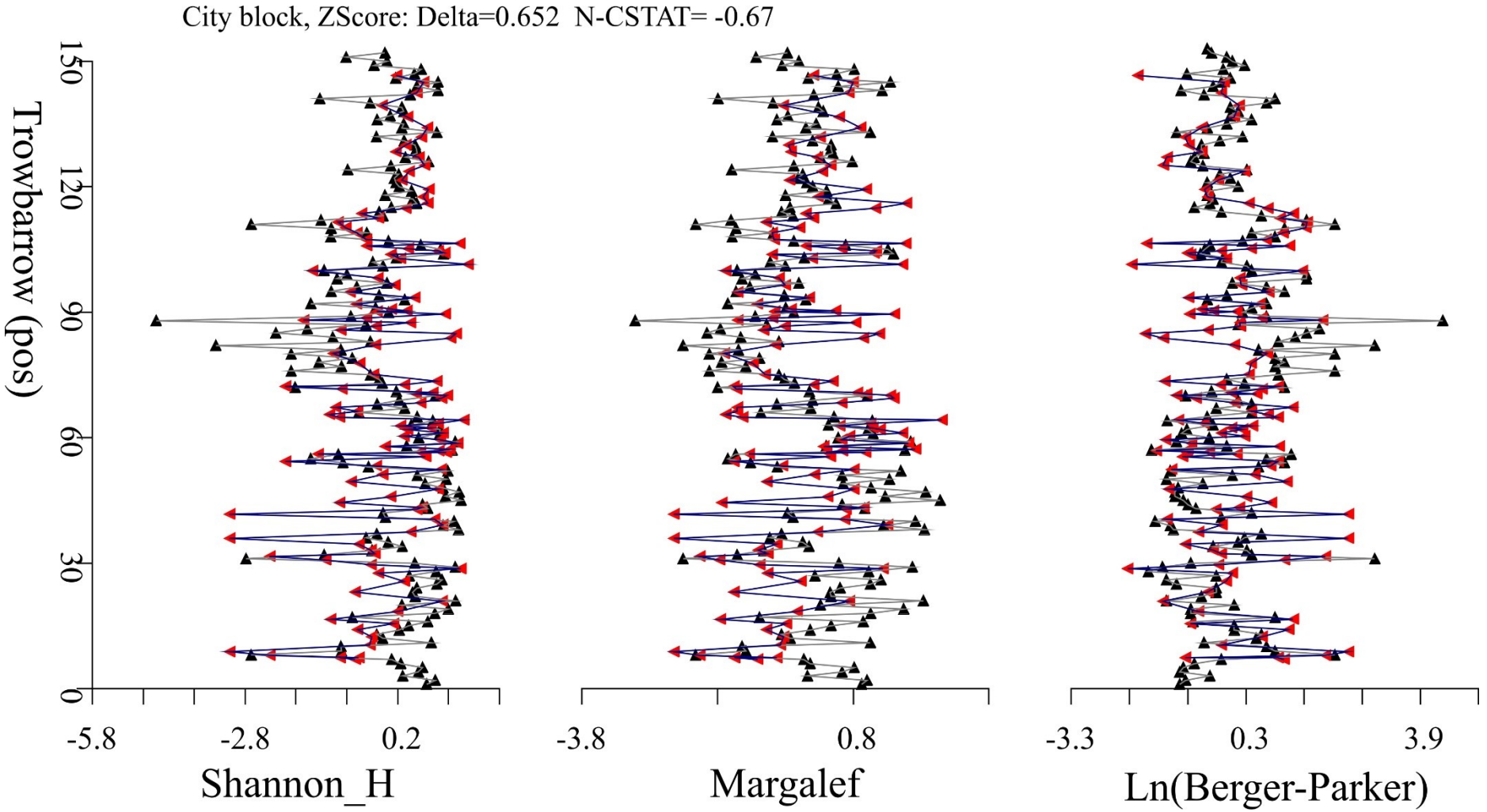

Fig. S15. The overlaid slotted diversity data for Trowbarrow (in black) and Ballyadams (in red). Diversity indexes have been plotted with data scaled to a mean of zero and a standard deviation of 1 (i.e. Zscore). The y-axis is the sample position at Trowbarrow, and in the case of Port Eynon data are the estimated positions (possibly non integer) using the slotting metric and scaling indicated.

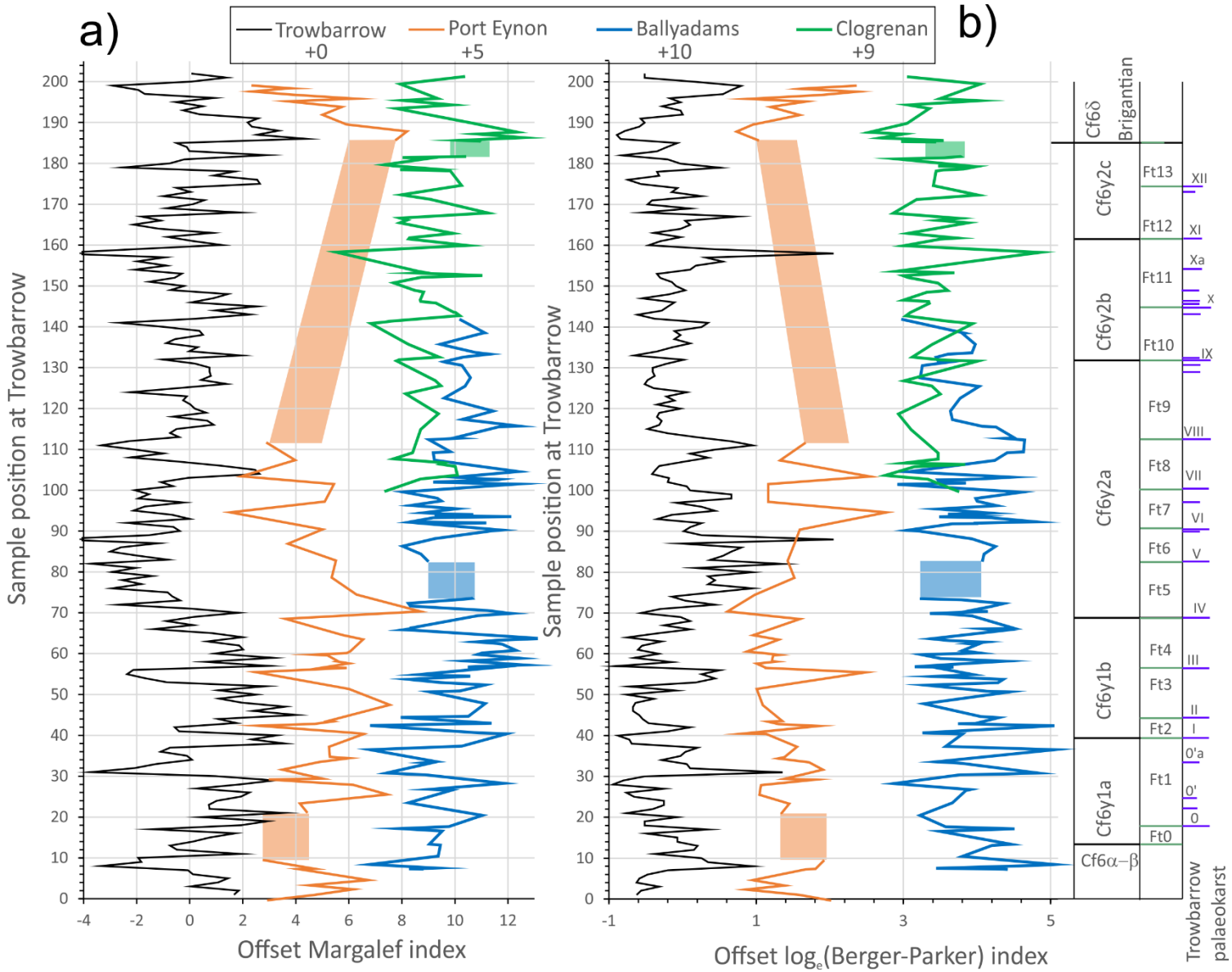

Fig. S16. Summary of diversity data in the sections, with sample positions at Trowbarrow based on the slotting analysis. The inferred hiatuses are displayed as square coloured blocks. For each section the data is displayed with the a) Margalef and b) Berger-Parker indexes. Offsets applied to the mean Margalef diversity indices are shown in the top key. i.e. offsets of 0, 5, 10 and 9 for Margalef and 0, +1.5, +4 and +3.5 for Log_e(Berger-Parker) respectively.

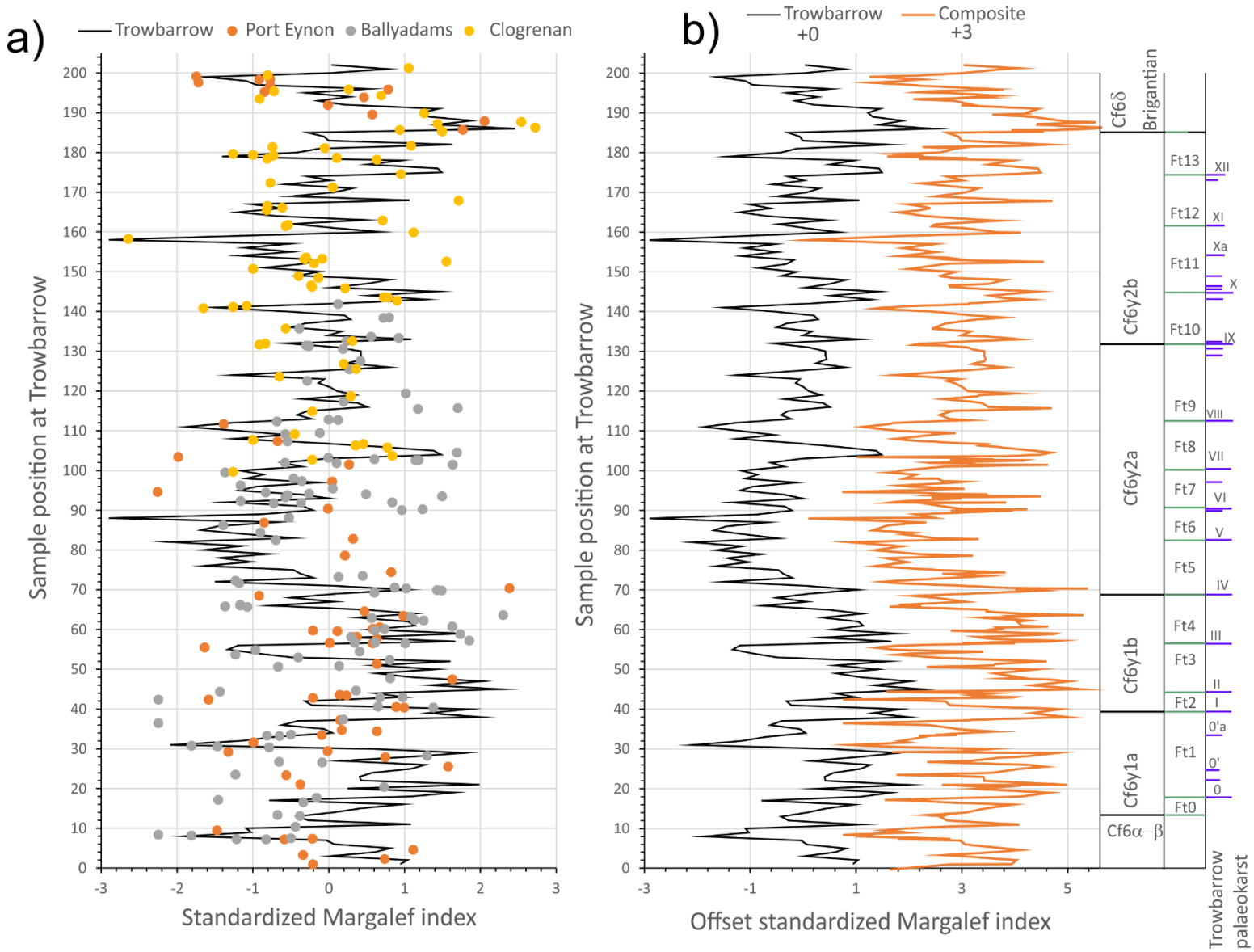

Fig. S17. Standardized composite diversity indices for the sections. The data have been standardized by converting all data to section-means of zero and standard deviation of 1.0, to try and account for the between section-differences in the range of the diversity indices. A) Shows the data for Trowbarrow as a line and the other sections as dots as a visual assessment of the mis-match between the sets of data. B) shows the Trowbarrow data as the black line and a composite of the entire dataset displayed with a mean offset of +3. The difference between these two curves is a measure of the disparity in the datasets, and also possibly incomplete parts at Trowbarrow such as over the Woodbine Shale interval (upper Ft4) and in Ft5 and Ft7.

Table S6. Diversity indices using in the slotting analysis for Trowbarrow. Position is the sample number ordered from the base of the section. Ln(BP)= Log_e (Berger-Parker)

Position	Shannon_H	Margalef	Ln(BP)	Height (m)	Position	Shannon_H	Margalef	Ln(BP)	Height (m)
202	2.832	5.218	-2.565	193.185	175	3.316	7.809	-2.615	160.915
201	3.139	6.551	-2.565	192.035	174	2.657	4.66	-2.120	159.765
200	2.778	5.218	-1.872	190.485	173	2.736	5.19	-2.197	157.605
199	1.772	2.274	-1.253	186.585	172	2.476	4.152	-1.792	156.285
198	2.095	3.219	-1.386	185.735	171	2.998	5.714	-2.464	155.555
197	2.245	3.46	-1.504	184.885	170	2.831	5.281	-2.526	154.355
196	2.992	6.093	-2.225	183.085	169	2.558	4.27	-1.946	153.355
195	2.653	4.617	-2.079	182.975	168	3.212	7.048	-2.590	151.515
194	2.999	5.655	-2.327	182.185	167	2.098	3.336	-1.299	150.385
193	2.783	4.905	-2.079	181.235	166	2.431	4.062	-2.015	150.065
192	2.864	5.533	-2.048	181.205	165	2.144	3.031	-1.946	149.315
191	3.374	7.736	-2.621	179.545	164	2.426	3.967	-2.079	148.605
190	3.308	7.339	-2.565	178.505	163	3.079	6.007	-2.442	147.825
189	3.233	7.503	-2.639	177.015	162	2.513	4.328	-2.079	144.935
188	3.404	8.507	-2.833	174.305	161	2.78	5.255	-2.351	143.915
187	3.309	7.697	-2.944	172.005	160	3.11	6.37	-2.512	143.365
186	3.594	9.526	-2.890	169.555	159	2.025	3.04	-1.609	140.965
185	2.678	4.66	-2.120	168.855	158	0	0	0.000	140.065
184	2.823	5.049	-2.269	168.005	157	2.476	4.235	-1.734	139.645
183	2.861	5.148	-2.398	167.805	156	2.043	3.186	-1.504	139.045
182	3.418	8.06	-2.872	166.535	155	2.458	4.289	-1.872	138.445
181	2.771	4.948	-2.251	166.015	154	1.946	3.083	-1.946	136.995
180	2.593	4.405	-2.079	164.995	153	2.713	4.853	-2.398	134.865
179	1.933	2.652	-1.540	163.815	152	2.648	4.598	-2.351	133.915
178	3.145	6.864	-2.398	162.975	151	2.197	3.641	-2.197	133.495
177	3.016	6.059	-2.367	162.115	150	2.67	4.941	-2.140	132.705

176	3.34	7.708	-2.793	161.515	149	2.523	4.431	-2.015	131.425
148	3.066	6.602	-2.234	130.635	117	2.97	5.824	-2.335	93.72
147	2.988	6.068	-2.603	129.735	116	3.016	6.059	-2.367	92.9
146	2.771	5.218	-2.159	128.485	115	2.72	4.66	-2.526	91.95
145	3.259	7.697	-2.251	127.755	114	2.58	4.415	-2.251	90.82
144	3.015	6.115	-2.335	126.105	113	2.625	4.755	-1.846	89.39
143	3.261	7.444	-2.663	124.725	112	1.906	2.885	-1.386	89.01
142	2.94	5.388	-2.428	123.625	111	1.099	1.82	-1.099	87.94
141	1.894	2.502	-1.705	121.875	110	2.025	3.04	-1.609	86.96
140	2.476	4.152	-1.792	120.775	109	2.441	4.168	-1.946	85.91
139	2.845	5.525	-2.159	119.775	108	2.02	2.919	-1.705	85.06
138	2.867	5.664	-2.079	118.375	107	2.691	4.784	-2.037	83.89
137	2.705	4.604	-2.159	117.275	106	3.059	6.348	-2.367	82.74
136	2.558	4.27	-1.946	116.775	105	3.291	7.618	-2.420	81.99
135	2.866	5.461	-2.197	115.975	104	3.326	7.792	-2.464	80.84
134	2.845	5.148	-2.398	115.075	103	2.781	5.102	-2.234	79.74
133	3.248	7.093	-2.708	112.575	102	2.507	4.075	-2.251	78.44
132	2.548	4.146	-2.037	110.215	101	2.626	4.529	-1.992	77.64
131	2.871	5.346	-2.269	109.365	100	1.946	3.083	-1.946	76.84
130	2.996	5.907	-2.457	107.965	99	2.21	3.622	-1.386	76.34
129	3.011	5.907	-2.457	106.965	98	2.095	3.219	-1.386	75.74
128	3.022	5.955	-2.428	105.665	97	2.67	4.941	-2.140	74.64
127	2.886	5.592	-2.526	104.165	96	2.322	3.46	-1.792	74.04
126	3.153	6.551	-2.565	102.765	95	2.025	3.04	-1.609	72.24
125	2.714	4.784	-2.442	101.865	94	2.582	4.498	-2.197	71.34
124	2.216	2.912	-1.992	101.165	93	2.877	5.148	-2.398	70.04
123	2.805	5.049	-2.269	99.965	92	1.792	2.791	-1.792	69.14
122	2.758	4.911	-2.159	98.165	91	2.54	4.547	-1.946	67.64
121	2.776	5.176	-2.398	97.065	90	2.691	4.784	-2.037	67.04
120	2.81	5.349	-2.079	96.265	89	2.254	3.622	-1.792	65.94
119	2.956	5.771	-2.367	95.765	88	0	0	0.000	64.99

118	2.65	4.529	-2.398	95.02	87	2.426	3.967	-2.079	63.89
86	1.748	2.569	-1.253	63.39	55	1.792	2.791	-1.792	31.6
85	1.386	2.164	-1.386	62.77	54	2.164	3.474	-1.609	31.2
84	2.043	3.186	-1.504	61.87	53	2.458	4.289	-1.872	29.95
83	2.48	4.328	-1.674	61.12	52	3.376	8.008	-2.773	29
82	0.6931	1.443	-0.693	60.89	51	3.022	6.239	-2.140	28
81	2.138	3.119	-1.872	60.39	50	3.354	7.669	-2.813	27.25
80	1.561	2.232	-1.099	59.49	49	3.109	6.269	-2.442	26.25
79	2.272	3.753	-1.705	57.69	48	3.319	7.112	-2.691	24.95
78	1.887	2.606	-1.609	56.84	47	3.508	8.757	-2.725	24.45
77	2.146	3.336	-1.705	56.24	46	3.349	7.541	-2.725	22.95
76	1.561	2.232	-1.099	55.69	45	3.527	9.192	-2.639	22.45
75	2.48	4.328	-1.674	54.29	44	3.082	6.235	-2.590	21.45
74	2.582	4.498	-2.197	53.29	43	3.142	6.923	-2.512	20.55
73	2.616	4.801	-2.015	51.5	42	2.624	4.598	-1.946	19.55
72	1.609	2.485	-1.609	49.5	41	2.653	4.755	-2.251	18.45
71	2.78	5.255	-2.351	48.8	40	3.449	8.446	-2.927	17.2
70	3.227	7.001	-2.615	47.95	39	3.319	7.491	-2.773	15.2
69	2.81	5.349	-2.079	47.4	38	3.495	8.723	-2.741	14.7
68	2.558	4.27	-1.946	47	37	2.552	4.415	-1.846	13.98
67	2.875	5.292	-2.303	46.6	36	2.431	4.062	-2.015	12.5
66	2.342	3.789	-1.946	44.25	35	2.686	5.049	-2.079	11.8
65	3.019	6.006	-2.398	41.66	34	2.847	5.242	-2.335	10.97
64	3.202	7.15	-2.803	39.79	33	2.5	3.882	-1.992	10.3
63	2.953	5.824	-2.335	39.36	32	1.946	3.083	-1.946	9.24
62	3.283	7.019	-2.603	38.88	31	1.04	1.443	-0.693	8.75
61	3.277	7.173	-2.657	36.9	30	2.992	6.139	-2.565	7.1
60	3.04	6.115	-2.375	36.1	29	3.461	8.352	-2.853	6.6
59	3.459	8.304	-2.708	35.2	28	3.238	7.048	-2.996	5.1
58	2.898	5.765	-2.197	33.9	27	2.93	5.422	-2.303	4.05
57	3.424	8.127	-2.962	33.3	26	3.305	7.413	-2.813	3.3

56	2.107	3.031	-1.540	32.3	25	3.248	7.093	-2.708	2.68
24	3.014	6.174	-2.303	1.65					
23	2.968	5.88	-2.303	1.3					
22	2.996	5.907	-2.457	1.25					
21	3.465	8.691	-2.813	0.9					
20	2.844	5.592	-2.120	0.36					
19	3.378	8.099	-2.565	0.2					
18	3.224	7.097	-2.565	-0.25					
17	2.272	3.753	-1.705	-0.55					
16	3.145	6.873	-2.539	-1					
15	2.921	5.903	-2.120	-1.7					
14	2.81	5.281	-2.120	-1.95					
13	2.552	4.415	-1.846	-2.85					
12	2.623	4.673	-1.897	-2.9					
11	3.185	7.089	-2.428	-4.8					
10	2.138	3.219	-1.792	-6.7					
9	2.146	3.336	-1.705	-8.25					
8	1.099	1.82	-1.099	-9.45					
7	2.726	5.094	-2.251	-11.35					
6	2.831	5.281	-2.526	-13.2					
5	3.085	6.602	-2.639	-14.4					
4	3.033	6.236	-2.674	-16.1					
3	2.853	5.194	-2.367	-17.35					
2	3.227	7.001	-2.615	-19.05					
1	3.128	6.83	-2.674	-20.8					

Table S7. Diversity indices using in the slotting analysis for Port Eynon. Position is the sample number ordered from the base of the section. Ln(BP)= Log_e (Berger-Parker). Position at TQ= position in the Trowbarrow section based on the slotting analysis and position revisions based on inferred hiatuses.

Position	Shannon_H	Margalef	Ln(BP)	Position at TQ	position	Shannon_H	Margalef	Ln(BP)	Position at TQ
64	1.561	2.232	-1.099	199.08	37	3.034	5.964	-2.590	60.56
63	2.406	3.736	-1.846	198.36	36	2.953	5.824	-2.335	60.14
62	2.245	3.509	-1.872	198.3	35	2.685	4.604	-2.159	59.73
61	1.677	2.276	-1.099	197.58	34	2.800	5.102	-2.234	59.6
60	2.333	3.736	-1.558	196.8	33	2.940	5.498	-2.251	58.18
59	2.992	6.139	-2.565	195.85	32	2.827	5.461	-2.197	58.08
58	2.254	3.622	-1.792	195.19	31	2.996	5.907	-2.457	57.61
57	2.901	5.643	-2.269	193.83	30	2.785	4.951	-2.335	56.63
56	2.705	4.911	-1.872	191.88	29	2.953	5.824	-2.335	56.53
55	2.978	5.816	-2.512	189.53	28	1.667	2.404	-0.981	55.48
54	3.395	8.097	-2.730	187.82	27	2.996	5.907	-2.457	51.38
53	3.266	7.657	-2.428	185.65	26	3.265	7.444	-2.375	47.46
52	1.792	2.791	-1.792	111.68	25	2.835	5.148	-2.110	43.55
51	2.425	3.883	-2.140	107.36	24	2.841	5.292	-2.303	43.39
50	1.332	1.864	-0.916	103.42	23	2.685	4.604	-2.159	42.78
49	2.788	5.341	-2.303	101.51	22	1.609	2.485	-1.609	42.35
48	2.812	4.998	-2.303	97.19	21	3.035	6.302	-2.639	40.5
47	0.693	1.443	-0.693	94.6	20	3.105	6.463	-2.327	40.35
46	2.672	4.911	-1.872	90.41	19	2.763	5.158	-1.910	37.22
45	2.376	3.613	-1.946	86.88	18	2.816	5.194	-2.079	34.73
44	2.811	5.422	-2.037	82.79	17	2.946	5.907	-2.169	34.39
43	2.756	5.255	-1.946	78.61	16	2.653	4.784	-1.749	33.48
42	3.145	6.200	-2.485	74.42	15	2.215	3.396	-1.558	31.62
41	3.458	8.605	-2.853	70.36	14	2.767	4.905	-2.079	29.39
40	2.245	3.509	-1.872	68.5	13	2.068	2.885	-1.674	29.19
39	3.068	5.653	-2.506	64.56	12	3.024	6.078	-2.398	27.85

38	3.025	6.445	-2.159	63.45	11	3.221	7.356	-2.420	25.51
10	2.431	4.062	-2.015	23.32					
9	2.643	4.349	-2.120	21					
8	2.008	2.652	-1.540	9.48					
7	2.582	4.598	-1.658	7.36					
6	2.369	4.024	-1.792	7.23					
5	3.133	6.647	-2.512	4.59					
4	2.636	4.405	-2.079	3.29					
3	2.988	6.068	-2.603	2.29					
2	2.651	4.604	-1.872	0.96					
1	2.069	2.824	-1.447	-0.37					

Table S8. Diversity indices using in the slotting analysis for Clogrenan composite. Position is the sample number ordered from the base of the composite section. Pos-S= position in either Clogrenan Quarry (Clog-Q) or the Clogrenan B corehole (Clog-B). Ln(BP)= Log_e (Berger-Parker). Position at TQ= position in the Trowbarrow section based on the slotting analysis and position revisions based on inferred hiatuses.

Pos-S	Position	Shannon_H	Margalef	Ln_BP	Section	Position at TQ	Pos-1	Position	Shannon_H	Margalef	Ln_BP		Position in TQ
23	69	2.736	4.865	-1.808	Clog-Q	201.22	10	56	2.542	4.905	-1.082	Clog-Q	181.68
22	68	1.735	2.422	-0.811	Clog-Q	199.4	9	55	1.846	2.502	-1.299	Clog-Q	181.36
21	67	2.306	3.821	-1.361	Clog-Q	195.86	8	54	2.243	3.41	-1.946	Clog-Q	181.1
20	66	1.748	2.525	-0.827	Clog-Q	195.37	7	53	1.099	1.82	-1.099	Clog-Q	179.61
19	65	2.671	4.386	-1.792	Clog-Q	194.3	6	52	1.787	2.164	-1.386	Clog-Q	179.36
18	64	1.735	2.276	-1.504	Clog-Q	193.42	5	51	1.751	2.519	-0.879	Clog-Q	179.17
17	63	2.765	5.128	-1.805	Clog-Q	189.81	4	50	2.192	3.616	-1.038	Clog-Q	178.64
16	62	3.209	6.811	-2.319	Clog-Q	187.65	3	49	2.058	2.414	-1.310	Clog-Q	178.43
15	61	2.95	5.359	-1.856	Clog-Q	187.16	2	48	2.503	4.309	-1.411	Clog-Q	178.14
14	60	3.23	7.054	-2.165	Clog-Q	186.27	1	47	2.67	4.727	-1.447	Clog-Q	174.56
13	59	2.562	4.708	-1.308	Clog-Q	185.61	46	46	1.845	2.463	-0.842	Clog-B	172.28
12	58	2.833	5.434	-1.887	Clog-Q	185.38	45	45	2.35	3.547	-1.678	Clog-B	171.18
11	57	2.818	5.446	-1.411	Clog-Q	185.27	44	44	2.908	5.728	-1.992	Clog-B	167.85

43	43	1.748	2.415	-1.099	Clog-B	166.55	12	12	2.525	3.95	-1.471	Clog-B	125.55
42	42	2.013	2.67	-1.386	Clog-B	166.09	11	11	2.008	2.621	-1.354	Clog-B	123.57
41	41	1.667	2.404	-0.981	Clog-B	165.44	10	10	2.591	3.858	-1.922	Clog-B	118.67
40	40	2.561	4.41	-1.792	Clog-B	162.87	9	9	2.171	3.189	-1.749	Clog-B	114.85
39	39	1.98	2.769	-1.126	Clog-B	161.75	8	8	1.906	2.885	-1.386	Clog-B	109.14
38	38	2.113	2.73	-1.361	Clog-B	161.48	7	7	1.386	2.164	-1.386	Clog-B	107.65
37	37	2.743	4.948	-1.846	Clog-B	159.87	6	6	2.452	4.075	-1.846	Clog-B	106.67
36	36	0	0	0.000	Clog-B	158.21	5	5	2.285	3.94	-1.016	Clog-B	106.32
35	35	1.946	3.083	-1.946	Clog-B	153.59	4	4	2.531	4.492	-1.705	Clog-B	105.79
34	34	2.261	3.366	-1.163	Clog-B	153.25	3	3	2.727	4.578	-2.104	Clog-B	103.64
33	33	2.101	3.057	-1.335	Clog-B	153.14	2	2	2.198	3.189	-1.526	Clog-B	102.72
32	32	2.884	5.517	-1.860	Clog-B	152.52	1	1	1.099	1.82	-1.099	Clog-B	99.64
31	31	2.138	3.219	-1.792	Clog-B	152.08							
30	30	1.386	2.164	-1.386	Clog-B	150.71							
29	29	2.07	2.956	-1.253	Clog-B	148.89							
28	28	2.277	3.301	-1.540	Clog-B	148.46							
27	27	2.324	3.174	-1.856	Clog-B	146.56							
26	26	2.302	3.188	-1.513	Clog-B	146.19							
25	25	2.385	3.76	-1.504	Clog-B	145.79							
24	24	2.656	4.433	-1.758	Clog-B	143.54							
23	23	2.703	4.5	-1.764	Clog-B	143.46							
22	22	2.649	4.659	-1.824	Clog-B	142.7							
21	21	1.55	2.056	-1.253	Clog-B	141.36							
20	20	1.099	1.82	-1.099	Clog-B	141.13							
19	19	1.099	1.82	-1.099	Clog-B	141.13							
18	18	1.28	1.303	-0.916	Clog-B	140.78							
17	17	1.951	2.729	-1.466	Clog-B	135.69							
16	16	2.395	3.883	-1.734	Clog-B	132.58							
15	15	1.882	2.377	-1.335	Clog-B	131.9							
14	14	1.636	2.274	-0.847	Clog-B	131.63							
13	13	2.379	3.736	-1.846	Clog-B	126.81							

Table S9. Diversity indices using in the slotting analysis for Ballyadams. Position is the sample number ordered from the base of the composite section. Ln(BP)= Log_e (Berger-Parker). Position at TQ= position in the Trowbarrow section based on the slotting analysis and position revisions based on inferred hiatuses.

position	Shannon_H	Margalef	Ln(BP)	Position at TQ	position	Shannon_H	Margalef	Ln(BP)	Position at TQ
118	2.079	3.366	-2.079	141.86	93	2.229	4.049	-0.956	102.81
117	2.418	4.324	-1.224	138.49	92	2.601	4.877	-1.253	102.61
116	2.335	4.219	-1.253	138.4	91	2.684	4.820	-1.584	102.54
115	1.902	2.643	-1.076	135.71	90	2.014	2.377	-1.558	101.93
114	2.219	3.988	-1.122	133.64	89	2.129	3.338	-1.204	101.8
113	2.467	4.503	-1.447	133.3	88	2.971	5.516	-2.135	101.45
112	2.390	3.528	-1.609	132.57	87	1.034	1.251	-0.452	99.53
111	2.200	2.771	-1.573	131.44	86	1.845	2.534	-1.069	98
110	2.069	2.824	-1.447	131.32	85	2.060	2.688	-1.052	97.36
109	2.362	3.461	-1.792	130.53	84	1.504	1.541	-0.782	96.229
108	2.434	3.786	-1.824	127.5	83	2.309	3.267	-1.576	95.44
107	2.236	3.579	-1.022	125.44	82	1.583	2.012	-0.875	94.448
106	2.150	2.791	-1.281	122.51	81	2.018	2.824	-1.447	94.165
105	2.484	4.637	-1.413	119.36	80	2.211	3.892	-1.329	94.021
104	2.415	3.474	-1.386	117.3	79	1.834	2.427	-1.099	93.797
103	2.475	5.609	-0.981	115.67	78	2.689	5.317	-1.564	93.52
102	2.200	4.865	-0.796	115.49	77	1.706	2.383	-0.854	93.253
101	1.645	3.191	-0.542	112.8	76	0.919	1.542	-0.254	92.267
100	1.854	3.367	-0.670	112.69	75	2.254	4.382	-1.068	91.968
99	1.353	2.222	-0.405	112.3	74	1.824	2.676	-1.066	91.845
98	1.447	3.024	-0.419	109.42	73	1.386	2.164	-1.386	91.771
97	1.587	2.377	-0.642	109.16	72	2.826	4.952	-2.005	90.229
96	1.706	2.422	-0.811	107.32	71	2.758	4.564	-1.824	90
95	2.869	5.594	-1.988	104.53	70	1.817	2.449	-1.122	88.125
94	1.708	3.188	-0.581	103.19	69	1.290	1.218	-0.800	86.25

68	1.619	1.911	-0.956	84.375	37	0.693	1.443	-0.693	53.7
67	1.791	2.203	-0.981	82.5	36	1.831	2.623	-0.768	52.92
66	2.580	3.829	-1.810	73.48	35	2.636	4.337	-1.743	52.31
65	2.178	3.376	-1.264	73.21	34	1.909	3.385	-0.921	50.83
64	0.693	1.443	-0.693	72.29	33	1.512	2.246	-0.606	50.63
63	1.400	1.516	-0.847	71.63	32	2.603	4.343	-1.772	47.75
62	2.530	4.428	-1.155	70.52	31	2.007	3.706	-1.003	44.63
61	2.328	4.647	-0.903	70.35	30	1.373	1.154	-0.758	44.37
60	2.711	5.223	-1.692	69.88	29	2.396	4.577	-1.074	42.94
59	2.647	5.310	-1.504	69.79	28	2.338	4.154	-1.308	42.89
58	2.387	4.049	-1.118	69.27	27	0.000	0.000	0.000	42.37
57	1.323	1.535	-0.550	66.23	26	2.555	4.116	-1.792	40.6
56	1.594	1.535	-0.956	66.08	25	2.659	5.150	-1.247	40.34
55	1.241	1.251	-0.789	65.81	24	2.257	3.463	-1.478	37.33
54	1.373	1.669	-0.693	65.69	23	0.000	0.000	0.000	36.48
53	2.920	6.461	-1.679	63.66	22	1.609	2.485	-1.609	33.54
52	2.603	4.737	-1.425	63.24	21	1.764	2.038	-1.335	33.29
51	2.130	3.997	-0.947	62.82	20	1.810	2.274	-1.253	33.18
50	2.514	4.798	-1.151	62.44	19	0.500	0.621	-0.223	30.78
49	2.220	4.973	-1.042	62.28	18	1.194	1.108	-0.629	30.6
48	2.666	5.510	-1.253	60.76	17	1.765	2.076	-1.281	30.34
47	2.173	4.237	-1.024	60.18	16	2.887	5.037	-2.179	28.24
46	2.626	4.052	-1.804	59.75	15	1.857	2.265	-1.145	26.73
45	2.846	5.658	-1.547	58.84	14	2.181	3.067	-1.204	26.54
44	1.937	3.612	-0.680	58.17	13	1.560	1.443	-1.386	23.48
43	2.749	5.826	-1.581	57.2	12	2.649	4.231	-1.828	20.41
42	2.612	4.066	-1.897	56.79	11	2.097	2.968	-1.478	17.64
41	2.380	3.679	-1.370	56.68	10	1.256	1.122	-0.542	17.15
40	2.702	4.625	-1.589	56.55	9	2.041	2.717	-1.558	16.54
39	1.099	1.820	-1.099	54.86	8	1.597	2.232	-0.588	13.35
38	2.443	3.770	-1.634	54.45	7	1.772	2.652	-0.847	13.08

6	1.748	2.569	-1.253	10.38
5	0.000	0.000	0.000	8.4
4	0.500	0.621	-0.223	8.17
3	1.609	2.485	-1.609	7.49
2	1.374	1.470	-0.693	7.28
1	1.565	2.020	-0.632	7.21

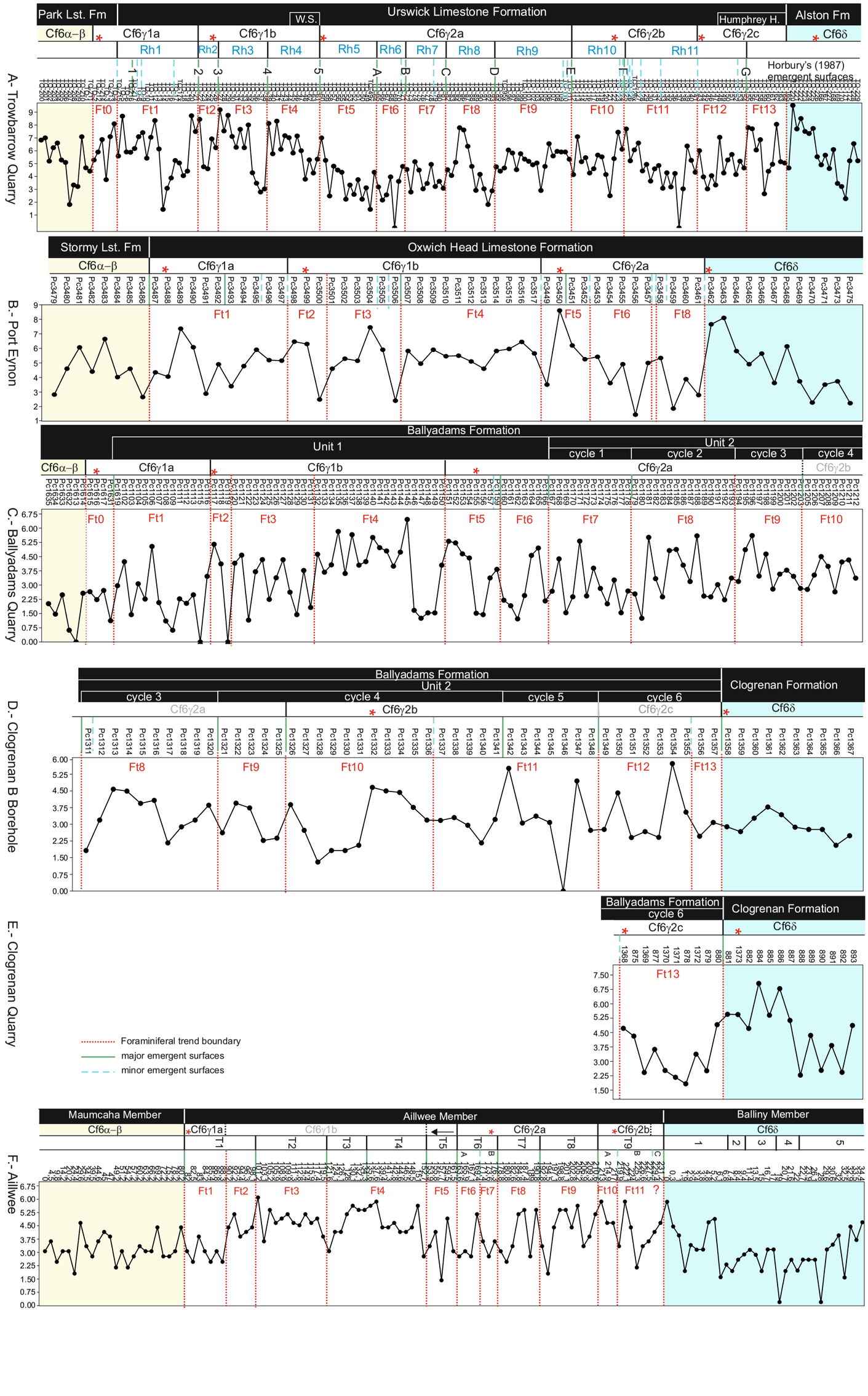

Fig. S1. Margalef diversity index in A. Trowbarrow Quarry, B. Port Eynon, C. Ballyadams Quarry, D. Clogrenan B Borehole, E. base of Clogrenan Quarry, F Aillwee sections. Other remarks as in Figs. 3 and 4.

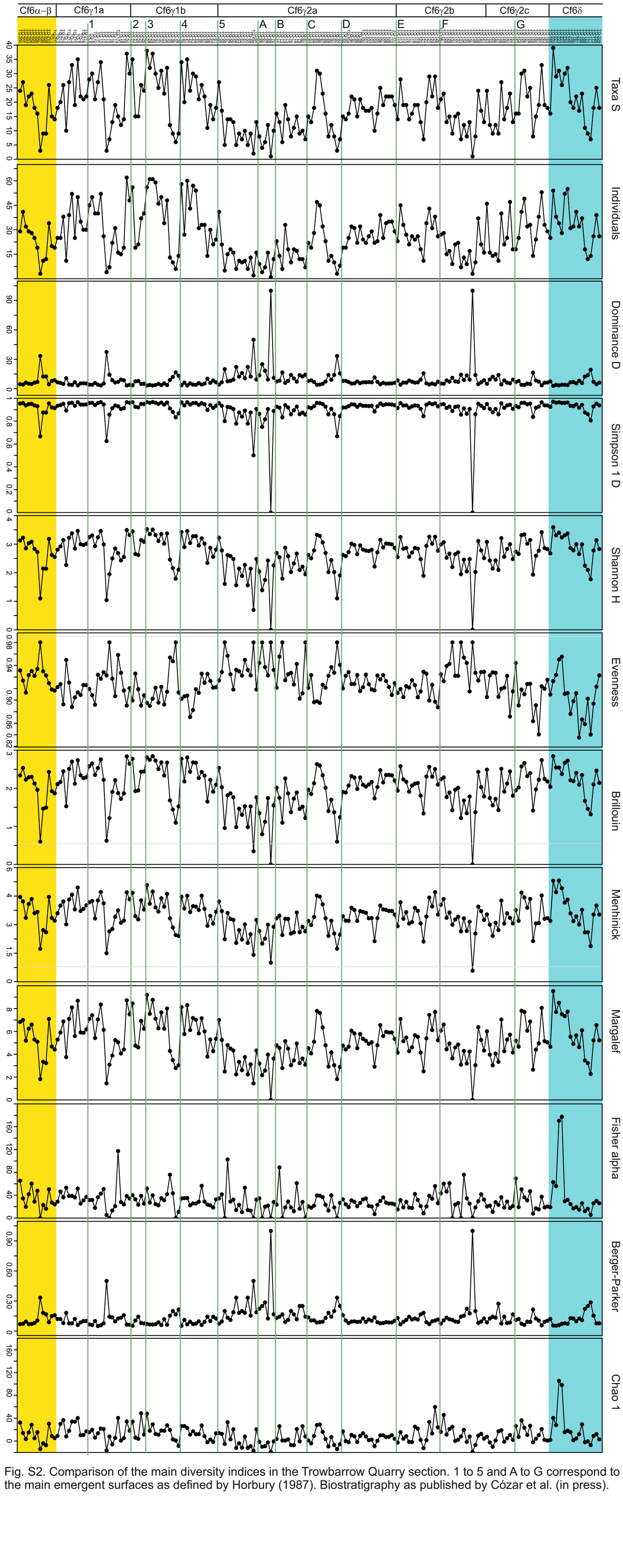

Fig. S2. Comparison of the main diversity indices in the Trowbarrow Quarry section. 1 to 5 and A to G correspond to the main emergent surfaces as defined by Horbury (1987). Biostratigraphy as published by Cózar et al. (in press).

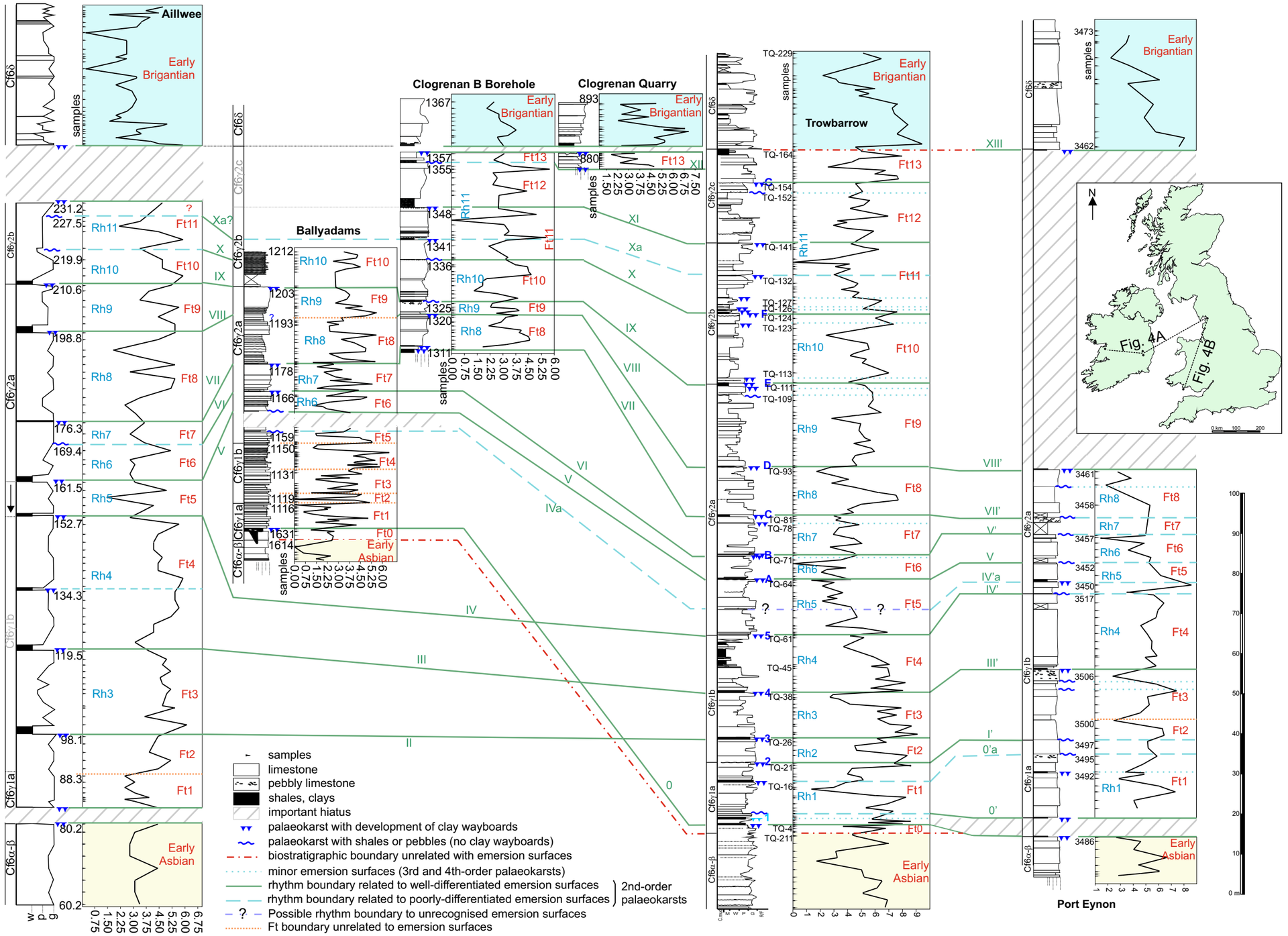

Fig. S3. Correlation of the foraminiferal trends (Ft), sedimentological rhythms (Rh) and major and minor emergent surfaces in the studied basins.

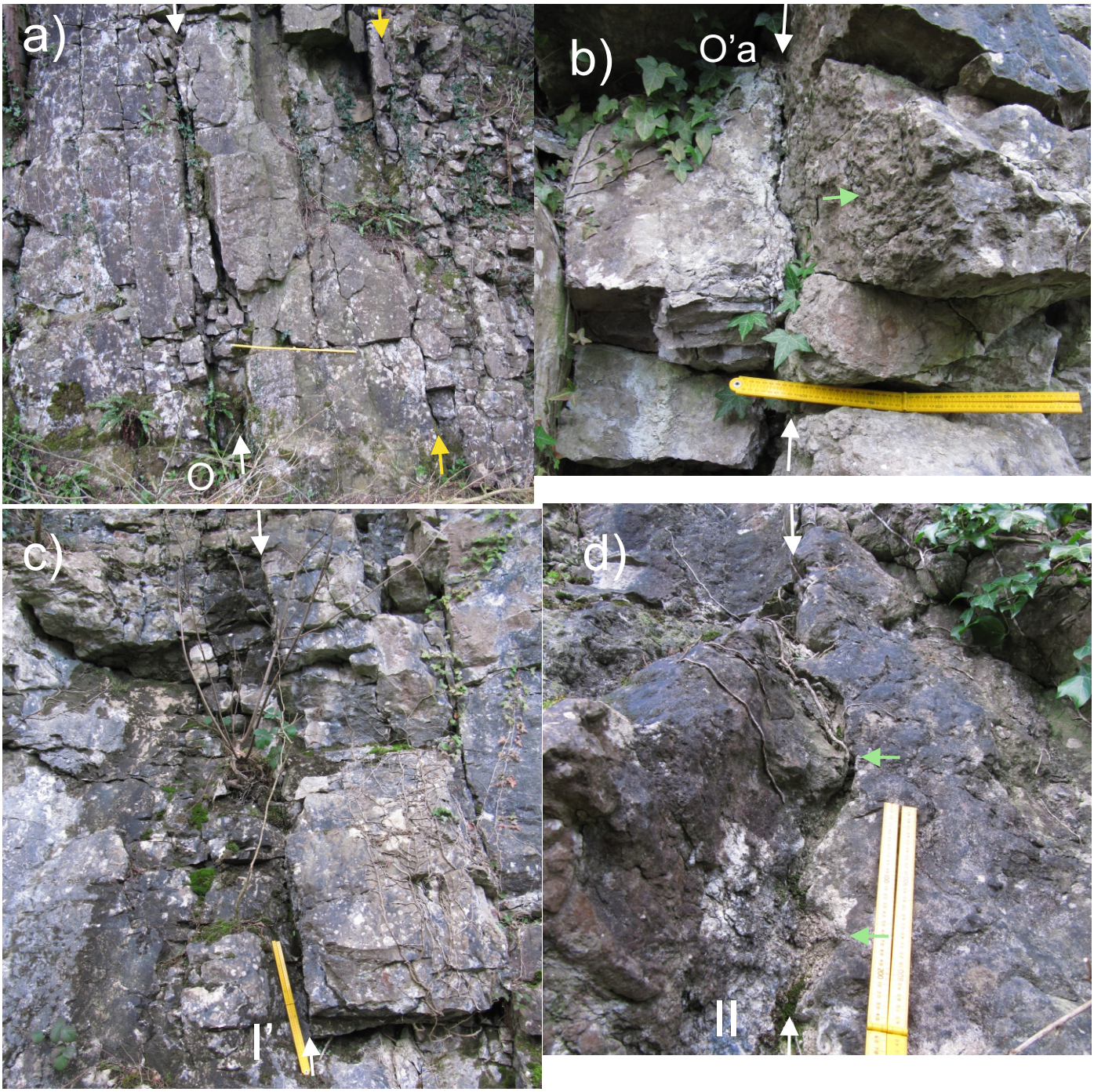

Fig. S4. Karst surfaces a) O, b) Oa, c) I and d) II in Trowbarrow Quarry. All sections young to the left in the photos. Scale shown by the 0.5 m ruler, when extended. a) The karstic surface (1 of Horbury, 1989) and surface O here, shown by white arrows. The rather more mammilated karstic surface at the base of the Urswick Limestone indicated by yellow arrows. b) The weakly mammilated surface show by white arrows, with a more irregularly pitted surface of the underlying bed (indicated by green arrow). C) The relatively flat karstic surface '2 of Horbury (1989) and our I surface. D) strongly mammilated karstic surface II (3 of Horbury, 1989), with a well developed silty fill of the surface. Green arrows show two prominent pits in the top of the underlying bed.

Fig. S5 continued. Karstic surface IVa at Burton Well Cliff, Silverdale [grid reference SD744465], where the beding is sub-horizontal. Surface IVa it can be clearly located between the underlying Woodbine Shale, and the overlying karstic surface V at the top of the cliff (neither shown in photo). e) shows a mammilated surface with no development of silty of silty paleosol at the contact (shown with white arrows). f) In contrast the surface (white arrows) some 10 m to the south displays an intermittent silty layer <1 cm thick which is preferentially weathered out like at the yellow ruler. Scale shown by 0.5 m ruler.

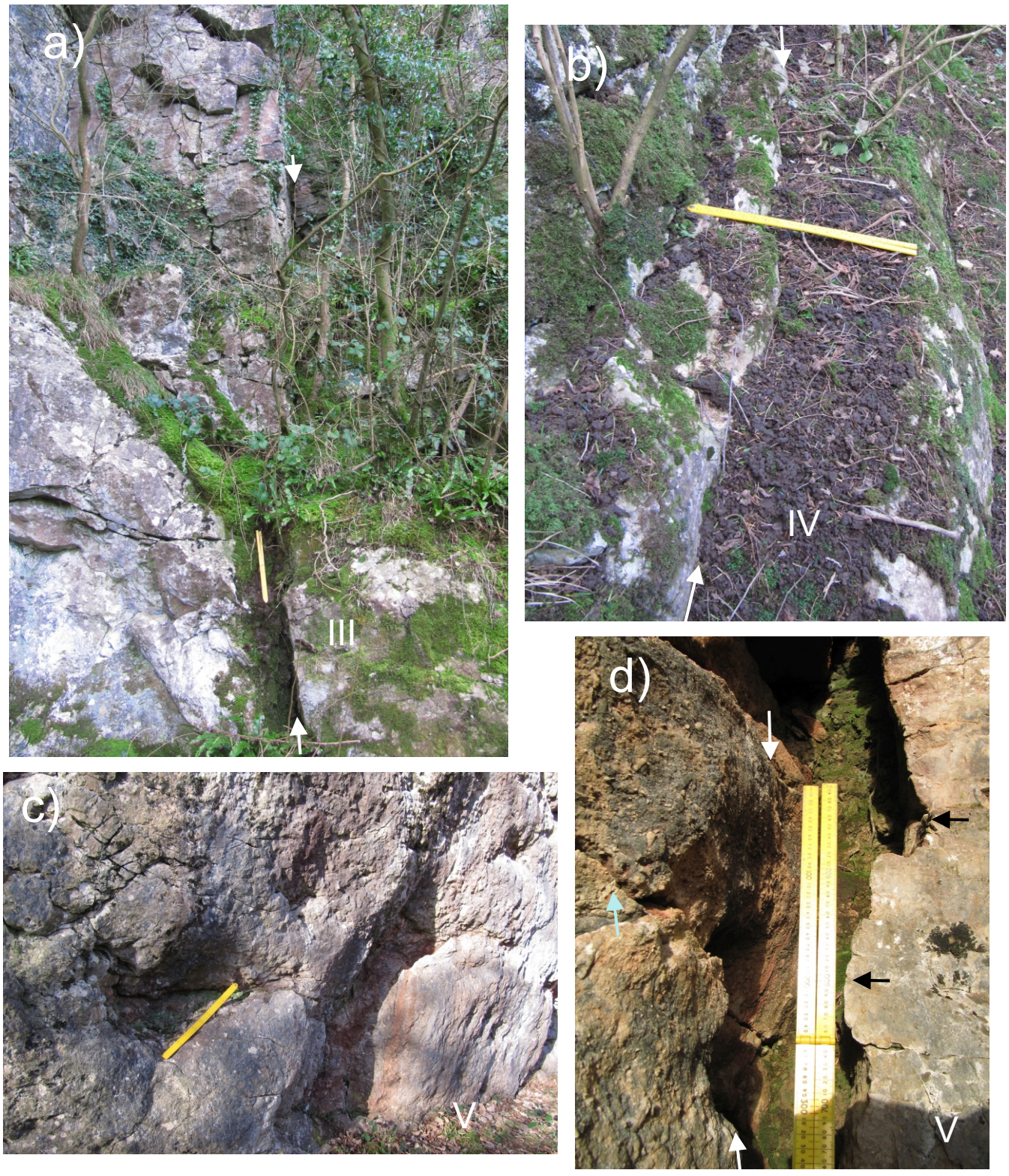

Fig. S5. Karstic surfaces: a) III, b) IV and in c), d) surface V in Trowbarrow Quarry. In a), b) beds young to the left in the photos; c) is the top surface of the underlying bed and in d) beds young to the right in the photo. a) The karstic surface 4 of Horbury (1989) and our surface III here shown by white arrows. The karstic surface is rather flat and strongly reddened, but has a well developed red silty palaeosol which the yellow ruler sits on. b) The very weakly mammilated surface IV (white arrows), with no silty palaeosol, which has a complex, strongly rootleted internal morphology described in detail by Horbury (1989). C) Very strongly mammillated and reddened karstic surface 'A' of Horbury (1989) and our V karstic surface. D) View of karstic surface V in the north part of the quarry (white arrows) showing the well developed silty palaeosol (underlying the ruler), and the rather irregular base of the overlying bed (black arrows). Red (hematite-bearing) fills occur in the cracks in the karstic surface shown with blue arrow. Scale shown by 0.5 m ruler.

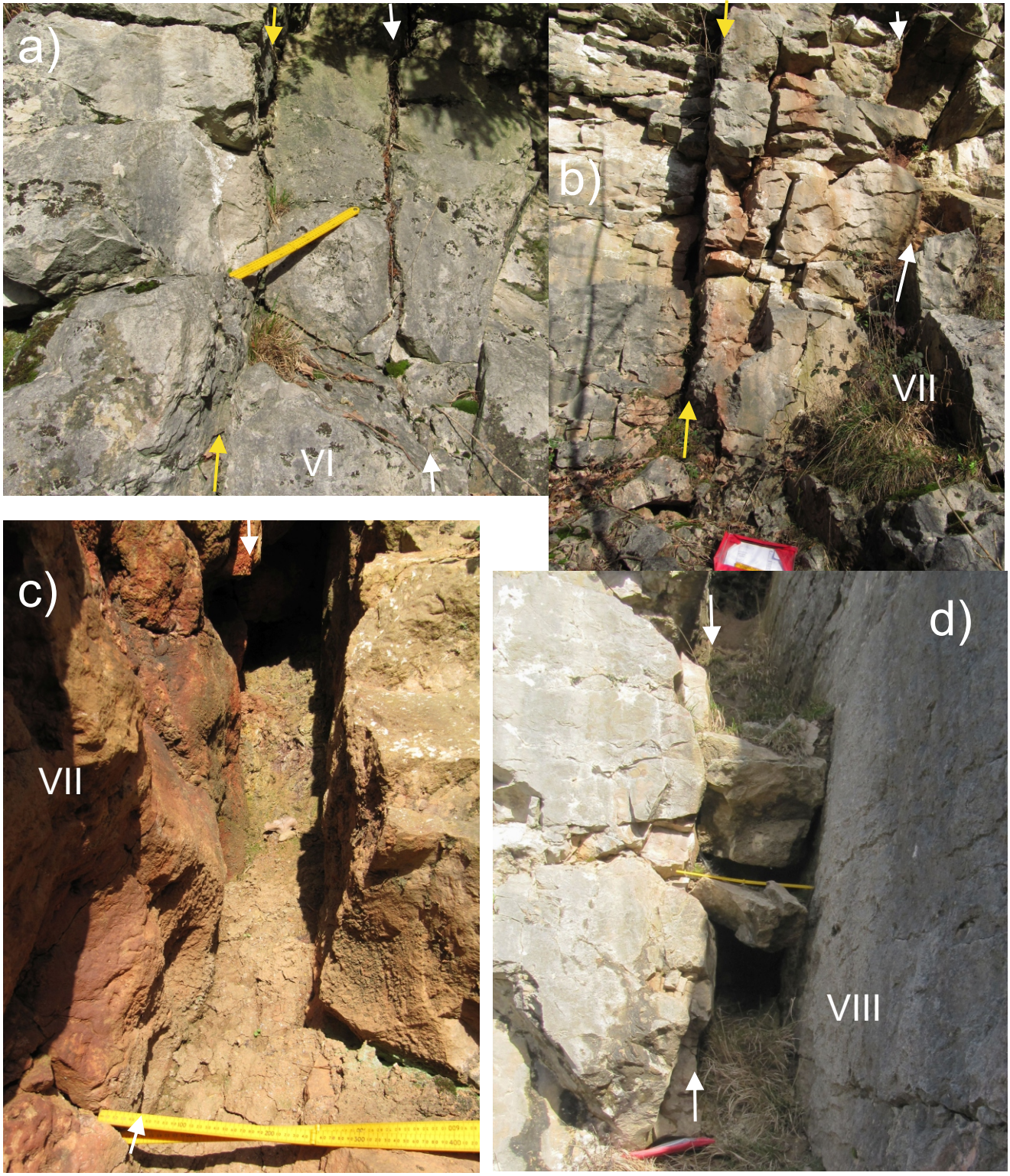

Fig. S6. Karst surfaces: a) VI, b), c) VII and, d) VIII in Trowbarrow Quarry. All beds young to the right in the photos. a) The rather flattish karstic surface B of Horbury (1989) and our surface VI here, showing an upper surface in white arrows and a lower surface in yellow arrows. The pitting on these surfaces is rather like shown in Fig. S5. b) The karstic surface C of Horbury (1989) in white arrows (our surface VII), and a lower weaker reddened karstic surface shown by yellow arrows. c) Detail of the very strongly mammillated and reddened karstic surface VII showing the very thick (25 cm) red silty palaeosol. In Trowbarrow this karstic surface is the most deeply pitted and reddened of any of the palaeosols. d) View of mammilated karstic surface VIII (white arrows), also showing the well developed silty palaeosol (underlying the ruler), and the flat base of the overlying bed which sits on the silty palaeosol.The blocks above and below the ruler are large fallen blocks. Scale shown by 0.5 m ruler, when extended, and 35 cm wide mapboard in b).

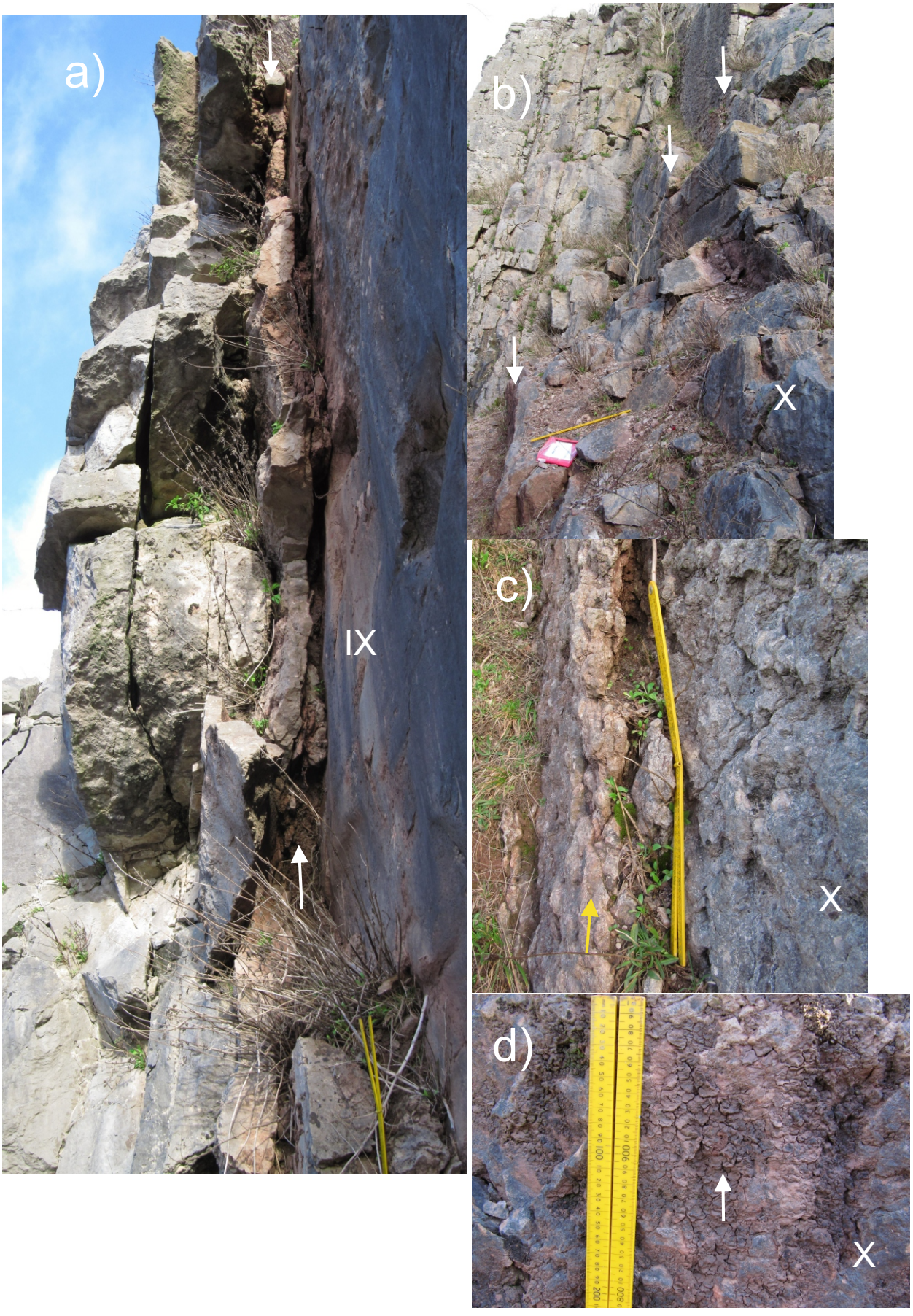

Fig. S7. Karstic surfaces: a) IX and b), c), d) X in Trowbarrow Quarry. Beds in a), b), c) young to the right in the photos, and d) is a photo of the base of a bedding surface. a) The concatenated karstic surfaces-calcrete-palaeosols E of Horbury (1989) and our IX surface (white arrows) which is weakly mammilated. b) View of the interval covering the many karstic surfaces and palaeosols designated F by Horbury (1989) and surface X here. White arrows show the three main karstic surfaces. c) Detail of the calcrete bed (yellow arrow) and overlying silty red palaeosol at the position fo the rightmost arrow shown in b). d) View of red, silty-clay on the middle karstic surface arrowed in a). The lowest karstic surface arrowed in b) has similar features to those shown in d). Scale shown by 0.5 m ruler, when extended in a and c) and 1 m ruler in b.

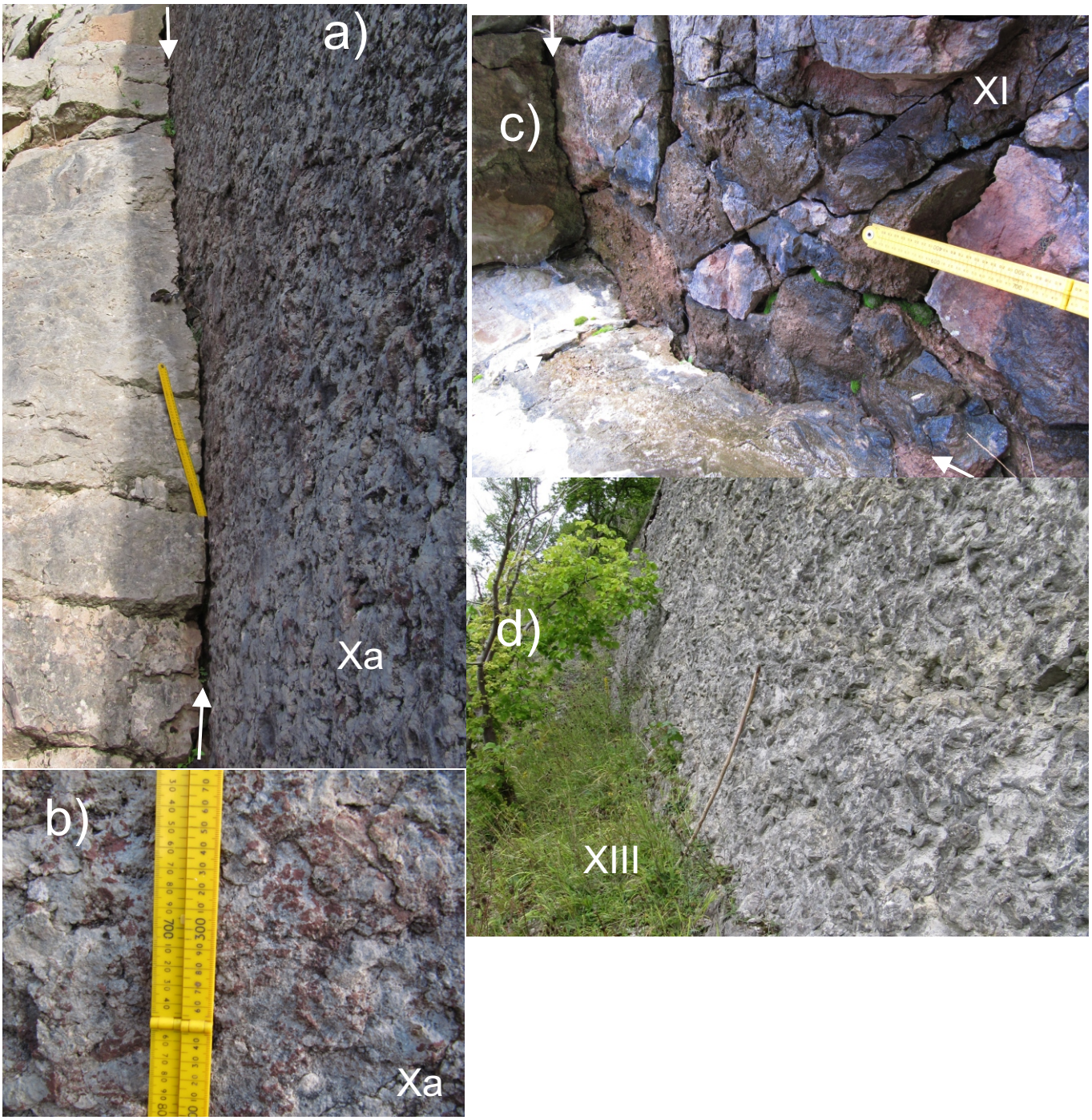

Fig. S8. Karstic surfaces: a), b) Xa and c), XI and d) the conformable surface XIII in Trowbarrow Quarry. a), c) and d) young to the right in the photos, and d) is a phot of the base of bedding surface overlying urface Xa. Scale shown by 0.5 m ruler, when extended in a and c) and 1 m stick in d). a) The rather flat karstic surface Xa (white arrows), and the rather irregular pitted surface of the overlying bed which contains extensive red mottling in its base (shown in b) and its lower few 10 cm. In this respect it is rather different in character to other palaeosols in the succession. c) Strongly reddened palaeosol-limestone XI, with the weakly mammilated karstic surface indicated by white arrows. d) The base of the Alston Formation shown by conformable surface XIII (which contains abundant brachiopod and large insitu coral heads), which rests on an underlying marine shale.

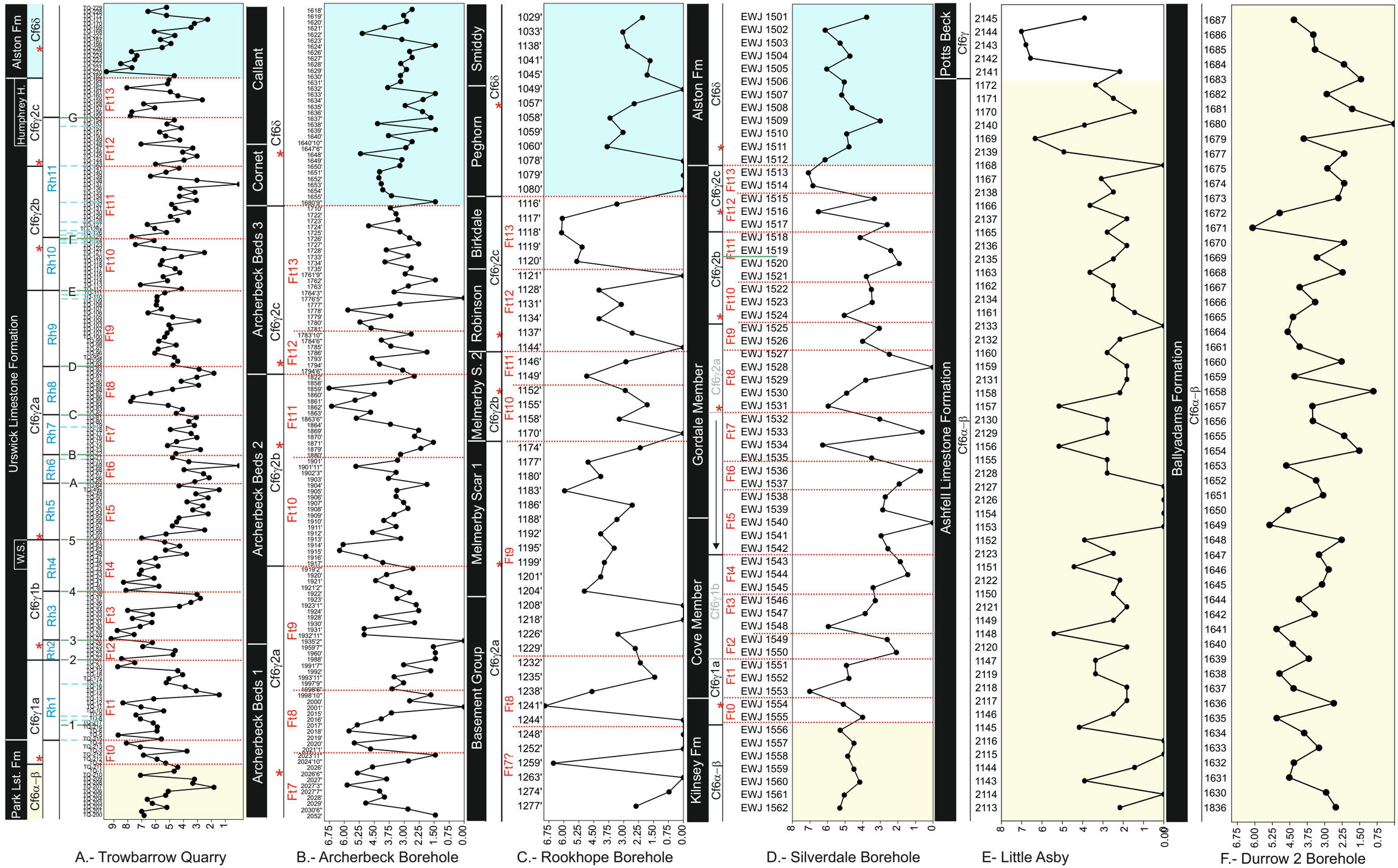

Fig. S9. Margalef diversity index in A. Trowbarrow Quarry, B. Archerbeck Borehole, C. Rookhope Borehole, D. Silverdale Borehole sections, E. Little Asby and F. Durrow 2 Borehole sections. The asterisks in the biostratigraphy column mark the precise position where guides of the foraminiferal assemblages/subzones are recorded sensu Cózar et al. (in press), Cózar and Somerville (2013), Cózar and Somerville (2004), Waters et al. (2017), Strank (1981) and unpublished data. Ft 0-Ft13 are foraminiferal trends with boundaries (dotted lines). Samples in all sections are placed equidistant, but differ in meter spacing.